110p.

Final Report

PRELIMINARY DATA

RAINFALL DETERMINATIONS BY METEOROLOGICAL SATELLITE RADAR

Prepared for:

NATIONAL AERONAUTICS AND SPACE ADMINISTRATION
WASHINGTON 25, D.C.

NASA CR-50,193

N63 17335

Code 1

By: *Arnett S. Dennis*

STANFORD RESEARCH INSTITUTE

MENLO PARK, CALIFORNIA

*SRI

OTS PRICE

XEROX $ 9.10 ph

MICROFILM $ 3.50 mf

SRI

April 1963

Final Report

RAINFALL DETERMINATIONS BY METEOROLOGICAL SATELLITE RADAR

Prepared for:

NATIONAL AERONAUTICS AND SPACE ADMINISTRATION
WASHINGTON 25, D.C.

By: Arnett S. Dennis

SRI Project No. 4080

Approved:

M. G. H. LIGDA, MANAGER AEROPHYSICS LABORATORY

D. R. SCHEUCH, DIRECTOR ELECTRONICS AND RADIO SCIENCES DIVISION

Copy No.....

ABSTRACT

The possibility of adding weather radar to meteorological satellite instrumentation has been discussed by a number of authors. In this report, the observations that such a satellite would make, if successful in the technical sense, are examined in the light of meteorological requirements. Consideration of the time variability of precipitation and the time intervals between successive satellite observations shows the two to be incompatible. To be of practical value in synoptic-scale analysis, instantaneous observations of precipitation must be updated once every hour or so, while local or mesoscale applications would require updating several times each hour. These requirements cannot be satisfied by means of a satellite radar system without the use of an absurdly large number of satellites.

The difficulties of detecting precipitation from a satellite are outlined, and certain specific systems that have been proposed for overcoming these difficulties are examined. It is concluded that no system proposed to date has any chance of detecting precipitation except at the satellite subpoint. However, this finding is of secondary importance, as overcoming this limitation would not remove the fundamental objections to the use of satellite-borne sensors to monitor precipitation.

ACKNOWLEDGMENTS

The work reported herein was performed in the Aerophysics Laboratory of Stanford Research Institute under the direction of Dr. M. G.H. Ligda, Laboratory Manager, and the immediate supervision of Mr. R. T.H. Collis, Head of the Laboratory's Radar Aerophysics Group. Both Dr. Ligda and Mr. Collis participated actively in the project, offering many valuable suggestions during its progress. Mr. R. E. Nagle, Research Meteorologist, was also active in the project, especially during its later stages. The concepts of the nature of precipitation patterns outlined in Sec. II-B were developed jointly by Mr. Collis, Mr. Nagle, and the author in a series of informal discussions, drawing upon earlier research which is referenced in the body of the report. The analysis of weather records and radar-scope photographs was carried out by Mr. F. G. Fernald, Research Meteorologist, and Messrs. A. H. Smith and R. A. Strader, Meteorological Technicians. The co-operative attitude displayed by all individuals mentioned is much appreciated by the author.

Thanks are due to the Illinois State Water Survey, the A. & M. College of Texas, and to McGill University for the provision of radar data for use in this study.

CONTENTS

ILLUSTRATIONS

TABLES

I INTRODUCTION, SUMMARY, AND CONCLUSIONS

This is the final report on a study of the meteorological value, both for operational and research purposes, of data that could be provided by various weather radar systems or obvious modifications or combinations thereof that have been suggested for incorporation in meteorological satellites. This report differs from a number of earlier treatments of the same subject, since it represents the approach of a meteorologist rather than an engineer. Much of the discussion, apart from certain sections dealing with specific radar systems, is applicable to any system which might be devised for monitoring precipitation from a satellite, including sferics detectors.

The first meteorological satellite observations, the TIROS I photographs of the Earth's cloud cover taken on 1 April 1960, were remarkable for a number of reasons. With a field of view several hundred miles across, they were able to show cloud systems associated with frontal cyclones and tropical storms in their entirety. The former conformed quite closely to models developed years earlier, notably by Bjerknes, on the basis of observations from the ground.[1]*

The success of TIROS I in observing clouds led some to anticipate similar results from satellite-borne weather radar equipment. A quote from an article published by two leading meteorologists in 1961 typifies these expectations: "Satellites equipped with radar could do a variety of jobs, depending on the wavelength of the signal. Some wavelengths would be reflected from the tops of clouds, providing a measure of cloud height; others would penetrate the clouds and be reflected back from raindrops or snowflakes, providing the vertical distribution of precipitating layers."[2]

---

*References are listed at the end of the report.

The feasibility of radar-equipped satellites is more questionable than was that of vidicon-equipped satellites during the planning and construction of TIROS I. Cameras carried by V-II rockets had successfully photographed clouds from 100 miles* altitude in 1947, 13 years before TIROS I was launched.[3] These photographs showed that the proposed systems had a good chance of success in the purely technical sense. More importantly, they revealed organization in the cloud cover relatable to specific synoptic situations and thus significant to meteorologists.[3,4] In contrast, no meteorological radar has ever been operated in a rocket or satellite, and it is by no means certain that the technical problems could be solved. However, this appears to be largely an academic question, as the evidence accumulated during the present study indicates that precipitation data from a satellite radar would be of negligible meteorological significance.

It is impossible in this report to duplicate exactly the lines of reasoning leading to this conclusion, as many of them advanced in parallel rather than sequentially. At the outset, various possible systems were considered in the light of the engineering difficulties they would present. A radar in a stationary orbit at 23,000 miles was shown to be out of the question for a number of reasons. Attention was therefore directed to satellite radars in low orbits, at altitudes of 400 to 600 miles. The assumption was then made that a sharp beam, of the order of 0.2 to 1 degree in width, could be scanned across the surface of the earth by such a satellite radar, and that all problems concerning power supplies, communication, and so on, had been solved.

The observations which such a satellite radar could obtain were simulated using observations of showers, hurricanes, and other precipitation patterns by ground-based radars, taking into account the loss of resolution and received power with range. It soon appeared that the most critical engineering problem was the loss of vertical resolution

---

*Nautical miles are used throughout this report.

for points off the satellite track, which caused precipitation return to be masked by ground clutter. The simulated satellite radar data showed that observations in a narrow strip along the satellite path would not be useful in identifying synoptic-scale features on weather maps. On the other hand, the low frequency of satellite observations ruled out their application to local and mesoscale analysis.

The possibility of extrapolating data from a narrow strip was next explored. Spatial correlation of the precipitation patterns proved to be very poor. This suggested a look at the variations with time. Here also, the correlation proved to be very low, with little predictability beyond an hour. When considered in the light of the periods of satellite orbits, this finding revealed that a single satellite could never be a successful precipitation monitor on a global scale, even if the swath-width limitation could be overcome.

Section II of this report reviews the historical background of the weather radar satellite concept, and then sets forth in detail the findings outlined in the above paragraph. Sections III and IV contain a review of our earlier work on resolution and sensitivity requirements, and examine some ideas advanced in the literature for detecting precipitation by satellite radar. In view of their complexity and the scant value of the data they could obtain, there appears little point in pursuing even those ideas offering some chance of technical success. In any case, no practical solution to the problem of vertical resolution for off-path points has been offered so far.

As instantaneous rainfall patterns are only loosely correlated with synoptic situations, it would appear that additional observations of such variables as pressure, temperature, and wind velocity would be preferable to rainfall-rate observations for filling in sparse-data areas of the weather map.

Where rainfall data is regarded as essential, attention should be directed to accrued amounts, rather than instantaneous rates. For areas of one million square miles or less, a few properly sited ground-

based radars would provide much better coverage than a satellite system. Where broader coverage is required, a system using gauges that would report on command to a communication satellite or an aircraft would be worth considering. However, the fact that no one has considered it worthwhile to develop systems to use the vast quantities of precipitation data accumulated every day by ship radars and aircraft radars in all regions of the world indicates that the meteorological community at large does not feel any pressing need for detailed precipitation data from remote areas.

II PRECIPITATION OBSERVATIONS FROM SATELLITES

A. Historical Background

One of the earliest published references to radar-equipped satellites was made by Wexler at the Third Symposium on Space Travel in May 1954.[5] A study of the uses of the data that might be obtained from such a satellite was published by Widger and Touart in 1957.[6] In both cases, the radar was considered as one of a number of devices to be carried by the satellite, and the engineering problems involved were not explored. Widger and Touart noted that resolution would be impaired as compared with ground-based radar, and gave an illustration of this effect applied to a radar observation of a squall line.

A paper presented by Mook and Johnson in 1959 suggested a weather radar satellite as a means of providing three-dimensional precipitation data on a world-wide, round-the-clock basis.[7] Choices of frequency and power requirements were considered, but not exhaustively. The effects of beamwidth upon vertical resolution and the incoherent nature of the radar return from precipitation were not mentioned.

In 1959, the National Aeronautics and Space Administration issued a proposal request for a feasibility study of weather radar satellites. Over 30 manufacturing and research groups responded. Many of the proposals submitted were the outcome of considerable effort, devoted mainly to engineering considerations. The proposals were valuable in that, taken together, they served to pinpoint some of the technical difficulties facing a designer of a meteorological satellite radar. These include the high power requirements of active radar systems as opposed to passive scanning devices, the need for narrow beams, and so on. The most critical difficulty appears to be that of distinguishing precipitation echoes from those returned by the underlying surface in areas not directly beneath the satellite.

Partial results of the preliminary studies conducted by two firms in response to the National Aeronautics and Space Administration's

proposal request were presented at the Eighth Weather Radar Conference in 1960,[8,9] and one of these papers was later published in the Journal of Geophysical Research.[10] Keigler and Krawitz, discussing possible methods for precipitation/ground discrimination, mentioned multifrequency systems, cross-polarization techniques, and Doppler radars.[8,10] On the other hand, Katzenstein and Sullivan proposed a fan beam with Doppler shifts being used to fix locations. All of these suggestions are considered below (Sec. IV), along with some additional ones. At this point, we merely note that none of these approaches appears capable of solving the problem at hand, which is the detection of an incoherent signal superimposed upon a signal some 10 to 30 db greater, which is itself fluctuating widely from pulse to pulse. The multifrequency and Doppler systems have been examined closely by personnel of the Meteorological Satellite Laboratory of the U.S. Weather Bureau and rejected as impractical.[11,12]

Further consideration within government agencies has led to suggested specifications for a first-generation weather radar satellite based upon presently available components.[13] In these systems, the precipitation/ground discrimination problem is sidestepped by limiting observations to a strip, of 20 miles maximum width, directly beneath the satellite path. These systems are a far cry from those envisaged earlier as providing "continuous global coverage on a round-the-clock basis."

More recently, a memorandum from Diamond Ordnance Fuze Laboratories to National Aeronautics and Space Administration has pointed out that the design specifications of the ultimate weather radar satellite system must be derived from the radar-sensible characteristics of the phenomena to be observed, rather than on the basis of available components.[14] This applies not only to the resolution and sensitivity, but to the coverage and frequency of observation required. Accordingly, Sec. II-B is given over to an examination of the nature of precipitation, which will provide the background information needed to evaluate the potential of meteorological satellites equipped with precipitation-monitoring devices.

B. The Nature of Precipitation

1. Precipitation Patterns as a Function of Synoptic Situation

The correlation of precipitation forms and intensities with the various features of synoptic charts is accepted by meteorologists as a matter of course. Bjerknes paid close attention to precipitation patterns in developing his frontal cyclone model.[1] The tendency toward convective activity along cold fronts and stratiform precipitation ahead of warm fronts and north of active cyclone centers that he noted in northwestern Europe holds over much of the temperate zones. Some striking composite radar photographs of storms in the central United States which show close agreement with the large-scale pressure systems and fronts have been prepared by Smith and Ligda,[15] while the spiral rain bands of hurricanes are well known--e.g., Senn and Hiser.[16]

However, attempts to fit instantaneous precipitation patterns as revealed by radar to synoptic-scale features have not been generally successful. In many cases, there is no obvious relationship between the precipitation patterns shown on radar screens and the synoptic-scale pressure and temperature fields.

Radar observations show that precipitation tends to form in discrete cells, which are organized into systems covering a few hundred to several thousand square miles. These systems, occupying a range of sizes exceeding the field of view of a local observer, but often too small to be delineated on weather maps, are referred to as mesoscale systems or, simply, mesosystems.[17] The smallest ones can be thought of merely as clusters of precipitation cells, but the largest ones, such as the Mid-West squall lines, are identifiable on synoptic charts.[18] The size and lifetime of mesosystems are positively correlated.[19] Large mesosystems can retain their identity for 24 hours or more.[18]

The individual precipitation cells which make up mesosystems have typical lifetimes which range from 15 minutes for small, convective cells to over 2 hours for snow-generating cells in stable air.[20,21] The

motion of mesosystems is accomplished through development and dissipation of cells, as well as by translation of existing cells.[22]

Mesosystems can be identified from radar data in three ways. Those in which the density of precipitation cells is much higher than that in the surrounding area can be identified by inspection of the instantaneous pattern. In other cases, where the cell concentration does not vary so widely, the mesosystems are not recognizable unless time-lapse techniques are used. Viewing the events of several hours in this way can reveal well-defined vortices with diameters of 100 to 300 miles embedded within larger cyclonic storms.[23] A third approach, which is especially useful where the cell concentration is very low, is to perform time-integrations. Soane and Miles used this technique to identify mesosystems in showers in Rhodesia which appeared to be randomly scattered when viewed on an instantaneous basis.[24]

Examination of cases in which close agreement between synoptic-scale maps and instantaneous precipitation patterns has been observed shows that each usually involves a large, intense mesosystem, which effectively constitutes an entire storm at the time of observation--e.g., Ref. 15. In cases with no obvious agreement, the precipitation is generally distributed randomly within several mesosystems, each of which undergoes wide variations in size and intensity over short periods.

The movement of precipitation areas associated with cyclonic storms and fronts is accomplished through the development and dissipation of mesosystems, as well as by their movements. To quote Austin and Blackmer on cold-front precipitation in New England, "The investigators were impressed by the fact that the precipitation pattern, relative to the moving surface front, is continually changing. For example, at one time there may be a frontal band and a prefrontal band and then an hour later the prefrontal band will have disintegrated into an isolated shower, or isolated showers will develop into a band, and so forth."[25] Attempts to find significant correlations between echo coverage and parameters derivable from other meteorological observations were not successful. A tendency for squall lines that form along cold fronts

in the central United States to move away from the fronts into the warm air and persist there for several hours has been noted.[18] In such cases, another line tends to develop along the front within a few hours, but any attempt to locate and track such a front by radar alone would lead to quite erroneous results.

Squall lines and shower complexes that develop within uniform air masses produce substantial quantities of rain. For example, Goldie has found that about half the rainfall of southeastern England, a region frequently traversed by frontal systems, is not associated with frontal activity.[26]

Fluctuations in precipitation could be due to shifting precipitation patterns within stable cloud systems, or to rapid formation and dissipation of cloud systems. The observed stability of large-scale cloud systems that sometimes maintain their identity for several days[27,28,29] indicates that the former explanation is correct. From this, one can infer that, at a given instant, precipitation occupies only a fraction of the total cloud area in a storm. This has been confirmed by several authors from a comparison of radar data and TIROS cloud photographs.[30,31,32]

Cloud systems associated with convective activity typically show only 10% of the cloud area to be actually yielding precipitation at a given time.

It is possible to extend Soane and Miles' time-integration technique to longer periods and larger areas, in order to relate precipitation patterns to synoptic-scale features. This has been done for a number of storms by Nagle.[33] In comparing precipitation echoes with TIROS cloud pictures, Nagle prepared integrated pictures in which all activity during periods of several hours was entered, using a coordinate system moving with the precipitation pattern viewed as a whole. The integrated patterns showed quite good agreement with the TIROS cloud patterns. One of his case studies, that of the mid-west storm of 16 May 1960, is reproduced here as Fig. 1.

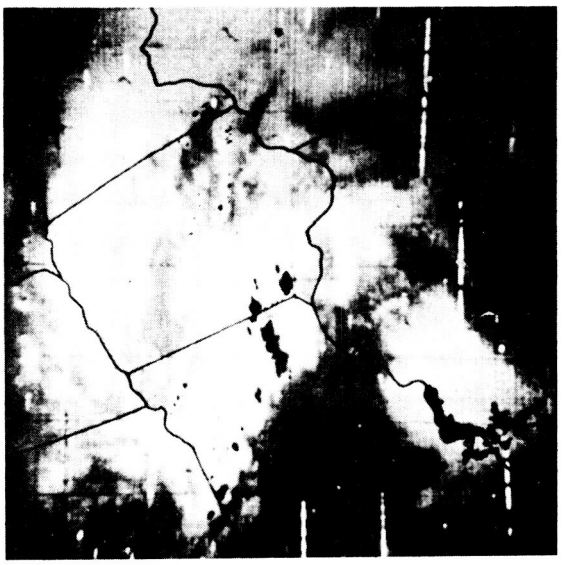

1500 CST

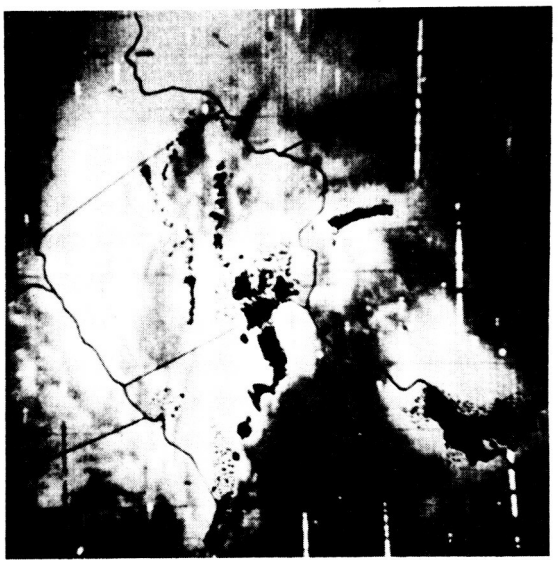

15—1600 CST

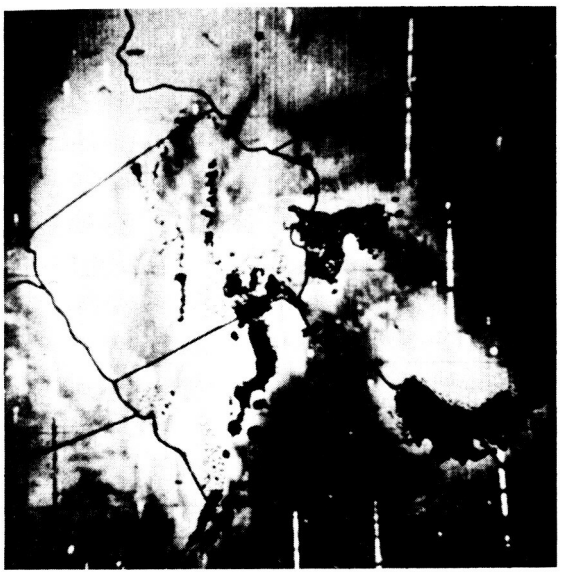

15—1700 CST

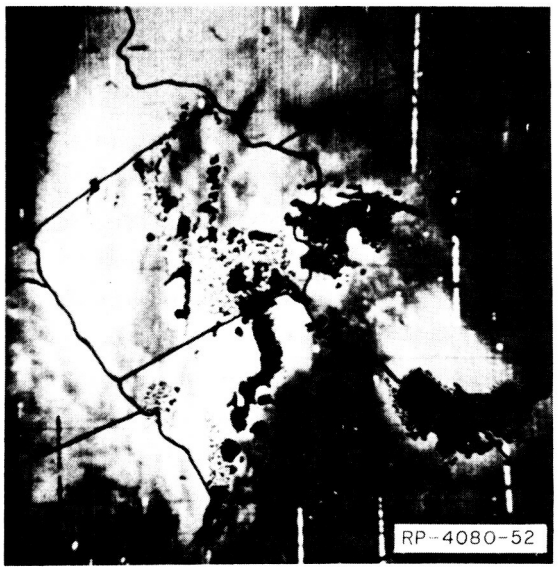

15—1800 CST

FIG. 1 INSTANTANEOUS AND TIME-INTEGRATED PRECIPITATION ECHOES SUPERIMPOSED UPON TIROS CLOUD PHOTOGRAPHS

The correlation between integrated rainfall patterns and cloud systems agrees with the well known fact that six-hourly rainfall accumulations are related to synoptic-scale pressure and temperature fields. In some parts of the world, the six-hourly rainfall totals are included in synoptic reports. It should be noted too that the so-called "present weather" section of the synoptic code involves some averaging in space and time, as in reports of "precipitation within sight, but distant from the station," "rain showers during the past hour," and so on. In summary, one can state that the instantaneous distribution of precipitation cells, being effectively a random sample of a function whose average value is relatable to the existing synoptic situation, cannot be used to locate fronts and pressure systems with any degree of accuracy.

There is a further possibility to be examined--namely, that the type of precipitation echoes observed could be used to identify fronts and pressure patterns (troughs, cols, etc.), even if their positions could only be estimated. Some observational programs have been carried out with ground-based radars in attempts to relate echo types and synoptic patterns.

Boucher has related the types of precipitation echoes observed in frontal storms of the northeastern United States to their locations within the storm system.[34] His classifications are as follows: (1) closely spaced, but distinct, shallow cells with tops quite uniform in height, (2) closely spaced cells protruding to varying heights above a region of generally continuous echo, (3) uniform echoes with broad streamers, originating as ice crystals, and (4) unstable cells, associated with heavy cumulus or cumulonimbus clouds. The various types are not mutually exclusive; rather, the probability of a given type of echo varies with position within a storm. The applicability of his results to the meteorological satellite radar is further limited by the fact that his types (1) and (3) ordinarily fall at rates below 1 mm/hr, and hence would not be detectable by most meteorological satellite radars proposed to date.

A study of precipitation echoes in the eastern Pacific Ocean by Ligda et al. shows that widespread, stratiform echoes are most likely to occur near low-pressure centers.[23] There do not appear to be any marked differences in the echoes associated with the various possible frontal configurations.

Kreitzberg has observed storms in the Seattle area with a vertically pointing radar and related the echo types to synoptic situations.[35] His results are similar to Boucher's. Some correlation between echo type and synoptic situation is evident, with large convective cells being most common in the vicinity of cold fronts. However, the distinctions are not clear-cut, and it is impossible, at least on the basis of data obtained so far, to lay down any rules for identifying fronts as warm, cold, or occluded, from radar observations of the associated precipitation.

2. The Statistics of Precipitation

The impossibility of adequately describing precipitation in terms of synoptic-scale systems has led some investigators, especially in the field of hydrology, to apply statistical techniques in analyzing it.[36] A useful concept in this work is the precipitation eddy spectrum, the transform of the correlation coefficient, which can be computed in both the space and time domains.[37] In any particular determination of spatial distributions, the information obtained is limited to those eddies larger than the resolution element but smaller than the total area observed. In a determination of fluctuations with time, information is obtained on eddies with periods longer than the interval between successive observations but shorter than the total period of observation. As a result, computed correlation coefficients depend upon the size of the area (or period of time) sampled and upon the resolution, in space and time, of the individual observations.

It is apparent that the common classification of precipitation echoes on radar screens as continuous, showery, or mixed is a description, in qualitative terms, of variations in the precipitation eddy spectrum.[38]

The continuous echoes are those in which the small eddy sizes corresponding to typical convective cell spacings (2 to 10 miles) are represented weakly, while the showery echoes are those in which these eddy sizes are prominent.

Analysis of precipitation echoes on radar screens has shown that the space-eddy spectrum is essentially continuous over the entire range of eddy diameters from less than one mile to over 500 miles, with a concentration in the range from 50 to 100 miles.[38] Similar results are found for the time-eddy spectrum, with eddy periods represented ranging from a minute or so up to several hours. Individual storms can show quite sharp peaks corresponding to the passage of regularly spaced mesosystems, but the positions of these vary from storm to storm.[39]

Correlation and autocorrelation coefficients have been measured for maritime precipitation echoes as a part of the present study, in order to permit an objective evaluation of the utility of instantaneous observations of precipitation in a 20-mile strip.[13] Plan-position-indicator records from the West Coast radar picket ships (Fig. 2) were chosen for analysis on a random basis, by months. In each picture, four rows containing five adjacent 20-by-20-mile blocks were laid out on east-west lines, two lines north of the origin and two lines south of it, placed so as to minimize range effects. The extent of precipitation in each block was determined by counting the number of 4-by-4-mile elements containing echoes. The procedure was then repeated for the pictures taken 30 minutes and 1 hour later. In all, 2880 blocks were examined for each station.

The sets of numbers obtained by the above procedure were analyzed to obtain the spatial correlation along an east-west line at intervals of 20, 40, 60, and 80 miles, and the autocorrelation at intervals of 30 and 60 minutes. The 30-minute autocorrelation was computed twice, for the first and second 30-minute intervals examined, to obtain information on the consistency of the data. The results indicate that the samples were adequate at Station 1, where precipitation is relatively frequent, but marginal at Station 7. No analysis was attempted for

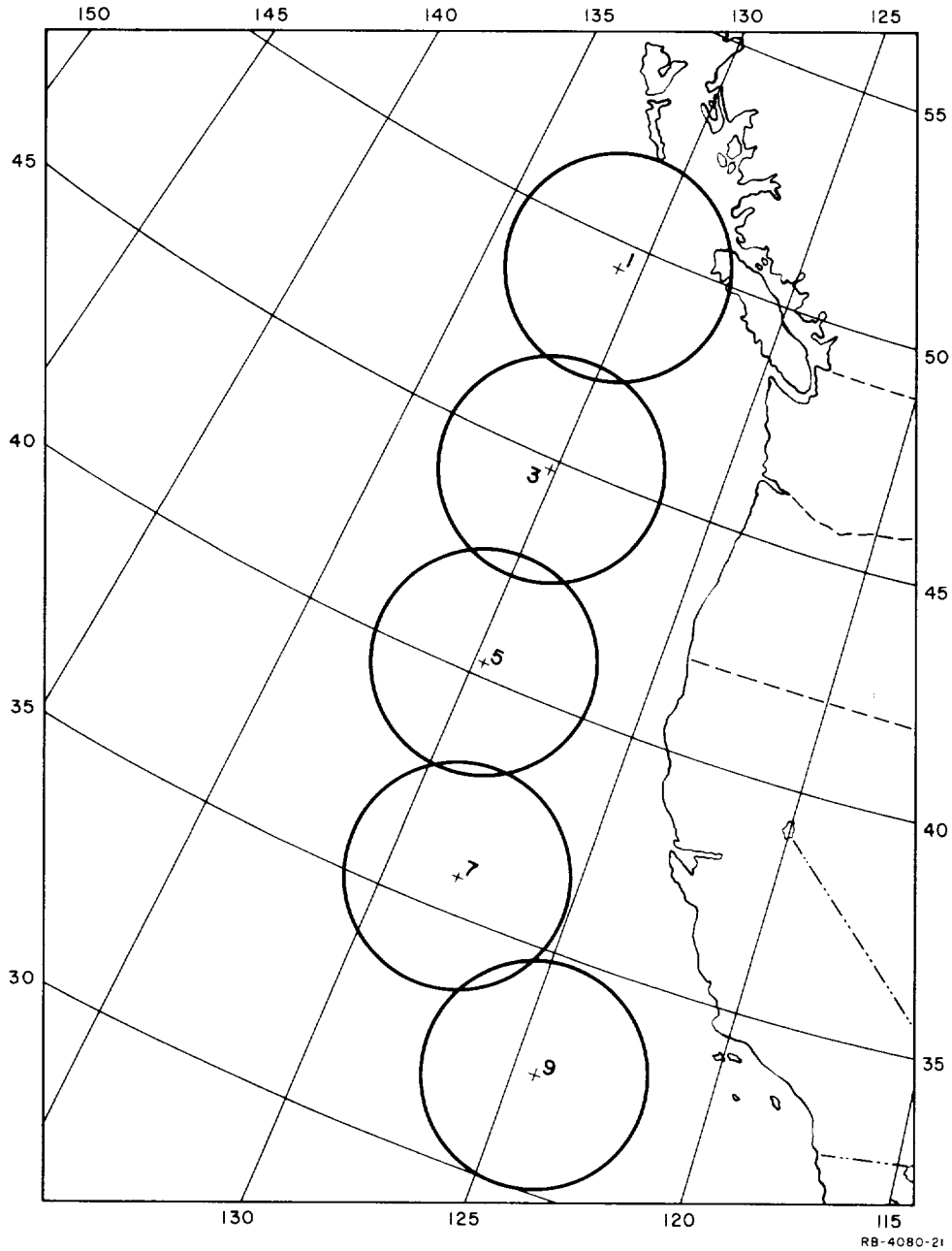

FIG. 2 POSITIONS OF WEST COAST PICKET SHIPS

Station 9, off southern California, where precipitation occurs only rarely (see Fig. 2).

Some consideration was given to making separate analyses for the cases with large areas of quasi-continuous echo. However, such cases obviously cannot be recognized on the basis of observations in a 20-mile strip. It is felt that the procedure followed, in which all combinations were lumped, corresponds most closely to the situation which would actually be faced in the utilization of satellite radar data. The nature of the results is illustrated in Fig. 3, a scatter diagram showing the precipitation counts on adjacent 20-by-20-mile blocks at Station 1. The concentration of points in the lower left-hand corner reflects the fact that most of the time neither block contains precipitation. Fourteen cases fall on Point 25, 25, in Fig. 3, which corresponds to a continuous rain shield extending across both blocks. The computed correlation coefficient is 0.86. The distribution of points is far from Gaussian, so there would be little value in a computed standard error of estimate.

Figure 4 shows the results for Station 1 for blocks 80 miles apart. The correlation coefficient is only 0.65, corresponding to a reduction in variance of roughly 40%. Examination of Fig. 4 suggests that the observed correlation is due mainly to the concentration of points in the lower left, and that otherwise the distribution is essentially random. In this connection it may be noted that Noel and Fleisher, who eliminated fair-weather cases from their sample, found that the correlation coefficient for five-mile squares dropped to 0.65 in only 10 miles.[37]

The results for the various cases examined are given in Table I. If one accepts a correlation coefficient of 0.80, which corresponds to a reduction of 40% in the error of estimate, as the minimum for useful extrapolation, it appears that observations in a 20-mile strip could be extrapolated to about 25 miles at Station 1, and to about 75 miles at the southern stations. There is no apparent trend from north to south in the autocorrelation coefficients, with the limit on useful extrapolation being somewhere between 30 and 60 minutes.

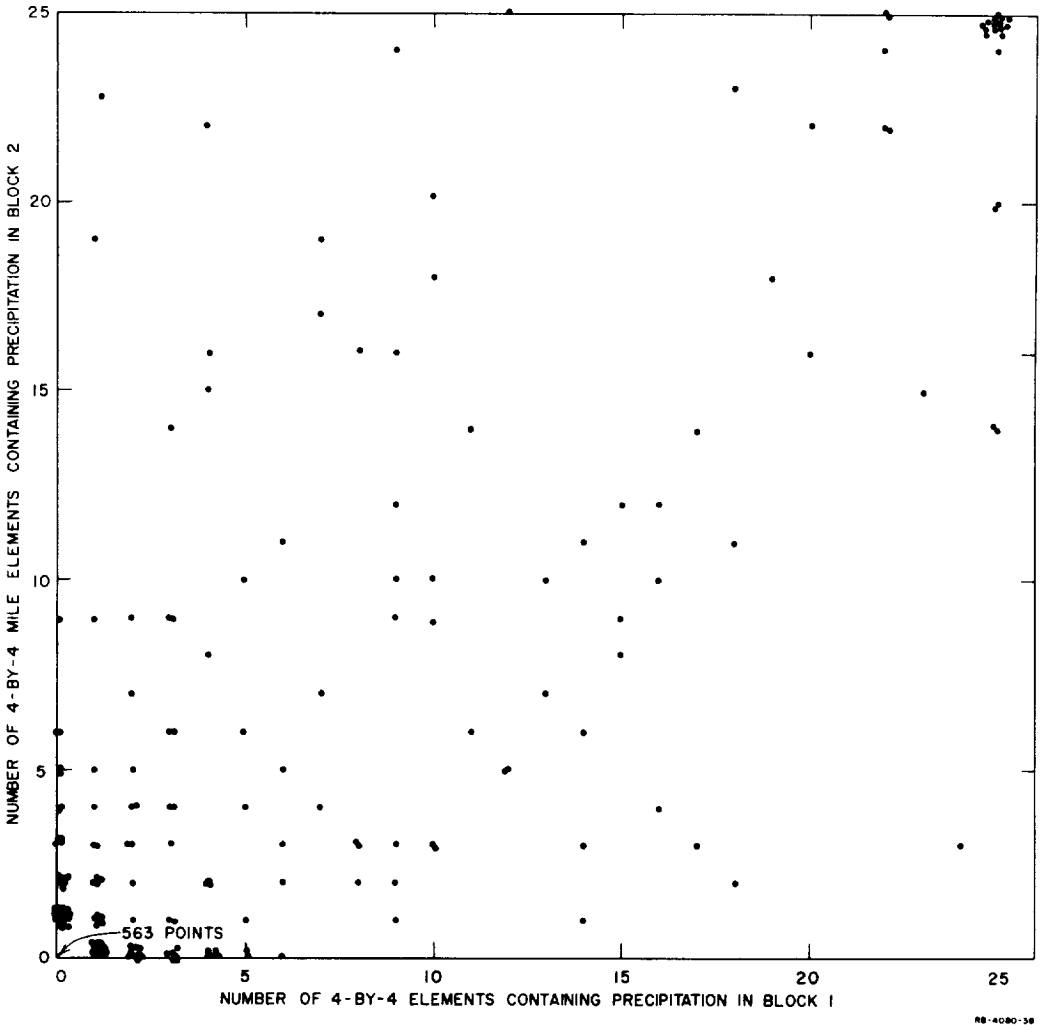

FIG. 3 SCATTER DIAGRAM COMPARING PRECIPITATION INCIDENCE ON 20-BY-20-MILE BLOCKS, WITH 20-MILE SEPARATION BETWEEN CENTERS

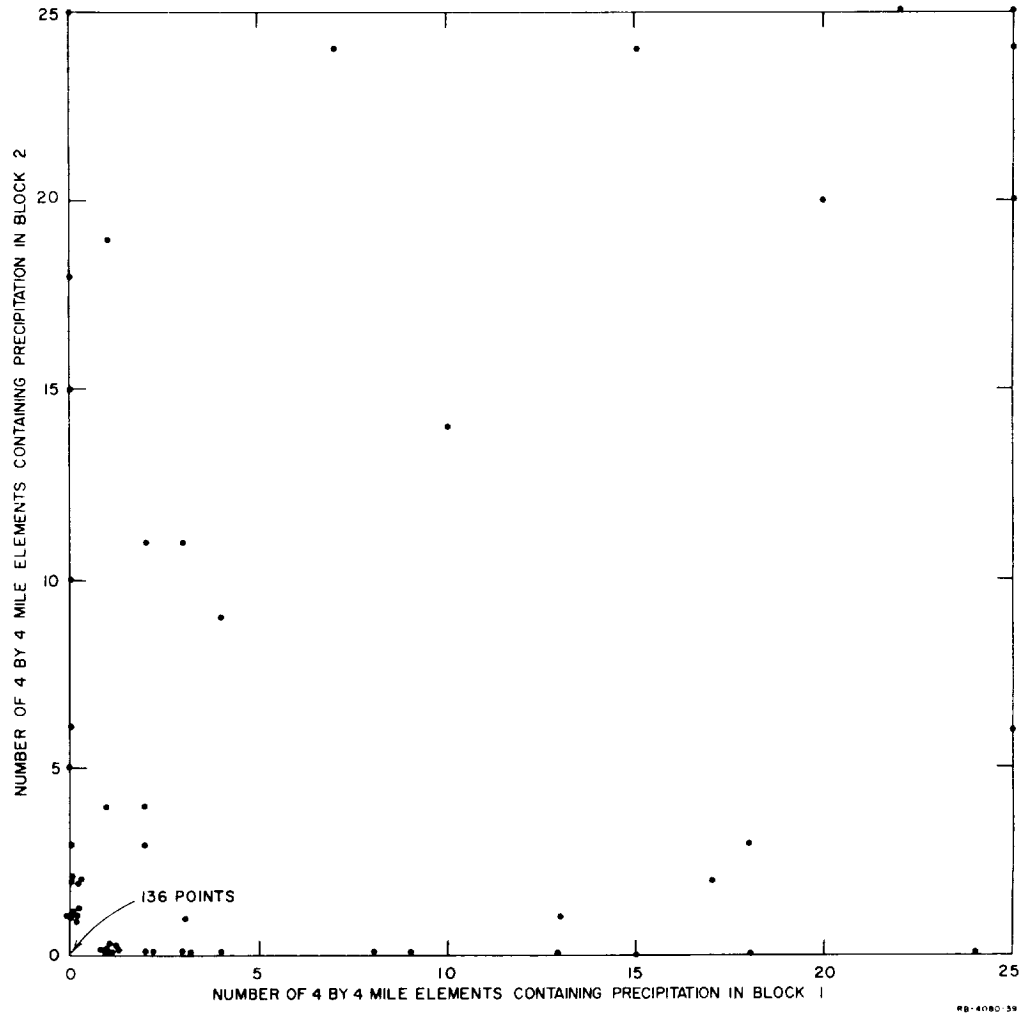

FIG. 4 SCATTER DIAGRAM COMPARING PRECIPITATION INCIDENCE ON 20-BY-20-MILE BLOCKS, WITH 80-MILE SEPARATION BETWEEN CENTERS

TABLE I

SUMMARY OR CORRELATION STUDY

(20-by-20-mile Blocks)

Station No.	Spatial Correlation Coeff				Autocorrelation Coeff	
	20 miles	40 miles	60 miles	80 miles	30 min	60 min
1	0.86	0.72	0.60	0.53	0.87 0.85	0.78
3	0.83	0.66	0.50	0.29	0.90 0.78	0.67
5	0.96	0.86	0.76	0.74	0.84 0.89	0.80
7	0.93	0.82	0.83	0.78	0.85 0.61	0.64

Showers were proportionately most numerous at the southern stations, yet the spatial correlations decreased most rapidly at the northern stations. This result is due to the use of 20-by-20-mile blocks, which are large enough to contain many convective cells, effectively averaging them out. (The rapid decrease in correlation noted by Noel and Fleisher down to 0.5 in 10 miles, is likely due in part to the use of 5-by-5-mile squares, as well as their elimination of fair-weather cases.)

It appears that the rapid decrease in correlation coefficients at the northern stations is due to the prominence of eddies with wavelengths in the range from 10 to 50 miles, too large to be averaged out in the 20-by-20-mile blocks. This indicates a tendency for precipitation there to be organized into small mesosystems. These were shown quite clearly in the convective situations. The showers tended to move along in small clusters or bands, with the groups separated by intervals of 10 to 50 miles (see also Soane and Miles[24]).

Further increases, through averaging, in the correlation coefficients for blocks some distance apart would not be likely unless

the averaging were over areas large enough to include several of these small mesosystems. It would also be necessary for the eddy spectrum to contain still larger components, extending across both blocks being compared. Some coefficients for 40-by-40-mile blocks have been computed to see if such averaging is of practical value. The results are not distinguishable from those for the 20-by-20-mile blocks. This suggests that in many cases the instantaneous precipitation pattern is determined largely by the locations and stage of development of small mesosystems and the cells within them, with the long wavelength components of the spectrum (greater than 100 miles) being of negligible importance. In this connection, it is of interest to note that the space-eddy spectrum derived by Noel and Fleisher, plotted against eddy length rather than frequency, has its maximum near 65 miles.[37]

The decrease in autocorrelation coefficients is due in part to translational effects. Adoption of a frame of reference moving with the precipitation elements slows the decrease, but does not prevent it. Convective cells which could be contained in a 5-by-5-mile square ordinarily last 20 to 40 minutes, while small mesosystems covering several hundred square miles have lifetimes of the order of two hours.[19] Some improvement over mere persistence forecasting can be achieved with radar data from ground stations by extrapolating positions of cells and mesosystems on the basis of observed velocities. Considerable difficulty would be experienced in applying this method to satellite data, as no determination of cell velocities can be made from the data itself (see Sec. II-C, below).

C. Fundamental Limitations

Precipitation observations by meteorological satellite radar would be characterized by poor spatial resolution, due to the long range of the targets. For a satellite at 600 miles, a 0.1° beam would be required to obtain roughly 1-mile horizontal resolution. However, such observations have a more critical limitation--the long period between successive observations in a given region--which arises from the characteristics of satellite orbits.

The essentials of useful orbits for weather observations are contained in a report by Dryden.[40] Placing a weather radar satellite in a circular, Earth-oriented orbit would minimize operational difficulties. The period of a circularly orbited satellite is a function of its height. A satellite at a height of 600 miles would travel at 4 miles per second, completing one revolution each 108 minutes. Although the orbital plane for any satellite is fixed in space, to a first approximation, there is an apparent westward motion of 15 degrees per hour due to the rotation of the Earth. Thus a satellite in a polar orbit returns to the same region* of the Earth once each 12 hours. This behavior is illustrated in Fig. 5.

Complex orbits can be worked out to improve coverage in certain areas at certain times. The time interval between observations in a given area cannot be reduced to less than one orbital period, however, and this interval cannot be maintained at any location for more than a few orbits at a time.

Any device used to observe precipitation systems on a given scale should up-date its information several times during the lifetime of such systems. If it does not, it cannot provide a reliable input to operational forecasts of their movement and development, and will provide nothing more than climatological data for the research worker. A single satellite radar, returning to a given part of the earth twice each day, is obviously unsuited to local and mesoscale observation, regardless of the instantaneous coverage it provides. Jones et al. estimate that mesoscale precipitation data should be up-dated 3 times per hour for operational applications, and 12 times per hour for research applications.[41] For local thunderstorms, the up-date frequencies needed are estimated at 12 per hour for operations and 20 per hour for research applications. The same requirements apply to any other device which might be proposed for observing instantaneous precipitation patterns

*"Region" is to be interpreted as a large area, hundreds of miles in extent. With a radar covering a 20-mile strip, as in Ref. 13, weeks could elapse between successive scans of a given point.

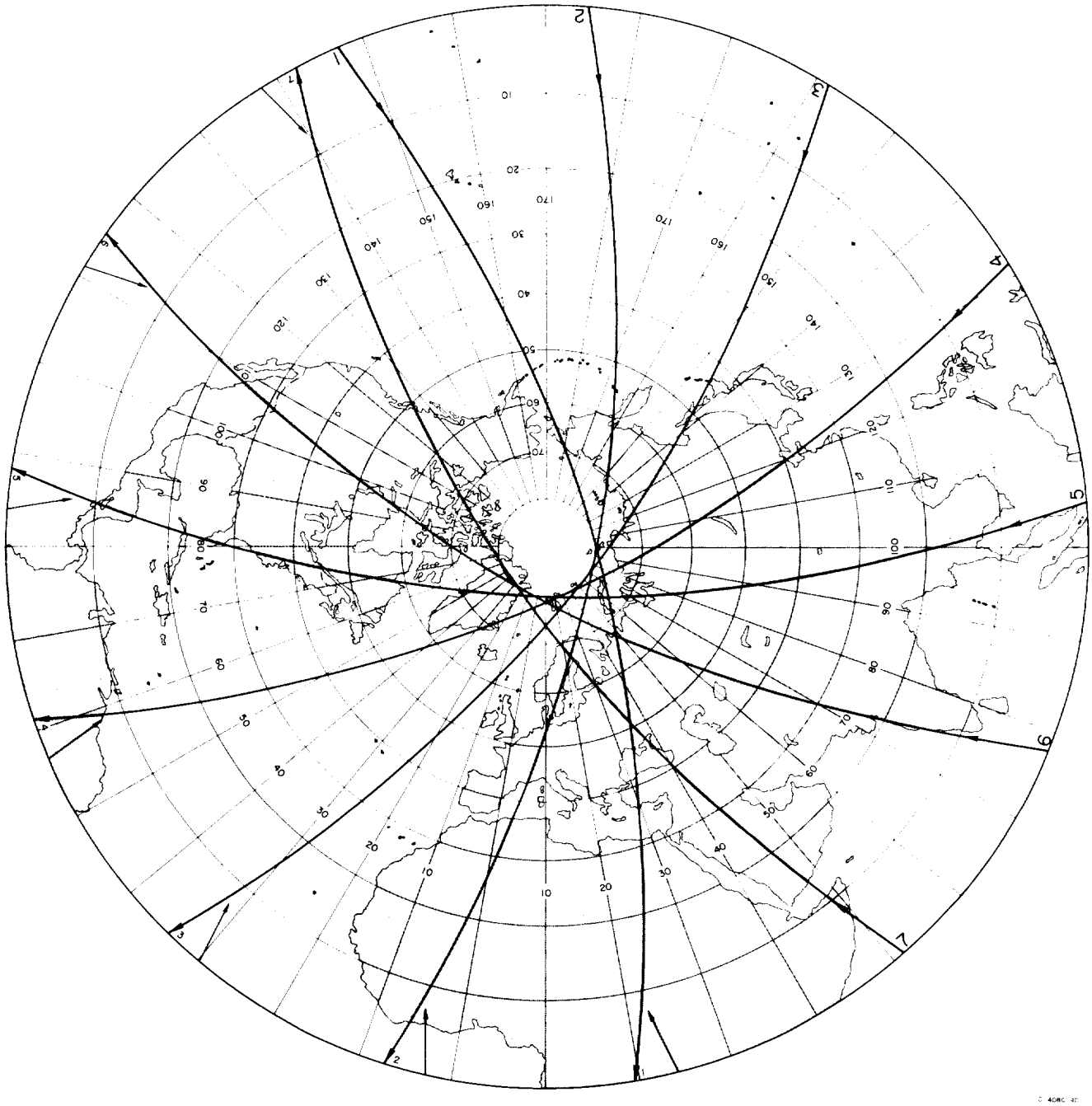

FIG. 5 SUCCESSIVE PATHS OF SATELLITE IN POLAR ORBIT AT 600 MILES

from satellites. (The lack of spatial resolution is also a sufficient reason for ruling out satellite radar as a tool for observing isolated showers, tornadoes, and other local phenomena.)

The above considerations show that practical applications for precipitation data from satellites must be sought on the synoptic scale. This makes sense in another way. A satellite's most obvious advantage is its ability to probe remote areas. It is a general rule in weather observing that interest in detail diminishes with distance. For example, an operational meteorologist is indifferent to the mesoscale structure of a storm 1,000 miles away from the area for which he is to issue forecasts.

The limitations inherent in attempts to use instantaneous observations of precipitation by themselves to derive synoptic-scale pressure and temperature fields are obvious, as explained in Sec. II-B-1. It would not be possible to locate the centers of low-pressure systems, except perhaps occasionally in the case of tropical storms. Active fronts could be located in a rough fashion but could not be classified as cold, warm, or occluded on the basis of precipitation observations alone.

It has been suggested that satellite rainfall data would be useful in monitoring the intensity of storms already located by conventional methods. However, the validity of the data obtained on any pass would be limited to a few hours. Jones et al. suggest up-dating synoptic-scale precipitation data once per hour for general applications.[41] If the observations were to be used merely as an aid to analysis of synoptic charts in certain key areas, up-dating every 6 hours would be sufficient. Either requirement would involve a multi-satellite system.

As only 10% or so of a cloud system produces radar-detectable precipitation at any one time, deducing cloud distributions from the locations of precipitation cells appears to be an impossible task. Therefore, the idea that radar observations of precipitation would be a satisfactory nighttime substitute for a camera-equipped satellite is incorrect.

It should be emphasized that the above discussion applies to a hypothetical satellite capable of observing storms in their entirety on a single pass. Observations in a 20-mile strip cannot be extrapolated to provide useful synoptic-scale coverage, as shown in Sec. II-B-2, and so would be of interest only to climatologists. Their value in climatology would be limited by the fact that radar reflectivity is not a unique function of rainfall rate. The commonly quoted expressions relating the two are average results. Variations about them of 50% or more are frequently observed in practice as a result of variations in drop-size spectra (Sec. III-A below). Data involving such gross errors would be virtually useless in studies of the atmospheric heat budget, which is one suggested application for satellite radar data.

In summary, a meteorological satellite radar, assuming it were technically successful, would be an extremely complex means of acquiring crude estimates of the instantaneous rainfall rate, a rapidly fluctuating function which is only loosely correlated with the prevailing synoptic situation. Such data would be of negligible importance to weather forecasters dealing with either local or large-scale systems, and would be too crude to provide reliable inputs to research programs involving climatology or the general circulation.

III PRECIPITATION DETECTION BY SATELLITE RADAR

A. Review of Basic Theory

The ability of radar sets to detect precipitation or cloud is due to scattering of incident radiation by the individual particles within the beam.[38,42,43,44] As the particles are randomly positioned and can move independently, precipitation echoes returned to a radar set are incoherent, showing fluctuations with range and from pulse to pulse. The average power from a contributing region filled with scatterers whose diameters are much less than the wavelength is, neglecting attenuation,

$$\bar{P}_r = \frac{\pi^4 P_t A_e h}{8 r^2 \lambda^4} |K|^2 \cdot Z \qquad (1)$$

where

P_t is the peak transmitted power,

A_e is the effective antenna aperture,

h is the length of a pulse in space,

r is the range,

λ is the wavelength,

K is a function of the dielectric constant of the scatterers, and

Z is the sum of the sixth power of the particle diameters per unit volume.[45]

The condition that the particle diameters be much less than a wavelength implies Rayleigh scattering. Rayleigh theory is applicable (1) to all cloud and precipitation particles, except large hailstones, at S-band, (2) to cloud particles, most raindrops, most snowflakes, and small hail at X-band, and (3) to cloud particles at K-band. The sixth-power law relating Z and D shows a pronounced bias toward large particles, which hampers attempts to measure water content by radar. For larger particles, deviations from Rayleigh scattering are noted, but

the bias toward large particles remains. Half the radar reflectivity of a shower can be contained in one small hail shaft, while dense cloud represents a negligible contribution to the total signal if even very light precipitation, such as drizzle, is present.

A great deal of work has been directed toward establishing empirical relationships between Z and rainfall rate, R, for rain (e.g., Fujiwara[46]), for snow (e.g., Gunn and Marshall[47]), and for hail (e.g., Douglas[48]). A widely quoted expression for rain is

$$Z = 200\ R^{1.6} \qquad (2)$$

where

Z is in mm^6/m^3 and

R is in mm/hr.[45]

This expression was derived using drop-size samples from steady light rain in temperate latitudes. Even under these limited conditions, deviations of the order of a few decibels are found, while the deviations in convective storms are even larger.[46] From the above, it is apparent that rainfall rate determinations based solely on measurements of radar reflectivity would be subject to large inherent errors, of the order of 25 to 50%, in addition to those which might arise from variations in equipment performance.

Whether or not precipitation in a radar beam is detectable can depend upon the sensitivity of the system or upon its sensitivity and resolution considered together. If the precipitation eddies are predominantly larger than the resolution element, sensitivity is the critical factor. If eddies smaller than the resolution element are present, the size of the resolution element is also important in determining whether or not the precipitation will be detected. If it is detected, the small eddies are smoothed, leading to a "smearing" of the precipitation pattern.

For a satellite 600 miles up, the minimum horizontal resolution element, barring some breakthrough in beam shaping, appears to be of the order of 4 miles. This is much larger than that possible with ground-based radars. It is possible, therefore, to estimate from observations of storms by ground-based radar how the same storms would look to a weather radar satellite system. Some work along these lines has already been done in connection with satellites,[6] and for other purposes as well.[49,50] This procedure is used in the following section in analyzing stepped-gain data from calibrated CPS-9 radar sets.

B. Resolution and Sensitivity Requirements--Case Studies

A thorough consideration of the resolution and sensitivity requirements for meteorological satellite radars must necessarily involve the statistics of precipitation--in particular, the statistics describing its spatial distribution. In this section, a number of case studies are presented as a preliminary treatment. These serve not only to clarify the nature of the problem, but will lead to preliminary estimates of the requirements for a radar capable of detecting precipitation in various situations.

Most of the case studies are based upon stepped-gain PPI records from a CPS-9 radar operated by the Illinois State Water Survey at Champaign, Illinois. The records have been analyzed, using calibration data provided, to give the average radar reflectivity in squares four nautical miles on a side. The records were corrected for range in accordance with Eq. (1), but not for attenuation. All data used were from points within 80 miles of the radar, to minimize difficulties due to partially filled beams. The reflectivity values were used to estimate how the same situations would appear to meteorological satellite radars with square horizontal resolution elements 4, 8, and 20 miles on a side, scanning back and forth across the satellite track. In this it was assumed that the depth of the precipitation exceeded the vertical resolution of the radar system.

Three points should be noted here. First, a satellite radar would not provide uniform resolution elements. Those removed from the satellite

path would be elongated transverse to it. Second, no correction was made for the small differences in range for targets along the satellite track and those off the track. Third, no information concerning variations in reflectivity with height has been included. Such information would be available for only a narrow strip along the satellite track, but it would be of some value. In effect, our presentation is that of an "extended" radar, capable of scanning in discrete steps and looking straight down everywhere in a strip some 100 miles wide, but with only one element of resolution in the vertical.

The reflectivity-area products computed for each resolution element have been converted to rainfall rates, using Eq. (2). The rainfall rates computed can be thought of as those required in widespread, uniform rain to yield the observed backscattering. In Ref. 13, the threshold of detectability--that is, the minimum detectable rainfall, assuming a filled beam--was set at 1 mm/hr. Later it was suggested that the threshold be set at 3 mm/hr.[14] In the results presented below, precipitation patterns as revealed by systems with thresholds at both 1 mm/hr and 3 mm/hr are shown, in order to show the changes that result from such a relaxation of requirements.

As a first example, a group of showers observed at 1440 CST on 20 May 1960 is presented (Fig. 6). Figure 6(a) shows the CPS-9 radar scope at full gain and 1-degree elevation, with the showers appearing west and northwest. As the CPS-9 is a very sensitive radar, some of the precipitation echoes may represent virga, rather than rain at the ground.

Figure 6(b) shows the situation with 4-by-4-mile resolution for five thresholds of detectability. If the satellite radar were capable of detecting any precipitation whatever in the beam, all the shaded area would necessarily be recorded as containing precipitation. With a threshold of 1 mm/hr, the area covered is reduced sharply, but the nature of the pattern is still apparent, particularly if one can measure the intensity of the stronger echoes. With the threshold set at 3 mm/hr, only six squares are filled in.

Figure 6(c) shows the situation with 8-by-8-mile resolution. With the threshold at 1 mm/hr, identification of the pattern is still possible, but at 3 mm/hr only one square is filled in. Detection of the showers would be a chancy business, depending upon whether or not there were individual showers in their mature stage at the instant of viewing the pattern.

The 20-by-20-mile view is shown in Fig. 6(d). Here no return is visible with the 3 mm/hr threshold, and only one square is filled in with the 1 mm/hr threshold. If the radar were capable of detecting any precipitation whatever, it would report the shower area as a solid area of precipitation over 100 miles long.

Consideration of a number of additional summer shower situations tends to confirm the findings in this particular case. In general, the detection and identification of showery areas (not of all individual showers) in warm, humid airmasses requires a sensitivity corresponding to a minimum detectable rainfall rate of 1 mm/hr and horizontal resolution of 8 miles, or a threshold of 3 mm/hr and horizontal resolution of 4 miles.

The detection of isolated showers in polar air masses would be more difficult, as they tend to be smaller in both horizontal and vertical extent and to produce lighter rainfall than showers in tropical air.

Figure 7 is a treatment of a severe squall line observed on the Illinois State Water Survey radar on 16 May 1960. On that date, Illinois was covered by a flow of tropical air, which formed the warm sector of a frontal disturbance moving by to the north. Several thunderstorm complexes moved through Illinois in association with the frontal wave. A detailed analysis of them has been provided by Wilk.[51] Figure 7 shows the situation at 1820 CST as seen by the CPS-9 at full gain, and by the various resolution-sensitivity configurations applied to the showers of May 20. Examination shows that this squall line could have been detected almost as well with a threshold of 3 mm/hr as with a threshold of 1 mm/hr, provided the resolution element was kept small. With the

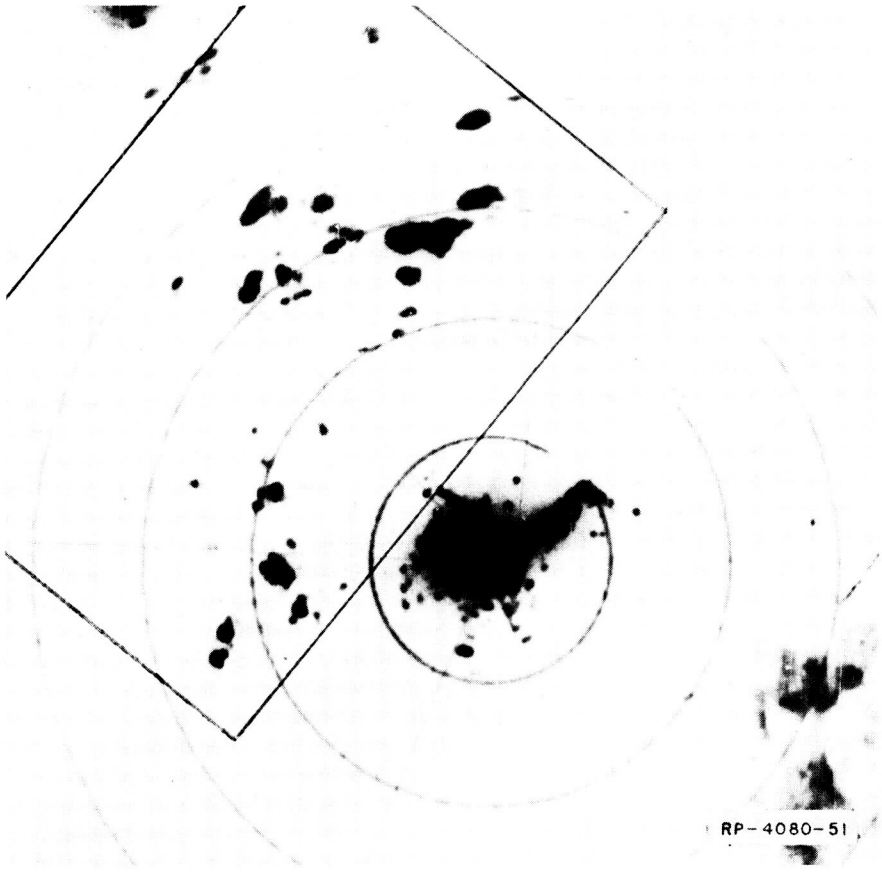

FIG. 6(a) PLAN VIEWS OF ISOLATED SHOWERS – ILLINOIS, 1440 CST, 20 MAY 1960
PPI-Scope Photograph, CPS-9 Radar

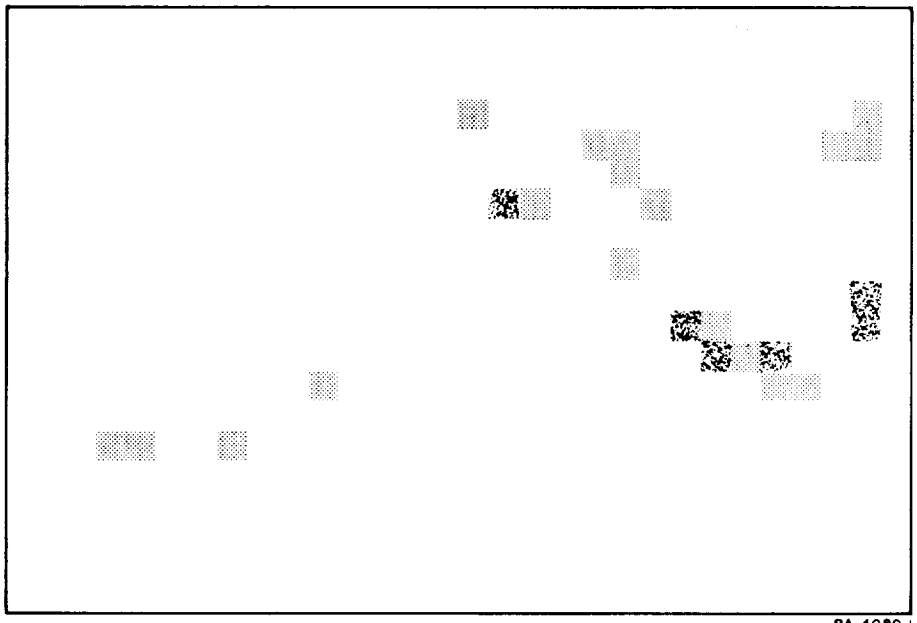

(b) 4 x 4 MILE RESOLUTION

FIG. 6(b) PLAN VIEWS OF ISOLATED SHOWERS – ILLINOIS, 1440 CST, 20 MAY 1960
Hypothetical Satellite Radar Display, 4-by-4-Mile Resolution

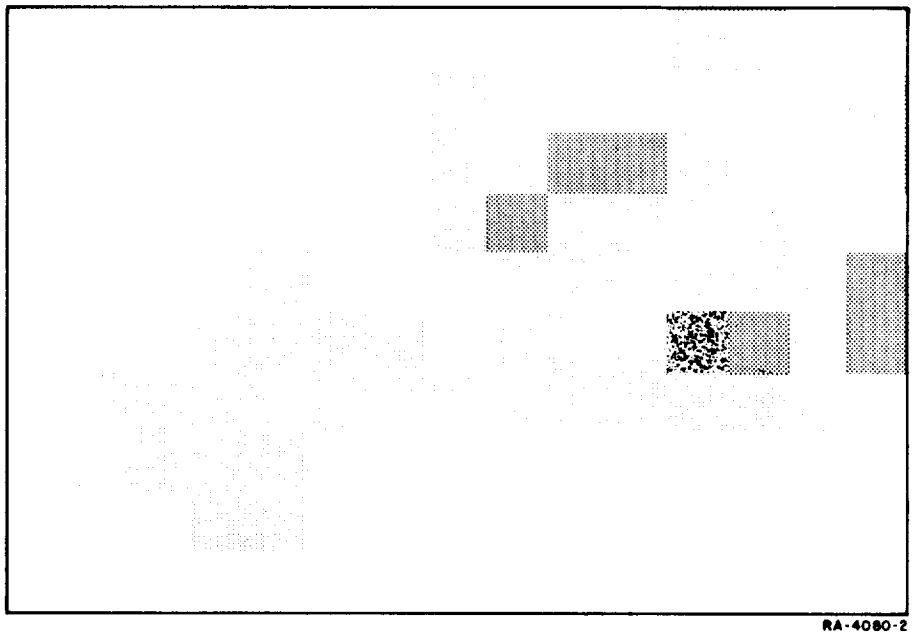

(c) 8 x 8 MILE RESOLUTION

FIG. 6(c) PLAN VIEWS OF ISOLATED SHOWERS – ILLINOIS, 1440 CST, 20 MAY 1960
Hypothetical Satellite Radar Display, 8-by-8-Mile Resolution

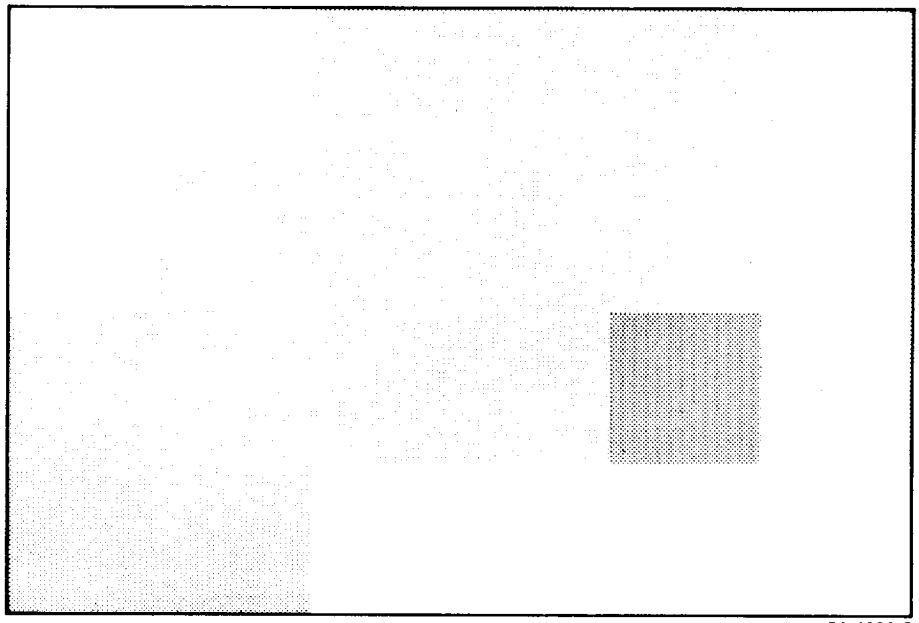

(d) 20 x 20 MILE RESOLUTION

FIG. 6(d) PLAN VIEWS OF ISOLATED SHOWERS – ILLINOIS, 1440 CST, 20 MAY 1960
Hypothetical Satellite Radar Display, 20-by-20-Mile Resolution

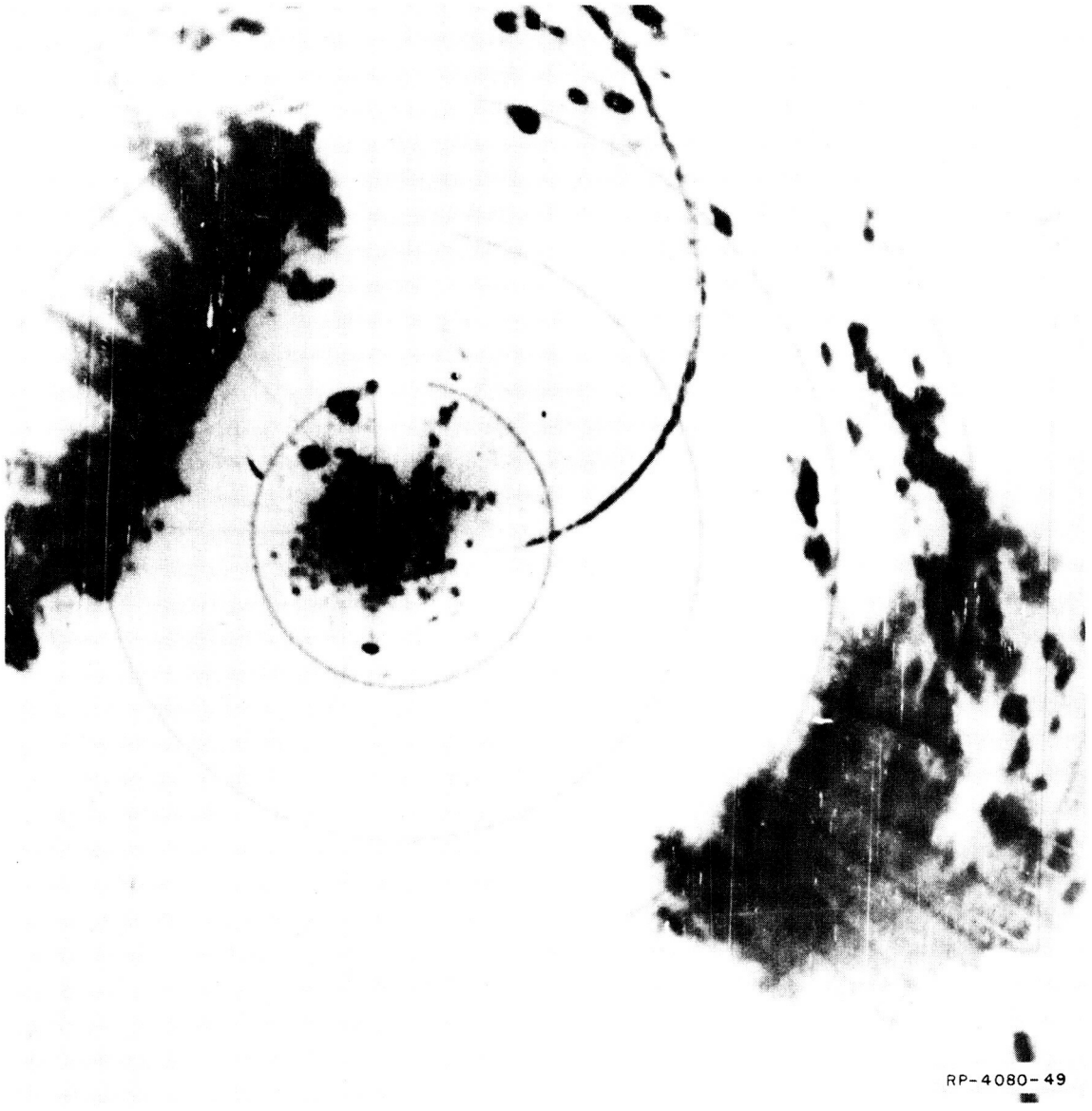

FIG. 7(a) PLAN VIEWS OF SEVERE SQUALL LINE – ILLINOIS, 1820 CST, 16 MAY 1960
PPI-Scope Photograph, CPS-9 Radar

(b) 4 x 4 MILE RESOLUTION

FIG. 7(b) PLAN VIEWS OF SEVERE SQUALL LINE – ILLINOIS, 1820 CST, 16 MAY 1960
Hypothetical Satellite Radar Display, 4-by-4-Mile Resolution

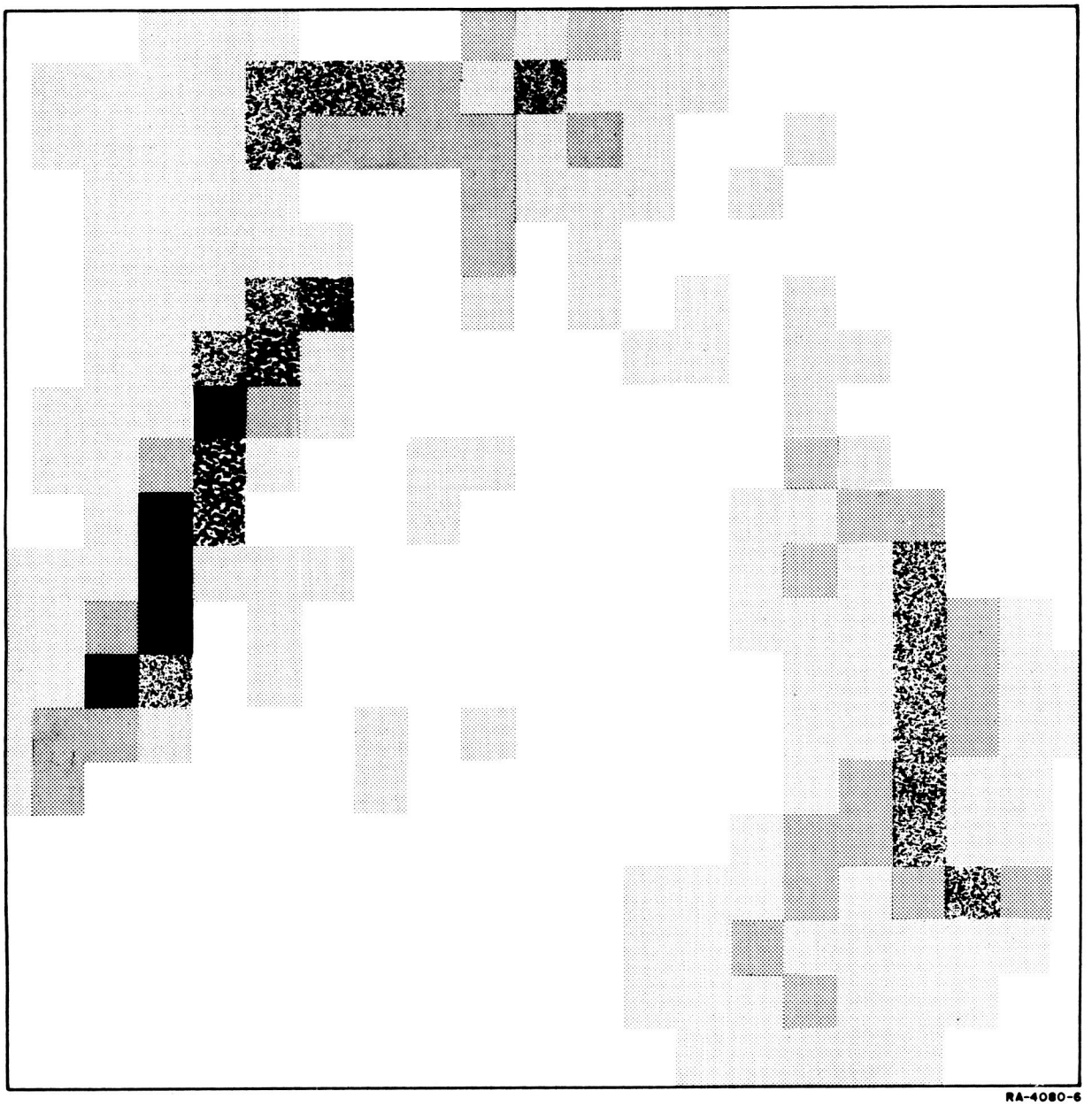

(c) 8 x 8 MILE RESOLUTION

FIG. 7(c) PLAN VIEWS OF SEVERE SQUALL LINE – ILLINOIS, 1820 CST, 16 MAY 1960
Hypothetical Satellite Radar Display, 8-by-8-Mile Resolution

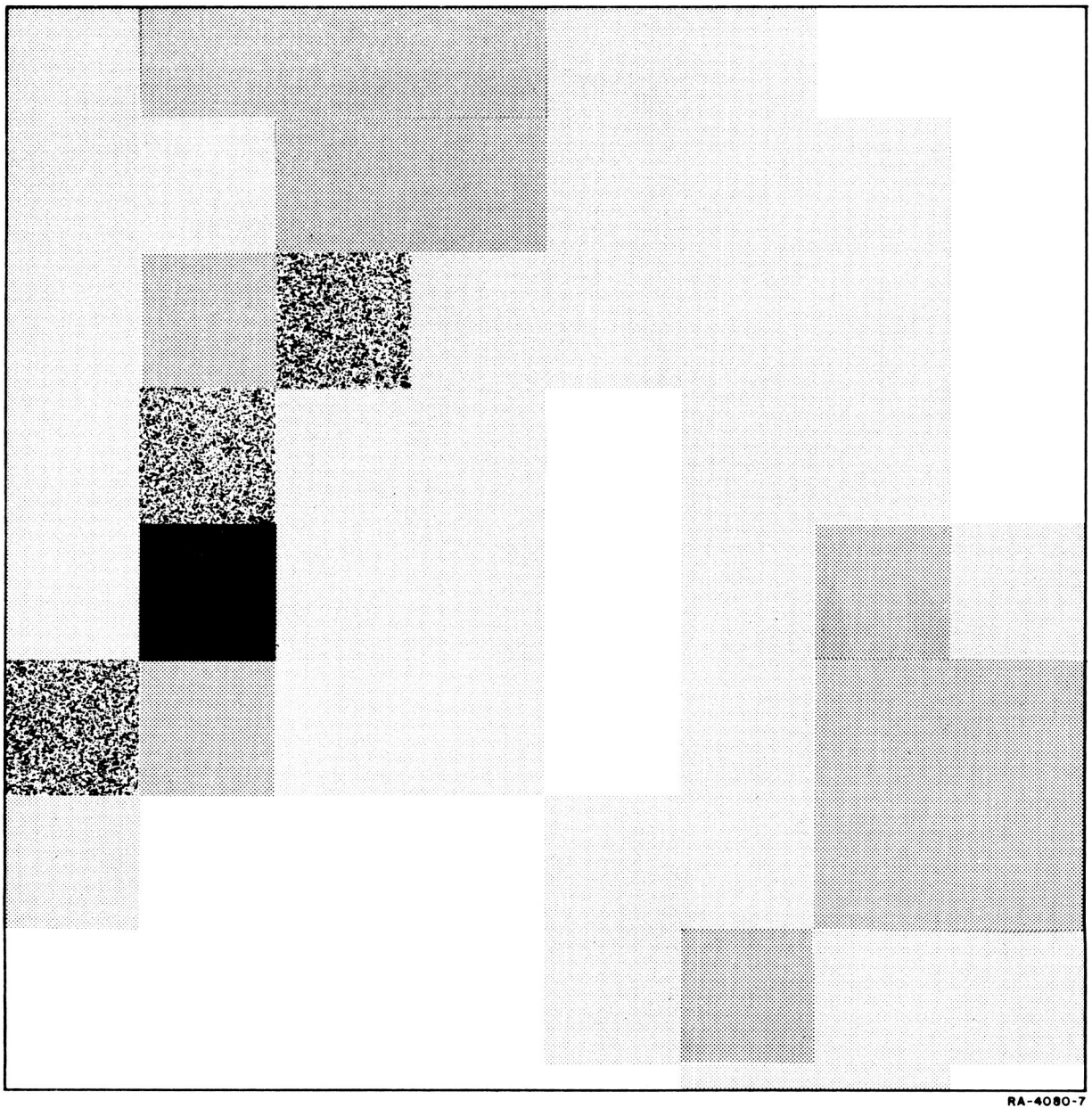

(d) 20 x 20 MILE RESOLUTION

FIG. 7(d) PLAN VIEWS OF SEVERE SQUALL LINE – ILLINOIS, 1820 CST, 16 MAY 1960
Hypothetical Satellite Radar Display, 20-by-20-Mile Resolution

resolution degraded to 20 by 20 miles, this is no longer true. Figure 7(d) shows that raising the threshold to 3 mm/hr in that case would have completely eliminated the moderate to heavy showers in the southeast corner. Four resolution elements would have been "painted in" in the strong squall line to the northwest, but it must be borne in mind that the squall line was then in its mature stage, accompanied by heavy rain and hail.[45]

Figure 8(a) shows a band of rain and snow showers observed at 1058 CST on 8 April 1960. Figure 8(b) is the representation for a system with 4-by-4-mile resolution and a threshold at 1 mm/hr, based on Fig. 8(a) and some additional photographs at higher angles of elevation. As only three cores remain, it would be impossible to say, without additional information, whether they were part of a band or merely isolated showers. Further degradation of the data eliminates the returns completely.

As one suggested function for a weather radar satellite is the detection of tropical storms at sea, the patterns which such storms would present are of special interest. Because of the high rainfall rates involved, one would expect the sensitivity requirements for the detection of tropical storms to be less stringent than those applicable to precipitation areas in the Temperate Zones.

Hurricane Debra of the 1959 season has been analyzed as a sample case, using radar reflectivity data obtained from a CPS-9 radar at the A. & M. College of Texas.[49] Figure 9 shows the situation at 2100 CST of 24 July 1959, as the hurricane eye was approaching the coast near Galveston. With 4-by-4-mile resolution, the hurricane eye and characteristic spiral bands are apparent with the threshold at either 1 mm/hr or 3 mm/hr. As Fig. 9(b) shows, increasing the resolution elements to 8-by-8-mile squares does not seriously impair the information content of the picture. With 20-by-20-mile resolution [Fig. 9(c)], there is no question of failure to detect the storm, but there is loss of detail; the position of the eye is no longer apparent and the pattern suggests a severe squall line rather than spiral bands. It appears that

8-by-8-mile resolution is required for accurate locating of tropical cyclones, while sensitivity corresponding to a minimum detectable rainfall rate of 3 mm/hr for a full beam would be satisfactory for their detection and location.

In the situations considered so far, the contributing regions have been considered to be filled in the vertical with scatterers. This is a reasonable assumption in the case of tropical storms and in showers with vertical extent of the order of 2 miles or more.

In stable situations, variations in the vertical must be considered. Particle growth in such cases, outside of the tropics, usually begins at the cirrus level, 4 to 8 miles up, and can continue all the way to the ground. Whether the particles, originally solid, reach the surface as snow, rain, or ice pellets (sleet) depends upon the vertical temperature distribution.

In cases where snow melts to rain, the melting region is marked by a layer of enhanced echo some 1000 to 1500 feet thick, known as the "bright band." A useful description of this phenomenon and a review of its causes are given by Battan.[52] Factors to be considered are (1) the change in the dielectric factor, $|K|^2$, of Eq. (1) from that of ice (~ 0.20) to that of water (~ 0.93), (2) the clumping of wet snow-crystals into large flakes, followed by collapse of the snowflakes into raindrops and possibly by the breaking up of the larger drops, (3) the increase in fall velocities upon melting, and (4) the growth by accretion of cloud droplets. No detailed explanation will be attempted here as there are still some discrepancies to be resolved.[47] Instead, we merely note that measurements show the reflectivity in rain below the melting level to average some 4 db above that in the snow above it, while the bright-band reflectivity typically exceeds that in the rain by 5 to 8 db.[47,52] Weak bright bands are sometimes observed in dissipating showers after the updrafts have died out, but convective activity does not ordinarily show bright-band effects.[20]

FIG. 8(a) PLAN VIEWS OF BANDED SHOWERS – ILLINOIS, 1058 CST, 8 APRIL 1960
PPI-Scope Photograph, CPS-9 Radar

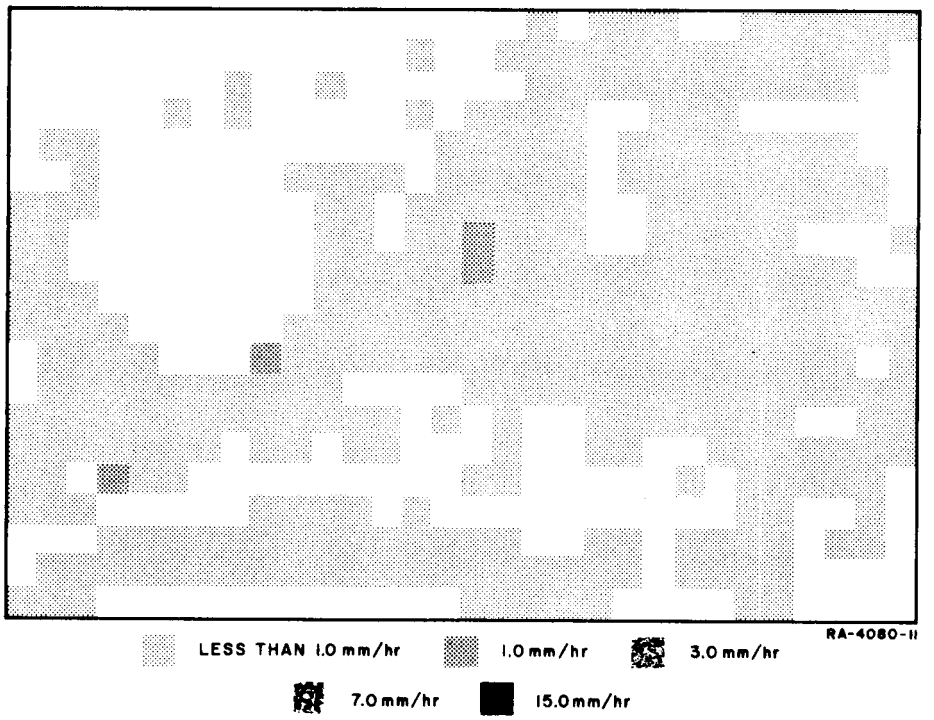

(b) 4 x 4 MILE RESOLUTION

FIG. 8(b) PLAN VIEWS OF BANDED SHOWERS – ILLINOIS, 1058 CST, 8 APRIL 1960
Hypothetical Satellite Radar Display, 4-by-4-Mile Resolution

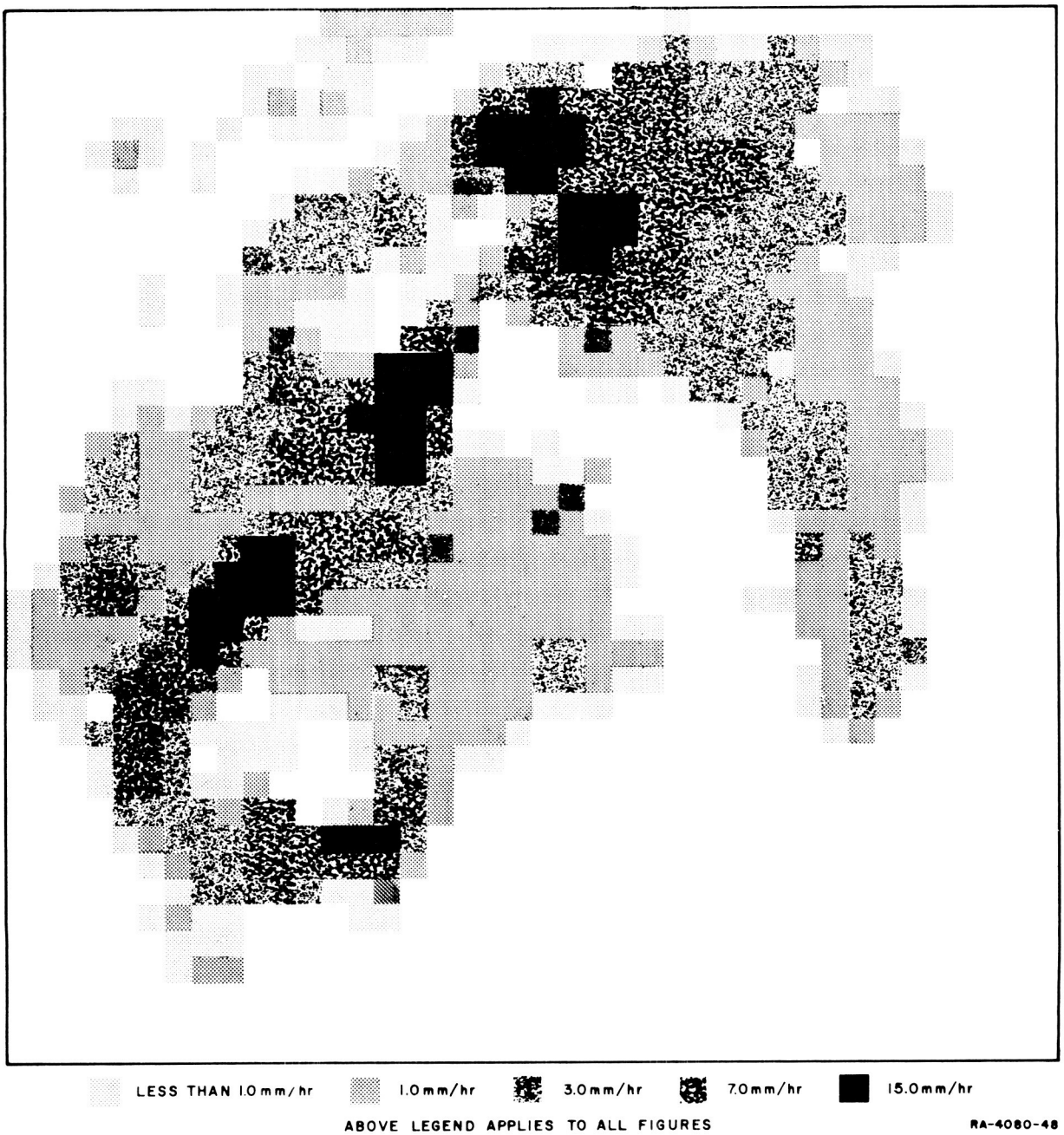

FIG. 9(a) HYPOTHETICAL SATELLITE RADAR DISPLAYS OF HURRICANE DEBRA – TEXAS COAST, 2100 CST, 24 JULY 1959
Display with 4-by-4-Mile Resolution

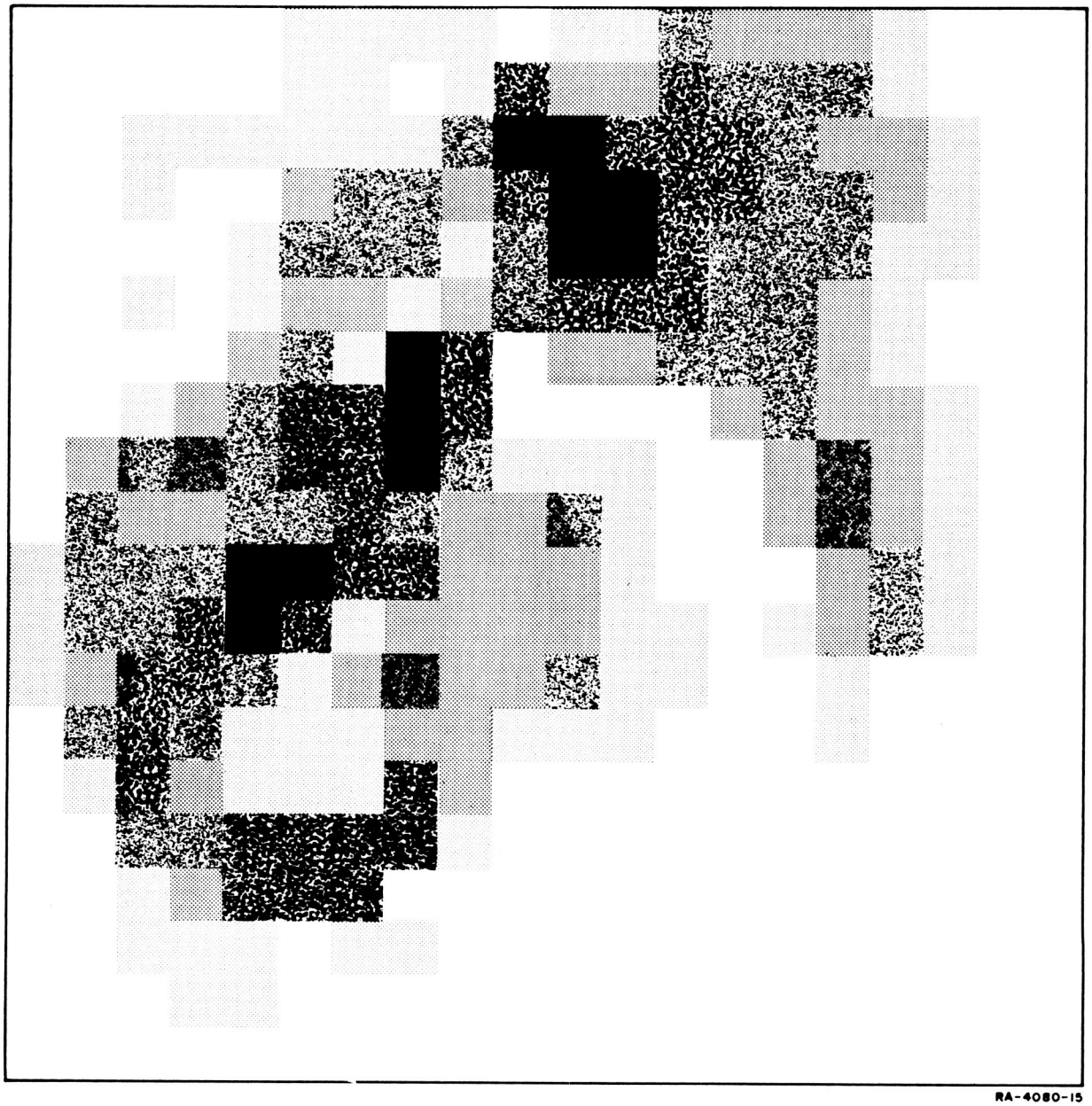

RA-4080-15

(b) 8 x 8 MILE RESOLUTION

FIG. 9(b) HYPOTHETICAL SATELLITE RADAR DISPLAYS OF HURRICANE DEBRA – TEXAS COAST, 2100 CST, 24 JULY 1959
Display with 8-by-8-Mile Resolution

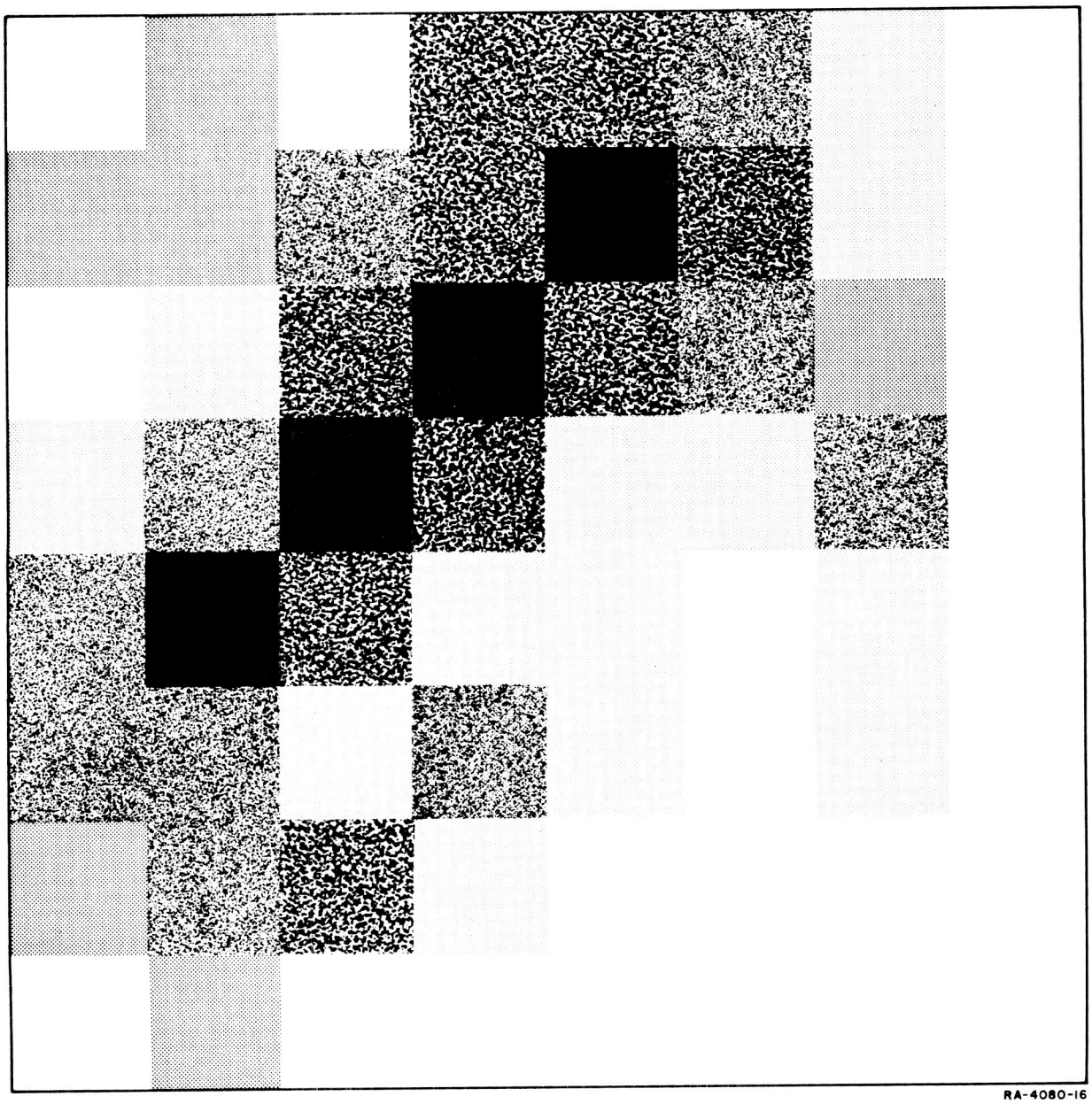

(c) 20 x 20 MILE RESOLUTION

FIG. 9(c) HYPOTHETICAL SATELLITE RADAR DISPLAYS OF HURRICANE DEBRA – TEXAS COAST, 2100 CST, 24 JULY 1959
Display with 20-by-20-Mile Resolution

It is apparent that the bright band, if present, can simplify detection problems considerably. For example, a system capable of detecting rain of 1 mm/hr filling the contributing region could detect melting snow corresponding to surface rainfall rates of 0.3 to 0.5 mm/hr, provided the melting snow also filled the contributing region. As the bright band is only 1,000 to 1,500 feet thick, but occurs in situations with widespread rain, it is apparent that vertical resolution is more important than horizontal resolution in determining whether or not it can be detected.

Wexler and Austin have reported on the vertical distribution of reflectivity in a number of storms in New England, showing quite uniform precipitation over areas of 100 square miles or more.[53] We have used their data to derive the equivalent Z, the sum of the sixth powers of the diameters per unit volume of small raindrops having the same reflectivity. The measured values have been averaged in the vertical over varying resolution elements to determine the response of a satellite radar to bright-band situations. No attempt has been made to allow for the various possible beam shapes; the results presented would apply to a rectangular beam with uniform gain throughout.

The situation at 1245 EST on 7 February 1953--one of rather light rain--is analyzed in Fig. 10. Inspection shows that, for bright band to be a significant factor in helping to detect precipitation, vertical resolution should be 5,000 feet or better. For a satellite radar 600 miles up using a 1-degree beam, this condition is satisfied only for nadir angles less than 3.5 degrees (see Sec. IV).

In cases where sufficient power is available to detect continuous precipitation without relying entirely upon the bright band, vertical resolution of 2 miles would be a reasonable standard. In stratified storms the reflectivity usually tapers effectively to zero some 3 to 5 miles above ground. Moderate or heavy rain showers ordinarily reach well over 2 miles in height, although some notable exceptions have been reported from the tropics where heavy rain sometimes falls from shallow cloud decks.[54]

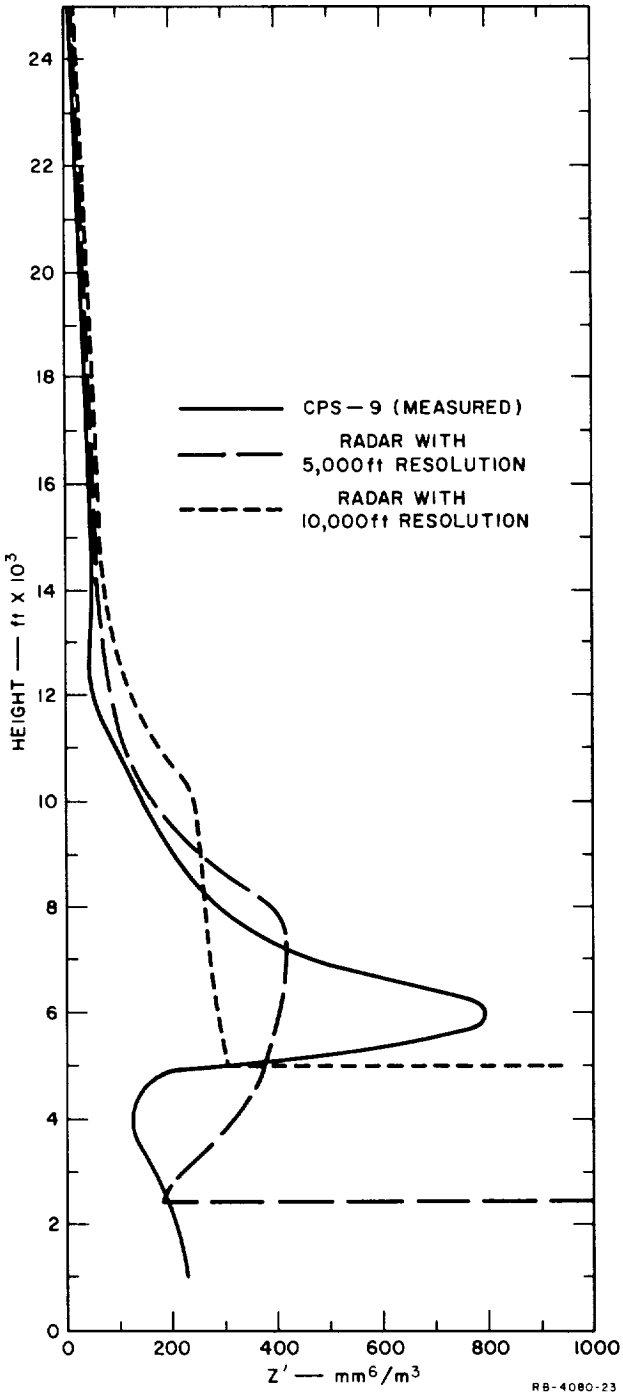

FIG. 10 VERTICAL PROFILE OF REFLECTIVITY IN A BRIGHT-BAND SITUATION – NEW ENGLAND, 1245 EST, 7 FEBRUARY 1953
(As a function of vertical resolution)

It might be thought that horizontal resolution would be unimportant in the detection of widespread rain, but case studies (not reproduced here) show that this is true only for systems with low thresholds--that is, with high sensitivity. With a threshold of 3 mm/hr, the resolution requirements are about the same as in the case of showers, because the system responds mainly to local intensifications of the reflectivity.

As snow above a bright band ordinarily yields a signal some 4 db weaker than that from the rain below, the sensitivity required for its detection is correspondingly greater. Snow reaching the ground unmelted would presumably be more difficult to detect than snow melting to rain at lower altitudes, as snowstorms are characterized by lower temperatures and less available moisture. Extensive radar studies of the 3-dimensional structure of snowstorms have been carried out at McGill University in Montreal, Canada during the past fifteen years. The radar data is now obtained on CAPPI (Constant Altitude Plan Position Indicator) presentations using a stepped grey scale to record signal intensity.[55] A set of calibrated CAPPI pictures taken during a snowstorm on 23 February 1961 was supplied by McGill University for use in the present study. Examination has shown that none of the echoes shown would have been visible to a radar with a 1-mm/hr threshold, regardless of resolution.

C. Statistics of Isolated Showers

The results derived in Sec. III-B on detection of showers were based on reflectivity measurements at a single location in Illinois. To fulfill the objectives of this study, they must be extended to other regions. Unfortunately, most available radar records are photographs of PPI presentations using a single, uncalibrated gain setting. The only dimension of a shower which can be measured from such a record is its horizontal extent. Therefore, some relationship between shower diameter and total radar reflectivity must be established before the photographs can be used in the present study.

It is not unreasonable to anticipate such a relationship. Many isolated showers consist of single convective cells, others of one mature

cell surrounded by small, developing cells and remnants of dissipating ones. There is a definite correlation between the height and diameter of a convective cell, with the two tending to be equal.[20] It is commonly accepted by meteorologists and pilots that tall thunderstorms tend to be severe, with heavy rain and perhaps hail. In recent years, this belief has been confirmed by Donaldson[56] and others, who have shown that vertical extent and peak reflectivity of convective cells are positively correlated. Combining these results indicates that shower diameter and total reflectivity must be correlated to some degree.

A series of detailed reflectivity measurements was made on isolated showers in Texas in May and June of 1961.[57] The reflectivity was measured for vertical slices through the core several times during the life of each cell. The processed data from which Ref. 57 was drawn have been made available for the present study by Texas A. & M.

In examining the data, the present author finds that the reflectivity at any point plotted against the distance to the edge of the shower yields an approximately straight line on a log-log scale. Some distortions arise from the finite size of the gain steps used. The relationship holds not only within individual showers, but for all the showers as a group. The results for a random sample of runs are shown in Fig. 11. A linear regression of log Z upon log $(r_o - r)$ yields

$$Z = 560\ (r_o - r)^{2.5} \qquad (3)$$

where r_o is the shower radius in nautical miles, r is the distance from the center in nautical miles, and Z is the reflectivity in $mm^6 m^{-3}$. The correlation coefficient is 0.87 and the standard error of estimate is near 5 db, smaller than the gain step interval.

The Texas measurements used in this analysis were all taken in warm air with dewpoints near 70°F. Several steps have been taken to see how far the results can be extrapolated. Figure 12 shows a scatter diagram of log Z vs. log $(r_o - r)$ for isolated showers occurring in tropical air in Illinois on 16 and 20 May 1960. The regression line for this case is

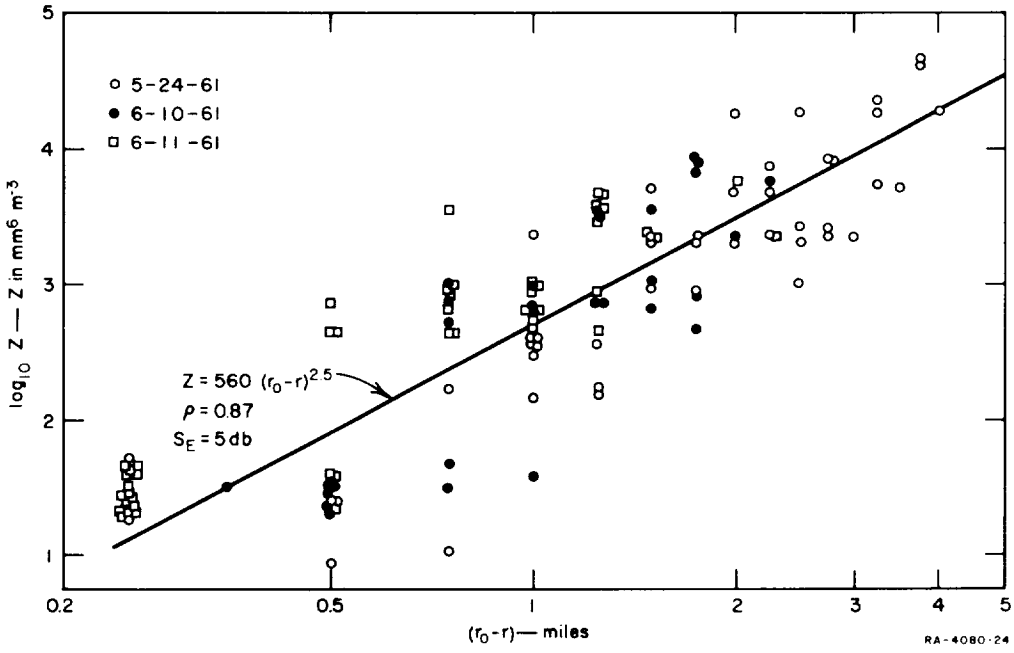

FIG. 11 REFLECTIVITY INSIDE ISOLATED SHOWERS IN TROPICAL AIR AS A FUNCTION OF DISTANCE TO SHOWER EDGE
(Measurements by Texas A. & M.)

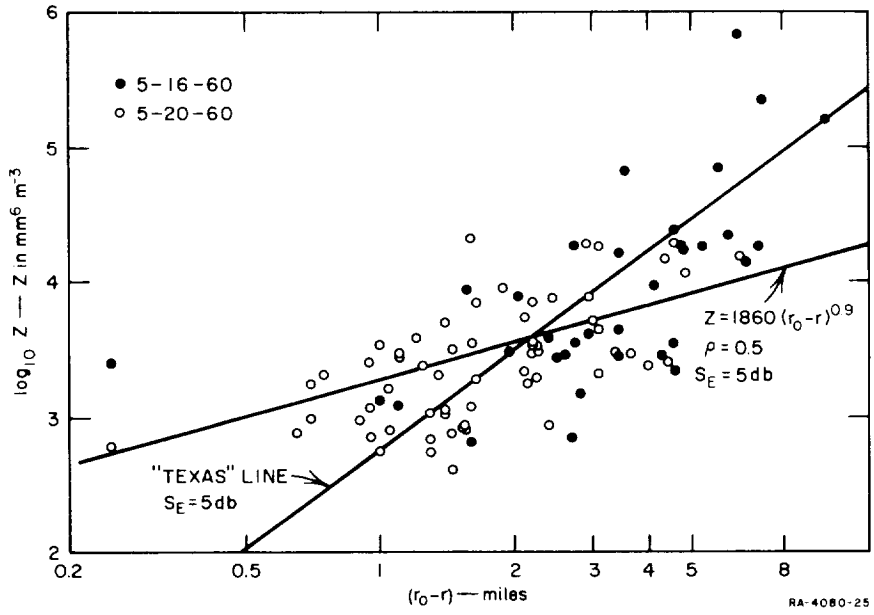

FIG. 12 REFLECTIVITY INSIDE ISOLATED SHOWERS IN TROPICAL AIR AS A FUNCTION OF DISTANCE TO SHOWER EDGE
(Measurements by Illinois State Water Survey)

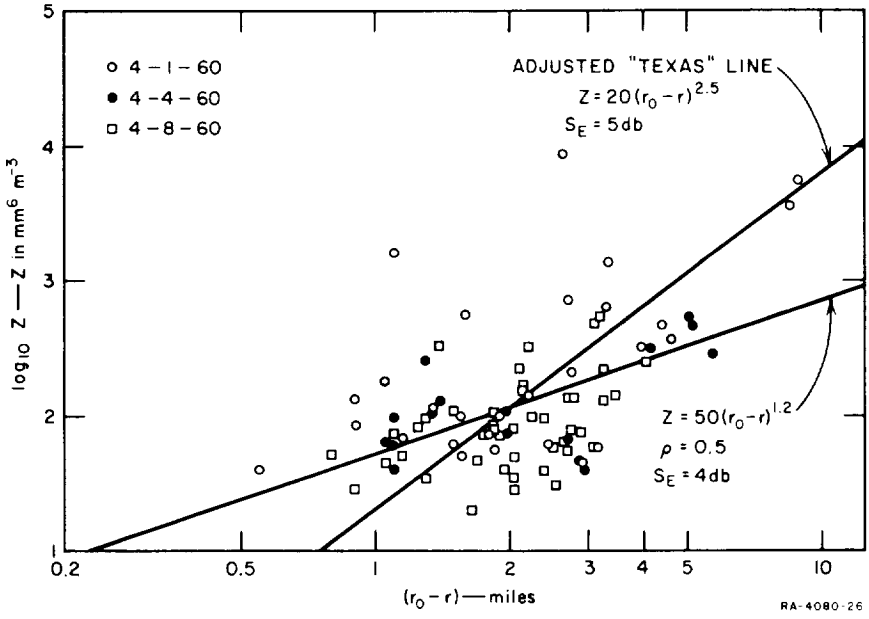

FIG. 13 REFLECTIVITY INSIDE ISOLATED SHOWERS IN POLAR AIR AS A FUNCTION OF DISTANCE TO SHOWER EDGE
(Measurements by Illinois State Water Survey)

$$Z = 1860\,(r_o - r)^{0.9} \quad . \qquad (4)$$

The correlation coefficient here is only 0.5, but the standard error of estimate is again close to 5 db.

The low correlation between log Z and log $(r_o - r)$ for the Illinois sample appears to be due to the large concentration of points near the mean. To check on this point, the regression line of Fig. 11 has been included in Fig. 12. Visual inspection shows that it fits the points as well as Eq. (4); this has been confirmed by computing the standard error about this line. The value found is 5.5 db, not significantly greater than the standard error about Eq. (4).

It is quite remarkable that the Texas curve [Eq. (3)] fits the Illinois data so well, not only in its slope but in passing through the middle of the distribution of points. In the upper right-hand region, which corresponds to observations of high reflectivity deep inside large showers, and hence is of great importance to this study, the Texas curve actually provides a better fit to the Illinois data than does Eq. (4). We conclude, therefore, that Eq. (3) provides a reasonable estimate of the reflectivity inside showers occurring in tropical air masses.

The derivation of a similar formula for the reflectivity within showers in cold air masses is more difficult. Showers in cold air are generally light and do not yield reflectivity values as high as those observed in warm, humid air. Most of them do not extend through more than one or two gain steps on stepped-gain records, and so fail to provide information needed to establish a systematic relationship. A sample of data obtained in Illinois on April 1, April 4, and April 8, 1960, is shown in Fig. 13. These showers formed with surface dew-points in the 30-to-40°F range. The concentration of data on a single gain setting (the first reduction below full gain) is apparent.

The regression line for this case is shown for completeness, but it is of little significance, the correlation coefficient being 0.5. The adjusted Texas line passes through the means of log $(r_o - r)$ and

log Z with a slope of 2.5. It thus differs from Eq. (3) only in the multiplying factor. Using it instead of the regression line raises the standard error for the sample from 4 db to 5 db. However, this is more than offset by the fact that it provides a better fit for the large showers, where much of the total reflectivity is concentrated. Figure 13 serves to emphasize that most showers which occur with surface temperatures near 32°F are only a few decibels above threshold for a CPS-9 at relatively short range, and hence would be completely invisible, even to a radar of comparable performance, at 600 miles.

In the following sections, we shall assume that

$$Z = C(r_o - r)^{2.5} \tag{5}$$

is a valid estimate of the reflectivity inside isolated showers, with C ranging from 500 in humid, tropical air, down to 20 in polar air with dewpoints near 32°F, and to still lower values in very cold polar and Arctic air masses.

Equation (5) emphasizes the concentration of reflectivity near shower centers. Let $\Sigma Z(r)$ be the total reflectivity in a horizontal circular slice of radius r centered on the shower center. Then $\Sigma Z(r_o)$ is the total reflectivity of a horizontal slice through the shower. Assuming circular symmetry and integrating lead to

$$\Sigma Z(r_o) = 0.4\, C\, r_o^{4.5} \tag{6}$$

and

$$\frac{\Sigma Z(r)}{\Sigma Z(r_o)} = \begin{cases} 1-4.5(1-\alpha)^{3.5} + 3.5(1-\alpha)^{4.5}, & r < r_o \\ 1, & r > r_o \end{cases} \tag{7}$$

where

$$\alpha = r/r_o.$$

Equation (7) is shown graphically in Fig. 14; inspection shows that the innermost fourth of the shower (in terms of area) contains about three fourths of its reflectivity. From this it is apparent that a shower which would be invisible to a radar whose resolution element coincided with it exactly could sometimes be rendered detectable by sharpening the resolution.

Figure 15 summarizes the findings of this section. The abscissa, r', is the radius of a circular resolution element coincident with the center of a circular shower. This shape was chosen for ease of calculation; in practice, the abscissa can be rescaled in terms of area of resolution without serious effect, except for very small values of r'. The ordinate for the solid lines if $\Sigma Z(r')$, the total reflectivity present in the beam, expressed on a logarithmic scale for showers of various radii with C set at 500. The ordinate for the dashed lines is the minimum $\Sigma Z(r)$ required for detection of the precipitation in the beam, for radars of various threshold sensitivities. These sensitivities are expressed in terms of R_{min}, the minimum detectable rainfall rate for steady rain filling the beam and following the $200\ R^{1.6}$ relationship of Eq. (2). Using this figure, one can estimate, for any combination of shower size, sensitivity and resolution, how far above or below the system threshold the signal will be. For Polar air with dewpoints near 32°F, the curves showing $\Sigma Z(r')$ would be lowered by roughly 14 db through the change in C.

The relationships between shower sizes and reflectivities just derived can be utilized in case studies of instantaneous shower patterns, but they become a more powerful tool when combined with statistics on shower-size distributions.

In the past, there has been a tendency for workers in the weather radar field to concentrate on large or unusual convective cells, rather than entire populations of cells. However, some useful histograms of cell diameters, depths and spacings in New England have been presented by Newell.[58] These indicate that the number of cells in a given diameter interval increases with <u>decreasing</u> size down to the resolution limits of the radar used.

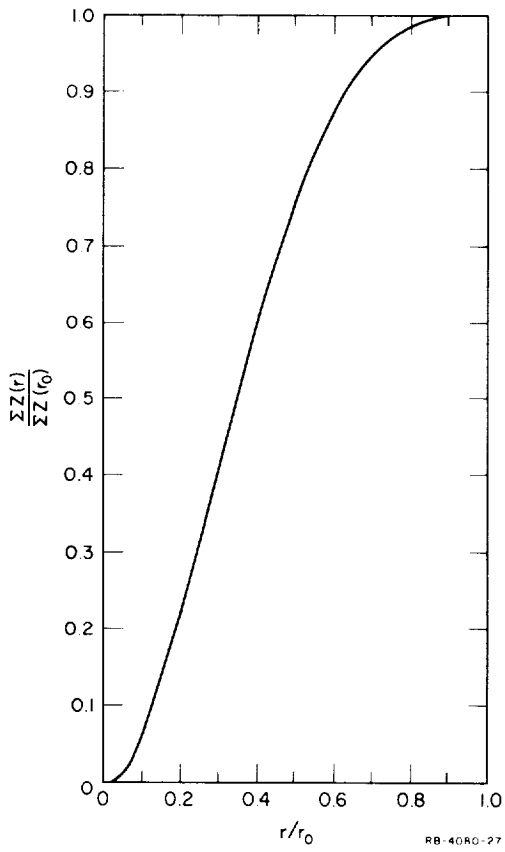

FIG. 14 FRACTION OF TOTAL REFLECTIVITY OF CIRCULAR SHOWER OF RADIUS r_0 CONTAINED IN CIRCLE OF RADIUS r (Centers Coincident)

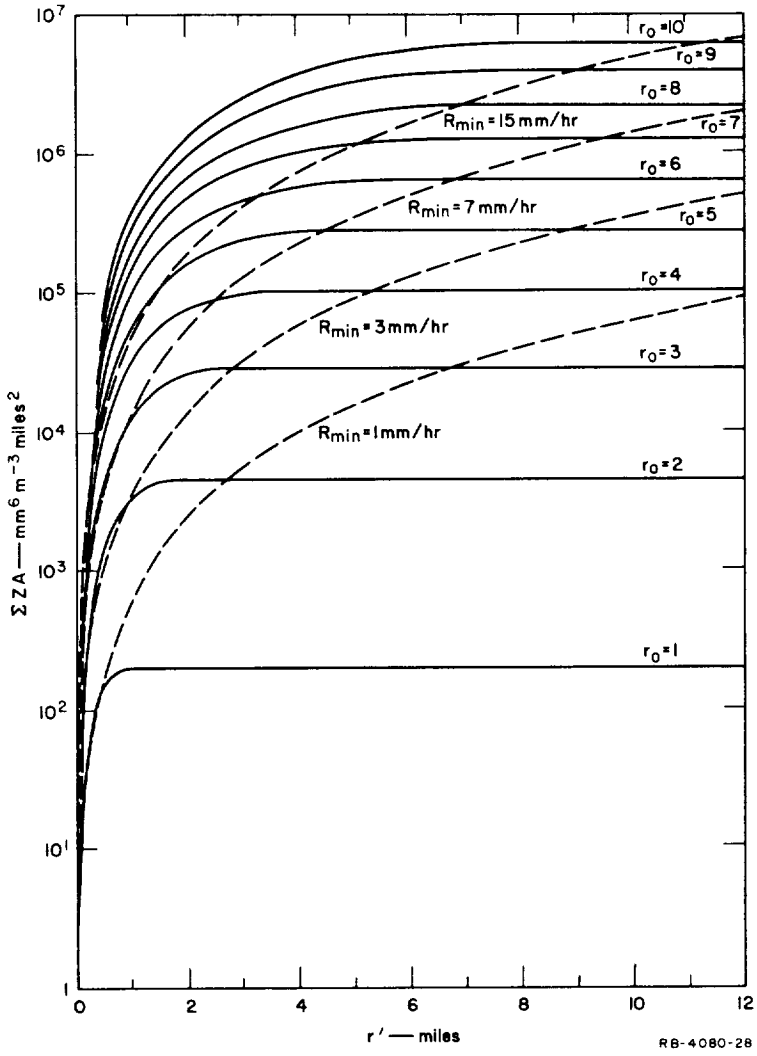

NOTE: Solid lines: Total reflectivity in circular resolution element of radius r′ centered upon shower of radius r_0, as a function of r′ and r_0.

Dashed lines: Total reflectivity required for detection of precipitation in circular resolution element of radius r′ as a function of r′ and R_{min}, the threshold rainfall rate for full beam.

FIG. 15 DIAGRAM FOR DETERMINING DETECTABILITY OF SHOWERS IN TROPICAL AIR AS A FUNCTION OF RADIUS, RADAR RESOLUTION, AND RADAR SENSITIVITY

As oceanic showers are of particular interest in the present study, PPI records from the West Coast radar picket ships and from Eniwetok have been used in establishing size distributions for isolated showers. To minimize variations due to beamwidth and possible loss of shallow showers at long ranges, only showers within 75 miles of the radars were included in the samples. Elliptical showers were arbitrarily assigned a radius found by averaging their major and minor axes.

A first inspection of the data indicated that the number of showers in a given size interval decreased exponentially with increased radius. Accordingly, scatter diagrams have been prepared for the various samples on semi-log paper and fitted with regression lines of the form

$$\log_{10} N = \log_{10} N_o - \beta' r_o^{\gamma} \qquad (8)$$

where N is the number of showers with radii between r_o and $r_o + dr_o$, $\log N_o$ is the intercept of the regression line upon the log N axis, γ is an arbitrary constant, and $(-\beta')$ is the slope of the regression line.

Figure 16 shows the results for a sample of 2429 showers observed on the Eniwetok radar from 4 April to 12 April 1960. The sample was obtained by counting at hourly intervals all the showers present between 25 and 75 miles. In computing the regression lines, the smallest shower size (r_o = 0.5 miles) has been omitted, since it is uncertain what the combined effects of beamwidth and threshold sensitivity would be for the very smallest showers. The very close fit to a straight line for the lower values of γ is obvious; the correlation coefficients, neglecting the small-sample-size correction, range from essentially 1 for γ = 1 to 0.98 for γ = 2. For the picket ships, where the computations were made with γ ranging from 0.5 to 2, the best correlations occur with γ in the range from 1 to 1.2. However, in no case is a significant improvement possible by choosing a value of γ other than 1. Therefore, discussion will be limited to the case with γ = 1--i.e., we shall assume that

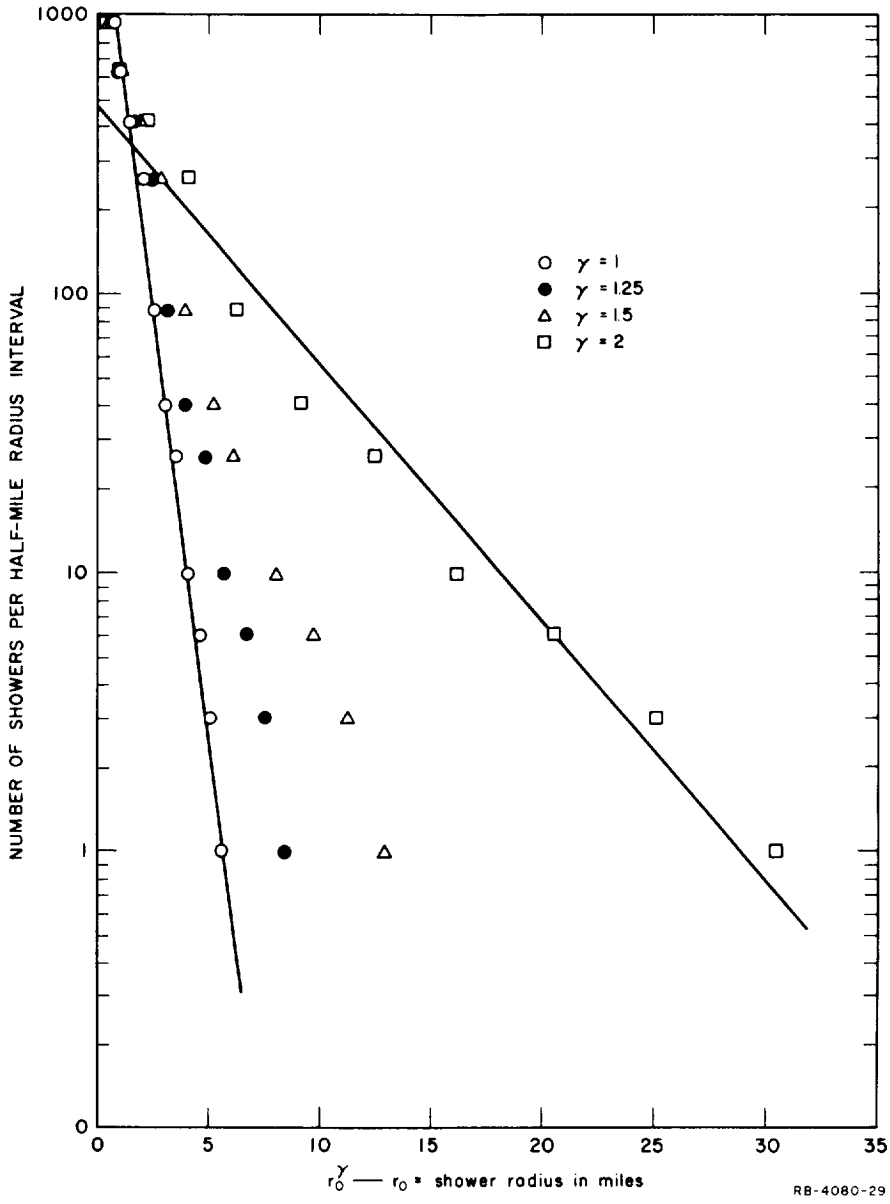

FIG. 16 OBSERVED SHOWER-SIZE DISTRIBUTION – ENIWETOK, APRIL 5 – 12, 1960

$$N = N_o \exp(-\beta r_o) \quad . \tag{9}$$

In the Eniwetok sample,

$$N = 5900 \exp(-1.45 r_o) \tag{10}$$

where N is expressed in miles^{-1}.
Upon integration over-all values of r_o, this yields for the total number of showers, 4,100--more than the original sample contained. It is possible that the exponential distribution breaks down for very small showers. However, Blackmer and Serebreny have found that cumulus clouds follow a similar law, and it is appealing to consider the shower-size distribution as the tail of the cumulus size distribution.[59]

There are two possible alternative explanations for the discrepancy. Some very small showers must pass undetected by any radar. Moreover, once a shower grows to detectable size, its apparent extent is increased along the beam by the pulse length (in space) and across the beam by twice the beam width. If we consider the loss of resolution as the sole explanation, and assume all showers were detected, agreement between the exponential frequency distribution and the total shower count is reached by considering that the radius of each observed shower was stretched about 0.35 miles by these factors. This is reasonable for the radar used (CPS-9) at the ranges in question.

The locations of the West Coast picket ship stations are shown in Fig. 2. It is seen that they cover a range of 22 degrees in latitude. Records were available from the ships' S-band radars over a period of a year, though with some gaps. One date to be examined in each month was chosen for each synoptic map time on a random basis, for each of the stations. Care was taken to avoid confusion between sea clutter and precipitation echoes. The areas covered by continuous precipitation were measured, and the showers tabulated by size.

In Fig. 17, the yearly size distributions for the five stations are shown on a log N vs. r_o plot. The regression lines are again fitted without regard to the smallest size interval, and the correlation coefficients are again near 0.99. This appears to justify the use of β as a parameter for comparing shower distributions in different areas. Adjusting the shower radii in these cases to fit the sample sizes indicates that apparent shower diameters were stretched by just over a mile. It is reasonable that this effect be larger for the picket ship radars than for a CPS-9, as their beams are somewhat broader, while the lower sensitivity resulting from use of S-band rather than X-band could play a part too by eliminating some of the smallest showers. In any event, these factors do not affect the determination of β.

The values found for β at Stations 1, 3, 5, 7, and 9 were 1.0, 0.8, 1.3, 1.4, and 1.4, respectively. The low value at Station 3 was due to a few large showers occurring during one period when a cold low was in that area. A larger sample was prepared to check on that station, which yielded a value near 1.1. Apparently the value 0.8 for the original sample represents a sampling error rather than some climatological peculiarity for that station. The general increase in β from south to north does appear valid, especially as the southern stations agree with the Eniwetok result.

Showers occurring over land during the spring were examined to see if they followed a similar law, using records from Champaign, Illinois, and Brize-Norton, England. The distributions fitted the semi-log form closely, with β being computed at 1.1 for the Illinois sample, and at 0.8 for the British sample.

For any shower distribution described by Eq. (9), the fraction of the total area of the showers contained in showers in any size interval is determined uniquely by the function β. Figure 18 shows $F(r_o)$, the fraction of the total area contained in all showers with radii greater than r_o, as a function of r_o and β.

A combination of the data contained in Figs. 15 and 18 provides a good estimate of the fraction of the area contained in a shower array

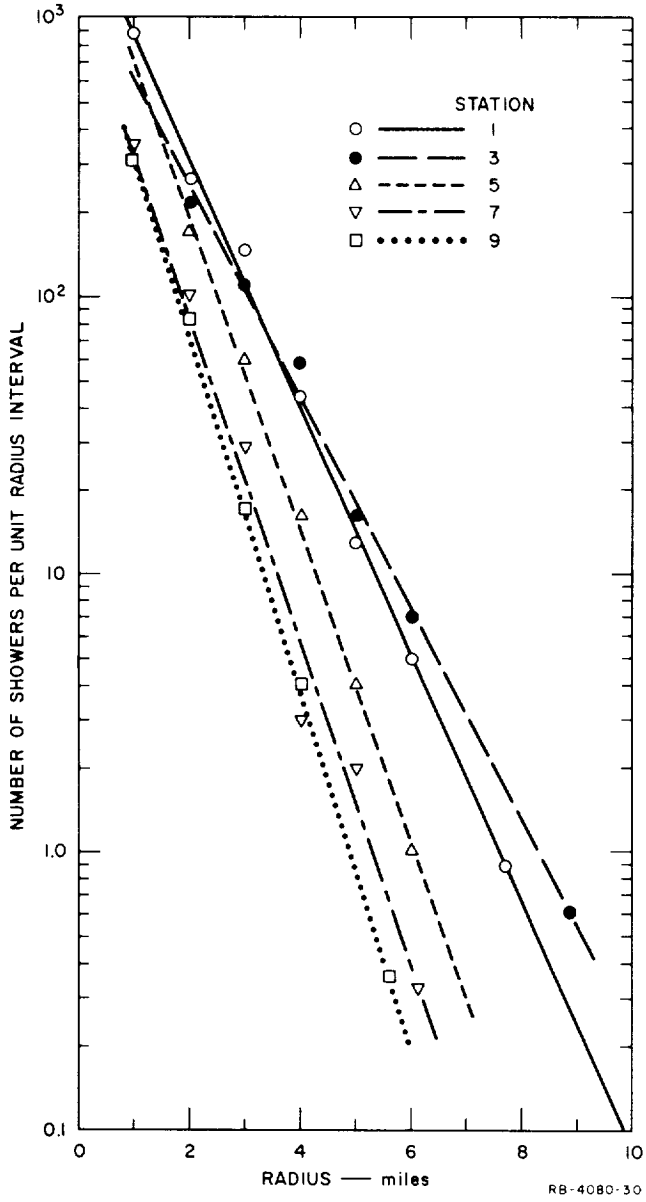

FIG. 17 OBSERVED SHOWER-SIZE DISTRIBUTION AT PICKET SHIPS (Annual Basis)

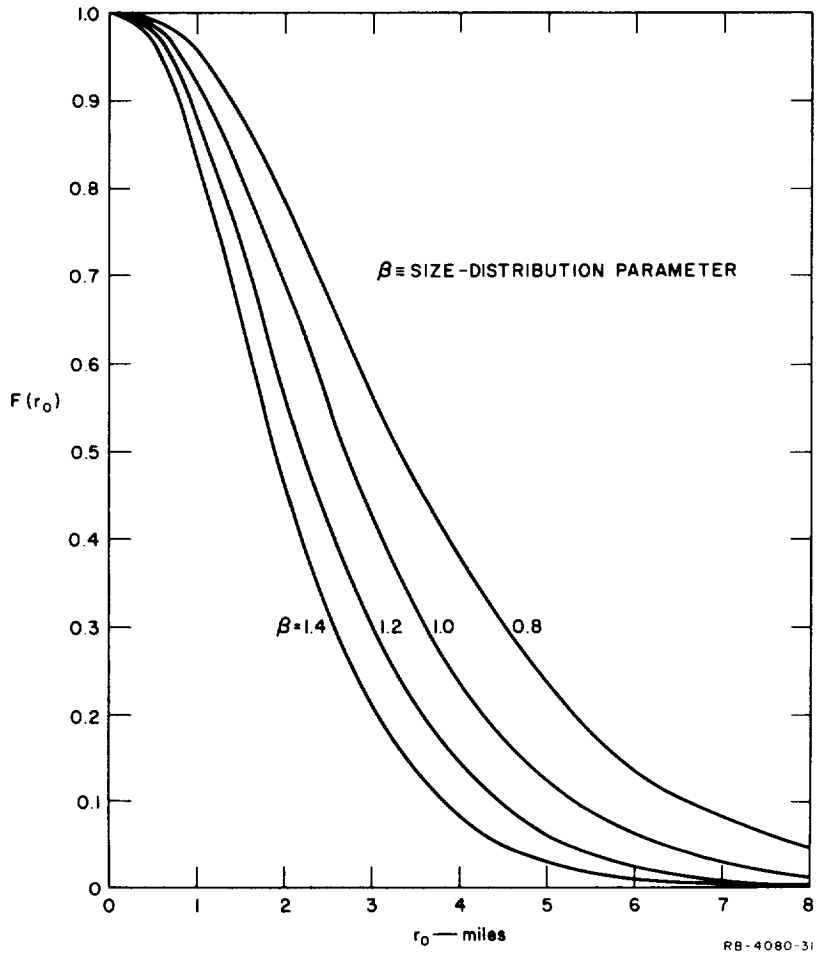

FIG. 18 $F(r_0)$, FRACTION OF AREA OF SHOWER ARRAY CONTAINED IN SHOWERS WITH RADII EXCEEDING r_0, AS A FUNCTION OF r_0

which would be visible to any proposed meteorological satellite radar. Results for radars with R_{min} of 1 mm/hr and 3 mm/hr are shown in Figs. 19 and 20, respectively. Here F is the fraction of the area of the shower array contained in showers big enough to be detected.

The "polar air" showers referred to in Figs. 19 and 20 are those occurring with dewpoints near 32°F. Snow showers in very cold polar and Arctic air masses would be invisible to any satellite radar suggested to date, including those described in Refs. 13 and 14.

D. Rainfall-Rate Distributions

Figures 19 and 20 show clearly that the success of a satellite radar in detecting isolated showers would depend upon its horizontal resolution as well as upon its sensitivity. Theoretically, its success in detecting large, uniform precipitation areas would be independent of resolution, and the fraction of such precipitation detected could be determined by comparing the instantaneous rainfall rate distribution with the threshold sensitivity. Large areas of truly uniform precipitation occur only rarely, but, in many cases, variations in rainfall rate within individual resolution elements are small enough to permit the application of rainfall rate distributions. This is particularly true for systems with low thresholds of detectability. One can make partial allowance for such variations as do occur by using distributions based upon averages over short intervals of time, rather than instantaneous values, but complete compensation is impossible because radar reflectivity is not a linear function of rainfall rate.

Heavy rain ordinarily occurs in bursts of several minutes duration associated with the passage of individual convective cells. Hourly distributions underestimate rainfall durations at high rates, because the bursts are smoothed out by the averaging process. On the other hand, hourly distributions overestimate the duration at low rates because some periods of no precipitation are included. These effects are illustrated in Fig. 21, which shows the annual rainfall rate distribution at Washington, D.C., as computed by Bussey for four different

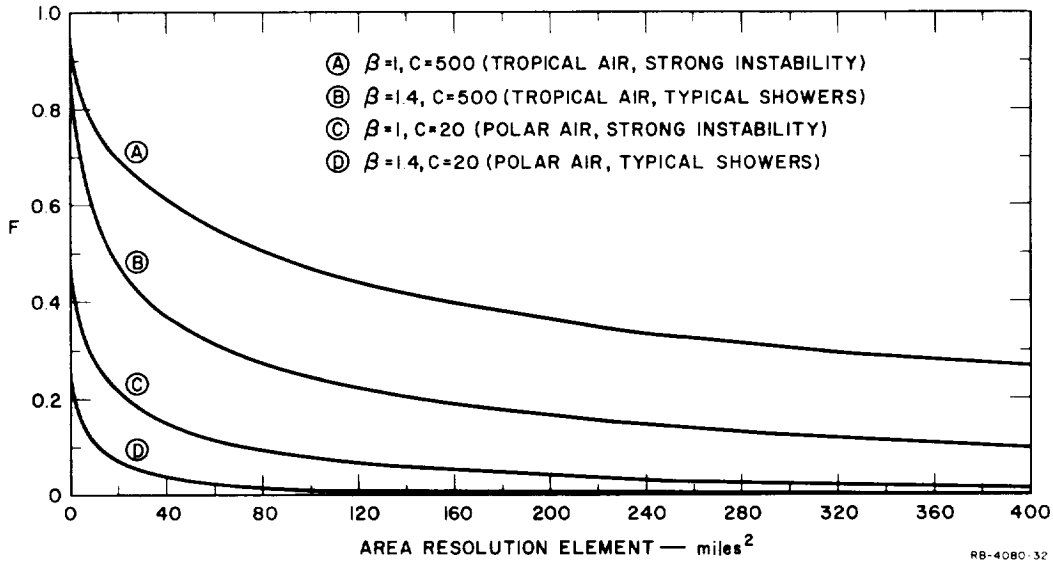

FIG. 19 F, FRACTION OF SHOWER AREA CONTAINED IN SHOWERS DETECTABLE BY RADAR WITH 1-mm/hr THRESHOLD IN CONTINUOUS RAIN, AS A FUNCTION OF RESOLUTION ELEMENT

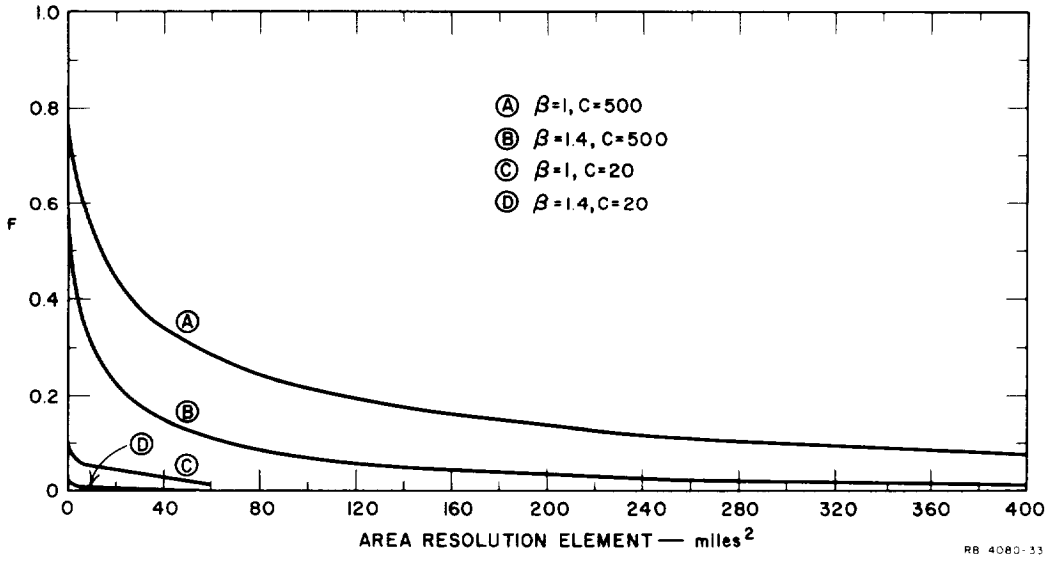

FIG. 20 F, FRACTION OF SHOWER AREA CONTAINED IN SHOWERS DETECTABLE BY RADAR WITH 3-mm/hr THRESHOLD IN CONTINUOUS RAIN, AS A FUNCTION OF RESOLUTION ELEMENT

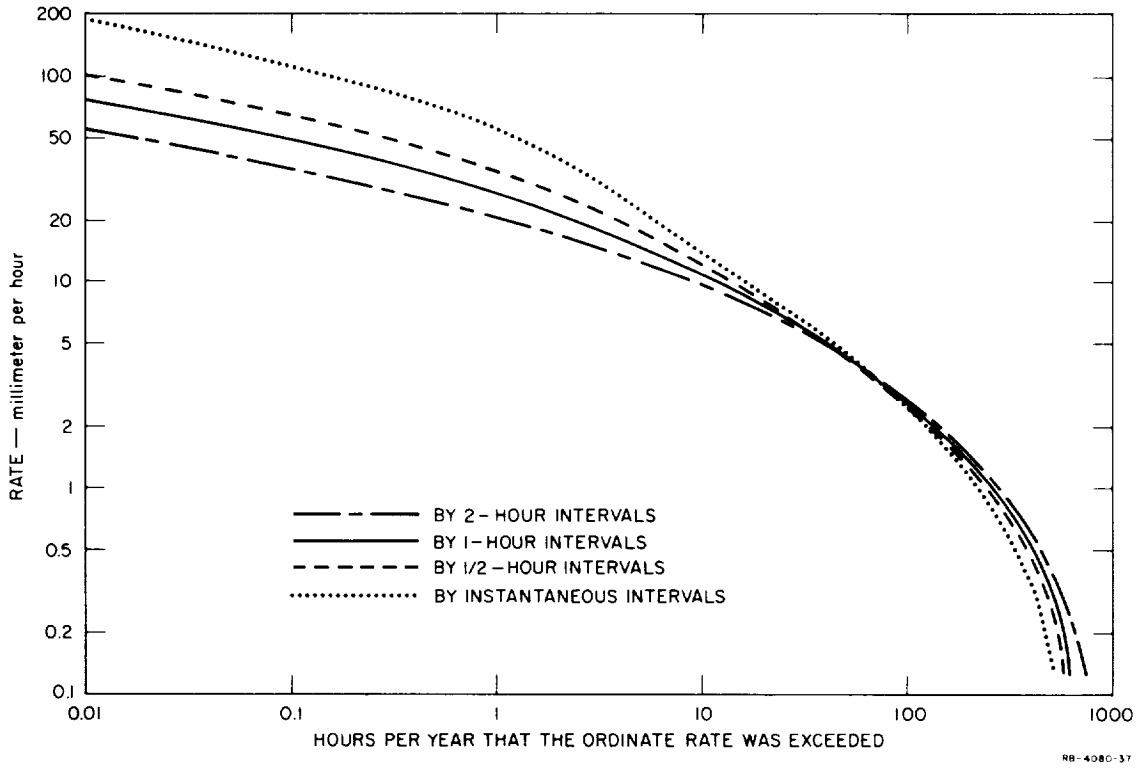

FIG. 21 ANNUAL RAINFALL-RATE DISTRIBUTIONS FOR WASHINGTON, D.C.
(After Bussey)

measurement intervals.[60] The cross-over near 3 mm/hr is of particular interest; it indicates that in this region the distribution is almost independent of measurement interval.

The most appropriate measurement interval for our purpose depends upon the resolution of the radar system being evaluated. As the spatial averaging occurs in two dimensions, the proper interval is somewhat longer than the width of the resolution element divided by the speed of translation of the precipitation pattern. The hourly distributions appear suitable for resolution elements 10 by 10 miles or larger; while for systems with 4-by-4-mile resolution, averages over 10 or 15 minutes should be used. Fortunately for our purposes, the cross-over in the Bussey curves near 3 mm/hr renders the question largely academic for systems with a 3-mm/hr threshold.* At the 1-mm/hr threshold, the difference between the curves is still small; using hourly data rather than 15-minute data for a system with 4-by-4-mile resolution leads to overestimates of duration amounting to only a few percent. As this is smaller than the uncertainties arising from the fact that the distribution curves are a function of location and season, we shall limit discussion to the hourly curves.

The available rainfall rate distributions to not distinguish between isolated showers and continuous precipitation. Before proceeding to use them to describe continuous precipitation alone, it is necessary to consider whether the removal of isolated showers changes the distributions significantly.

As noted above, heavy rain is generally associated with convective activity. However, the isolated shower category does not include all convective cells and, in fact, the most intense convective storms usually occur in complexes embedded in rather extensive precipitation areas. This point is illustrated by a comparison of Figs. 6 and 7 and has been noted by previous authors.[20,61]

---

*The position of the cross-over may vary somewhat with location, but it must occur in all diagrams of the form of Fig. 21.

The rainfall rate distributions produced by shower arrays conforming to the findings of Sec. III- C and typical Z-R relationships for showers (Ref. 46) have been calculated. In the derivation, instantaneous distributions in space are assumed to be statistically equivalent to time distributions at a point, following the procedure of Hamilton and Marshall.[62] The distributions obtained match observed rate distributions quite closely, indicating that no significant change in the distribution is caused by eliminating isolated showers.

A further complication that must be considered is the inclusion of snowfall (water equivalent) in the rainfall-rate distribution curves. Data from Japan and eastern Canada indicate that the reflectivity of snow aggregates per unit volume is given by[47]

$$Z = 2000\ R^{2.0} \quad . \qquad (11)$$

Making allowance for the lower dielectric constant of ice (0.20) as compared to that of water (0.93), one finds that the threshold rates in snow corresponding to 1 mm/hr and 3 mm/hr in rain are 0.7 mm/hr and 1.7 mm/hr, respectively. The reflectivity of fine snow, often observed under very cold conditions, would be smaller than indicated by Eq. (11), but significant snow aggregation occurs at temperatures as low as -15C.[63]

The effect of including snow in rainfall rate distributions is felt mainly at low rainfall rates. Snowfall-rate measurements made at Montreal in recent years show that snow rarely occurs at rates above 3 mm/hr (water equivalent).[64] The 1.7-mm/hr rate, which corresponds to the 3-mm/hr threshold in continuous rain, was exceeded about 8% of the time over a 2-year period. The 0.7-mm/hr rate, which corresponds to the 1-mm/hr threshold in continuous rain, was exceeded about 30% of the time.

The form of rainfall-rate distribution curves (including all forms of precipitation) has received attention from a number of authors. Cole and Sissenwine have obtained regression equations relating the percentage of the time certain hourly thresholds are exceeded at any station, to

the annual precipitation divided by the number of days per year with measurable precipitation.[65] Russak and Easley have extended their work to give the complete distributions in terms of these two parameters.[66] They note that the method would probably fail at stations with unusual orographic effects and in arid regions. It should be most reliable in the temperate zones, which are of greatest concern here (most activity in the tropics is showery).

The importance of location in determining the shape of the rainfall rate distribution curve, as opposed to mere changes in the number of rainy days, is illustrated in Fig. 22. It shows observed hourly distributions on a normalized basis for a station subject to heavy convective storms (Washington, D.C.), for a coastal station subject to cyclonic storms (San Francisco), and for an inland station in a dry region (Spokane). Only 25 to 40% of the area covered by continuous measurable precipitation is included at rates above the 1-mm/hr threshold, while a change of the minimum detectable rainfall rate from 1 mm/hr to 3 mm/hr would further reduce the areal extent of detectable precipitation echoes in certain climatic regimes by as much as 90%.

E. Analysis of Climatological Data

Sections III-B, C, and D, above, have provided answers to the question, "What fraction of the precipitation occurring in the beam of a meteorological satellite radar can be detected?" The answers obtained apply to a variety of precipitation forms and a variety of radar systems characterized by different resolution-sensitivity combinations. We now turn to a slightly different question--namely, "During what fraction of the time will the satellite radar actually see anything?" The data required to answer this question precisely are not available, and if they were, a complete analysis of them would be beyond the scope of the present project. However, a reasonable estimate can be made for some parts of the Earth's surface.

Since one obvious function of a satellite radar is the detection of precipitation over the oceans, the North Atlantic and North Pacific Oceans have been studied as sample areas.

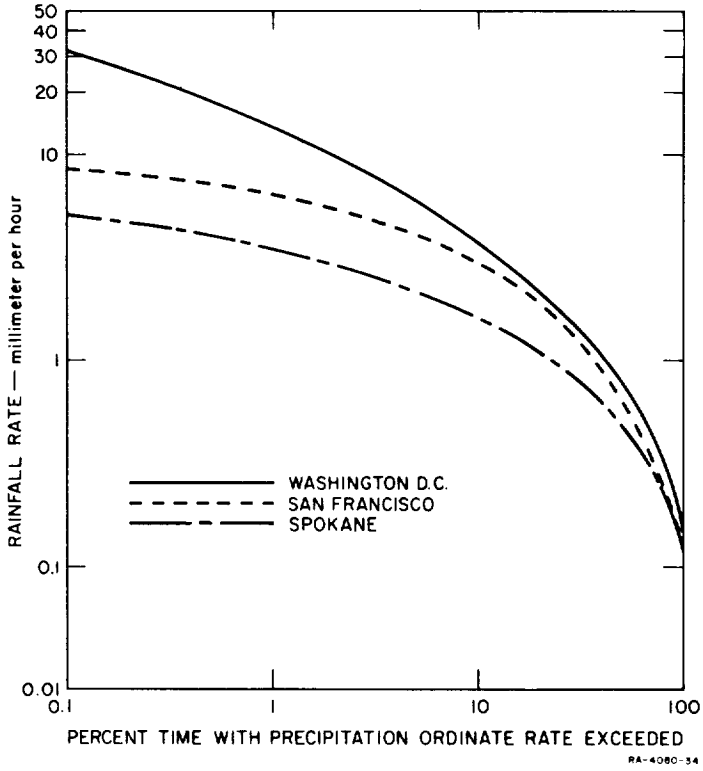

FIG. 22 NORMALIZED DISTRIBUTION OF HOURLY RAINFALL TOTALS

The basic data have been drawn from Volumes I and II of the U.S. Navy Marine Climatic Atlas of the World.[67,68] It includes maps showing the percentages of weather observations with precipitation, by months. Although it is not mentioned in the atlas, comparison of the maps with 5-year samples from a number of islands and weather ships, based on synoptic report summaries, shows that the percentages given in the atlas include observations of precipitation within sight and precipitation during the preceding hour.

The observations of precipitation given by the atlas can thus be considered as falling into four categories: (1) precipitation within sight or within the past hour, (2) drizzle, (3) widespread rain and/or snow, and (4) showers. The data provided in Refs. 67 and 68 were broken down into these categories according to the distribution of the precipitation reports in the 5-year samples, grouped in areas extending 5 degrees in latitude and longitude. The first category obviously makes no contribution to the fraction of the time echoes could be detected at a particular point. The second--drizzle--seldom produces measurable precipitation, and its detection by a satellite radar is out of the question. The remaining two categories can be broken down into detectable and non-detectable cases by use of Secs. III-C and D, if it is assumed that ship reports of showers correspond to isolated radar echoes and that reports of intermittent and continuous rain or snow correspond to quasi-continuous echoes.

Rainfall amounts are not reported from ships. Reports from islands are suspect, as islands tend to set off convective activity. Presumably the rates correspond most closely to coastal stations with prevailing onshore winds. From an examination of the distributions at a number of coastal stations, we have estimated the fractions of the continuous precipitation exceeding the 1-mm/hr and 3-mm/hr thresholds at low latitudes to be 40% and 12%, respectively. The corresponding fractions at 50°N are estimated at 30% and 6%. The percentages for 50°N correspond roughly to the values quoted above for the probability of snow yielding reflectivities corresponding to 1-mm/hr and 3-mm/hr rain. In view of this, and the large uncertainties involved throughout the procedure, no attempt was made to distinguish between reports of rain and snow.

The results for showers and continuous precipitation combined appear in Figs. 23 through 30. In all cases, a satellite radar with 4-by-4-mile horizontal resolution and a beam filled in the vertical is assumed. The figures appear low at first sight, but they agree with the picket ship data referred to in Sec. II-B, which is shown in Table II.

TABLE II

BREAKDOWN OF PRECIPITATION OBSERVED ON PICKET SHIP RADARS

(Area examined per ship: 188,500 mi^2 per season)

	Percent Coverage				
	Station	Location	Continuous Precipitation	Showers	Total
Winter	1	49N,131W	8.7	1.4	10.1
	3	45N,130W	6.2	1.7	7.9
	5	40N,130W	2.9	0.9	3.8
	7	36N,128W	2.8	0.9	3.7
	9	32N,124W	-	0.7	0.7
Summer	1	49N,131W	2.9	0.8	3.7
	3	45N,130W	0.1	0.5	0.6
	5	40N,130W	0.1	0.5	0.6
	7	36N,128W	-	0.1	0.1
	9	32N,124W	-	0.1	0.1

Comparison of these figures with the appropriate maps indicates that a satellite radar with a threshold of 1 mm/hr would detect roughly half the precipitation detected by the ship radars. Variations in the ratio occur from station to station, and between winter and summer.

An analysis of the picket ship data on a diurnal basis indicated a tendency for showers to be most numerous around 2200 local time, but it is impossible to lay down any quantitative rules for the North Pacific Ocean on the basis of such a limited sample. In any event, isolated showers make a relatively small contribution to the final results of Figs. 23 through 30 for areas north of 30°N.

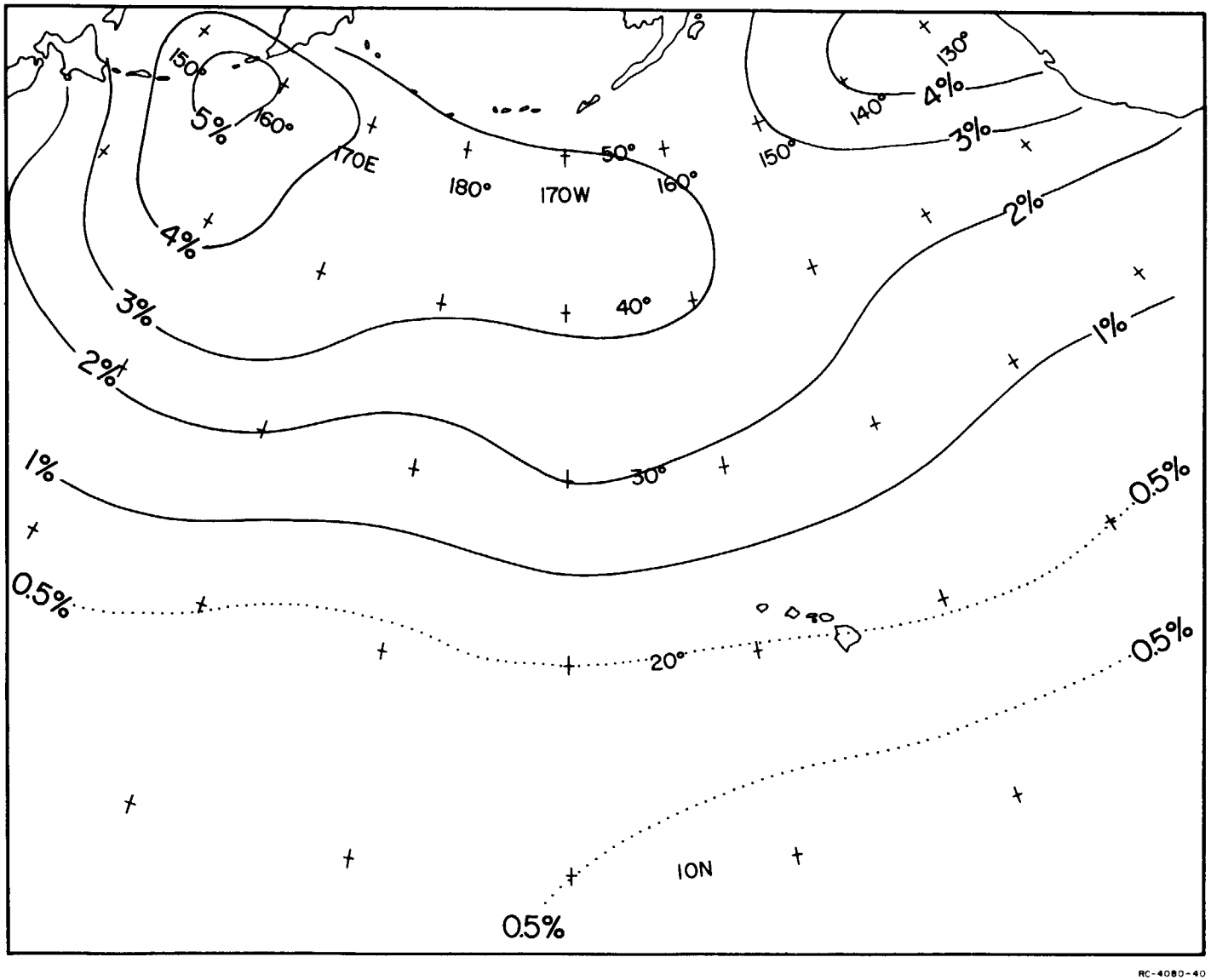

FIG. 23 ESTIMATED PROBABILITY OF OCCURRENCE OF PRECIPITATION DETECTABLE BY SATELLITE RADAR WITH 4-BY-4-MILE RESOLUTION – NORTH PACIFIC, JANUARY, 1-mm/hr THRESHOLD
(Beam filled in vertical)

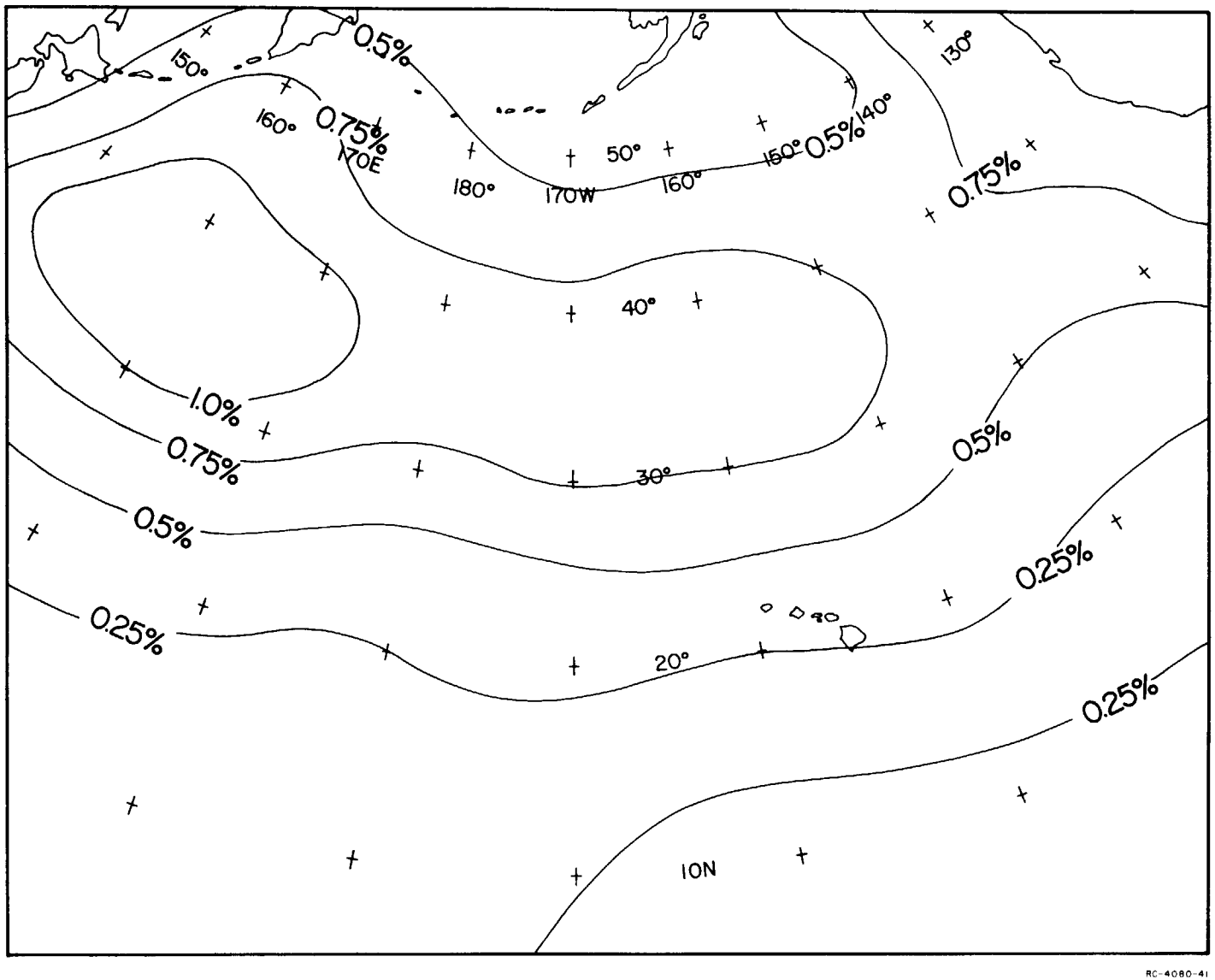

FIG. 24 ESTIMATED PROBABILITY OF OCCURRENCE OF PRECIPITATION DETECTABLE BY SATELLITE RADAR WITH 4-BY-4-MILE RESOLUTION – NORTH PACIFIC, JANUARY, 3-mm hr THRESHOLD
(Beam filled in vertical)

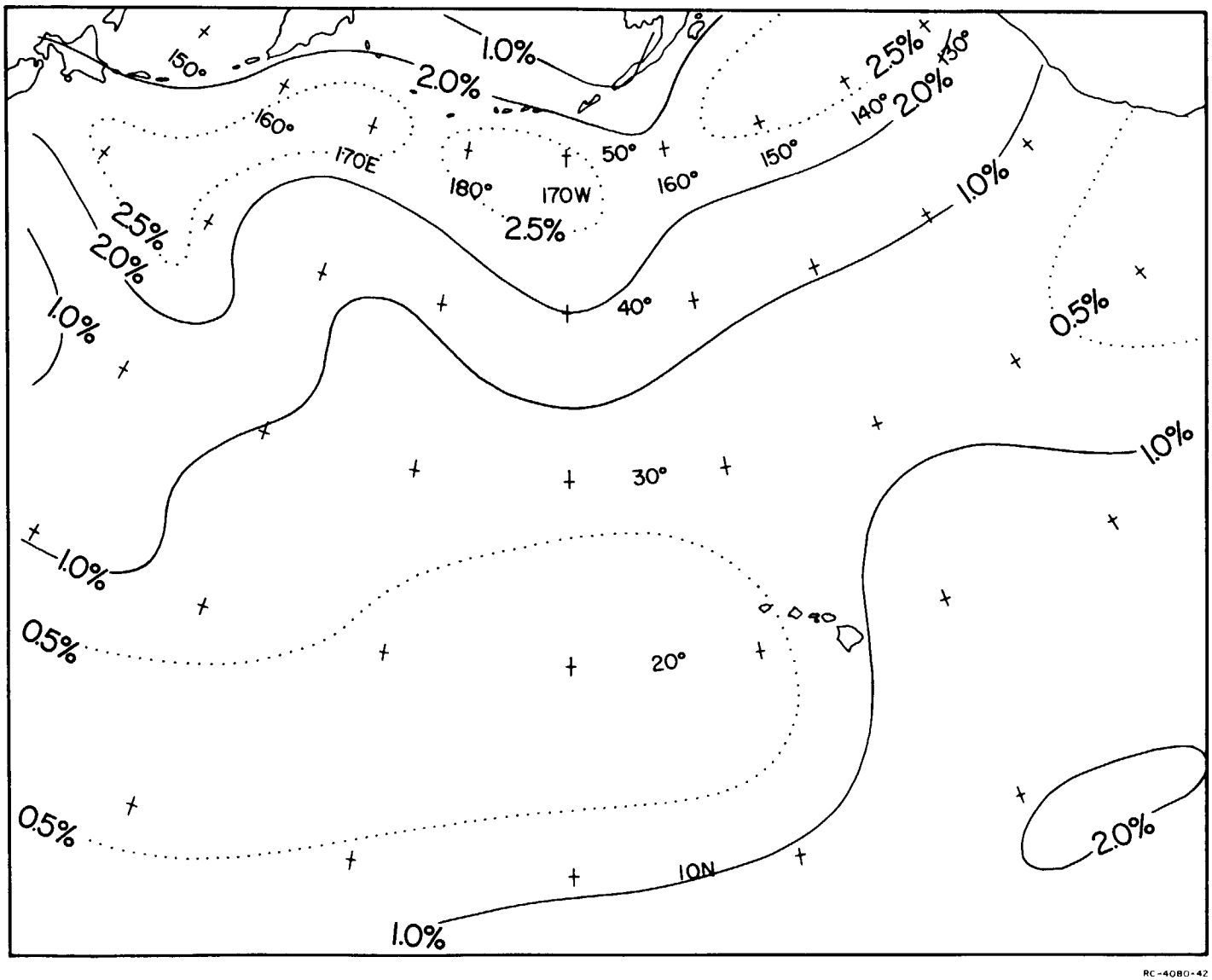

FIG. 25 ESTIMATED PROBABILITY OF OCCURRENCE OF PRECIPITATION DETECTABLE BY SATELLITE RADAR WITH 4-BY-4-MILE RESOLUTION – NORTH PACIFIC, JULY, 1-mm/hr THRESHOLD
(Beam filled in vertical)

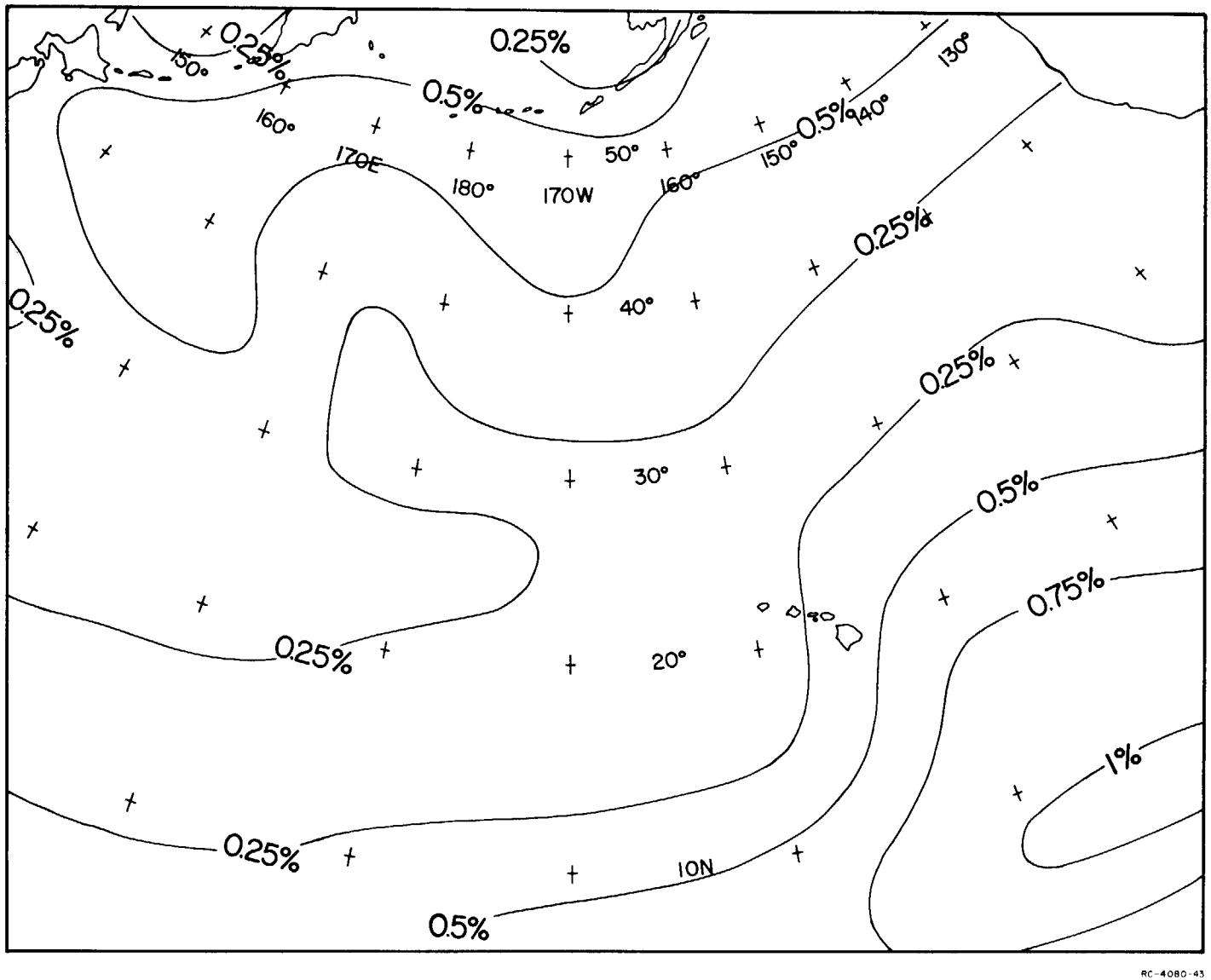

FIG. 26 ESTIMATED PROBABILITY OF OCCURRENCE OF PRECIPITATION DETECTABLE BY SATELLITE RADAR WITH 4-BY-4-MILE RESOLUTION – NORTH PACIFIC, JULY, 3-mm hr THRESHOLD
(Beam filled in vertical)

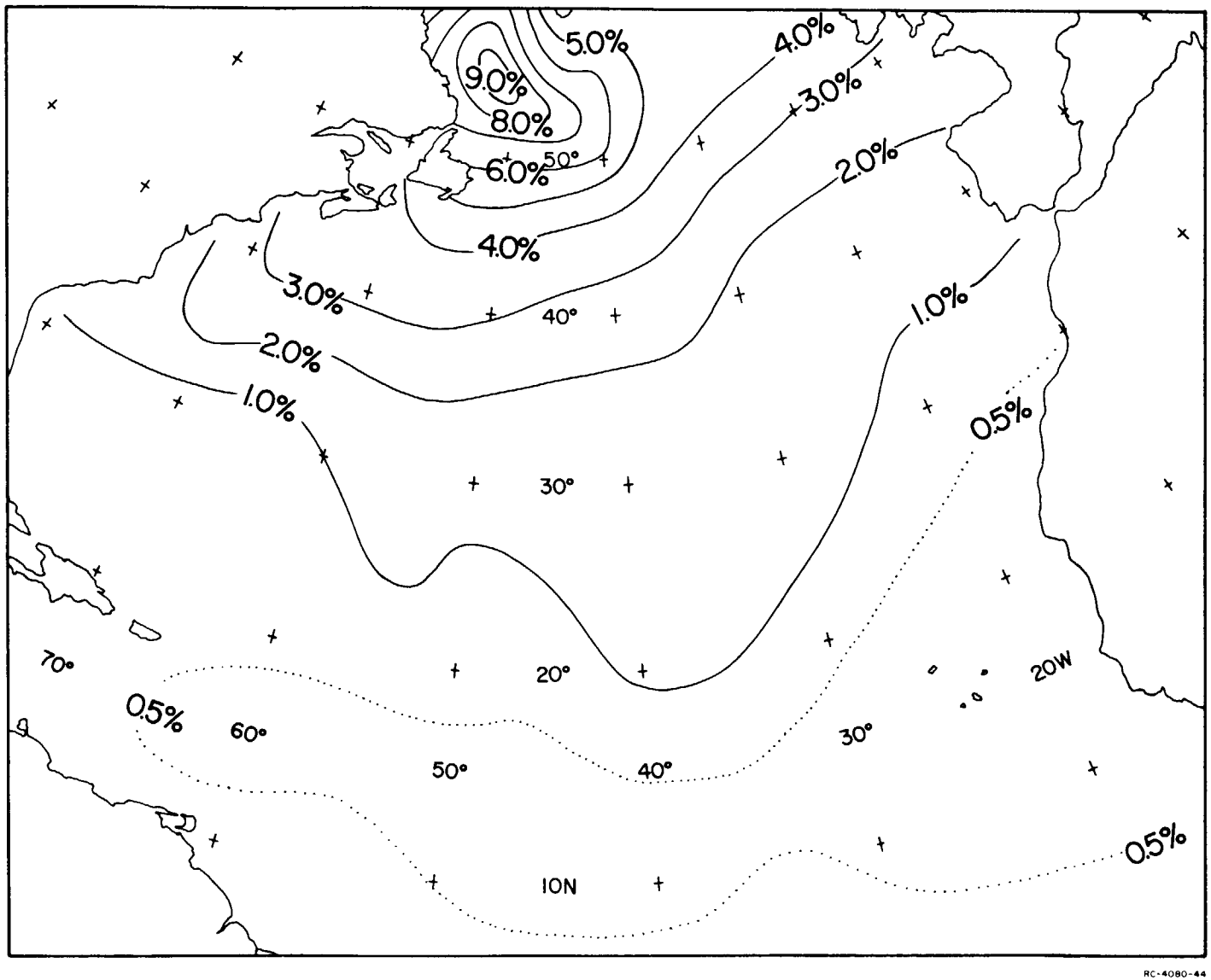

FIG. 27 ESTIMATED PROBABILITY OF OCCURRENCE OF PRECIPITATION DETECTABLE BY SATELLITE RADAR WITH 4-BY-4-MILE RESOLUTION – NORTH ATLANTIC, JANUARY, 1-mm/hr THRESHOLD
(Beam filled in vertical)

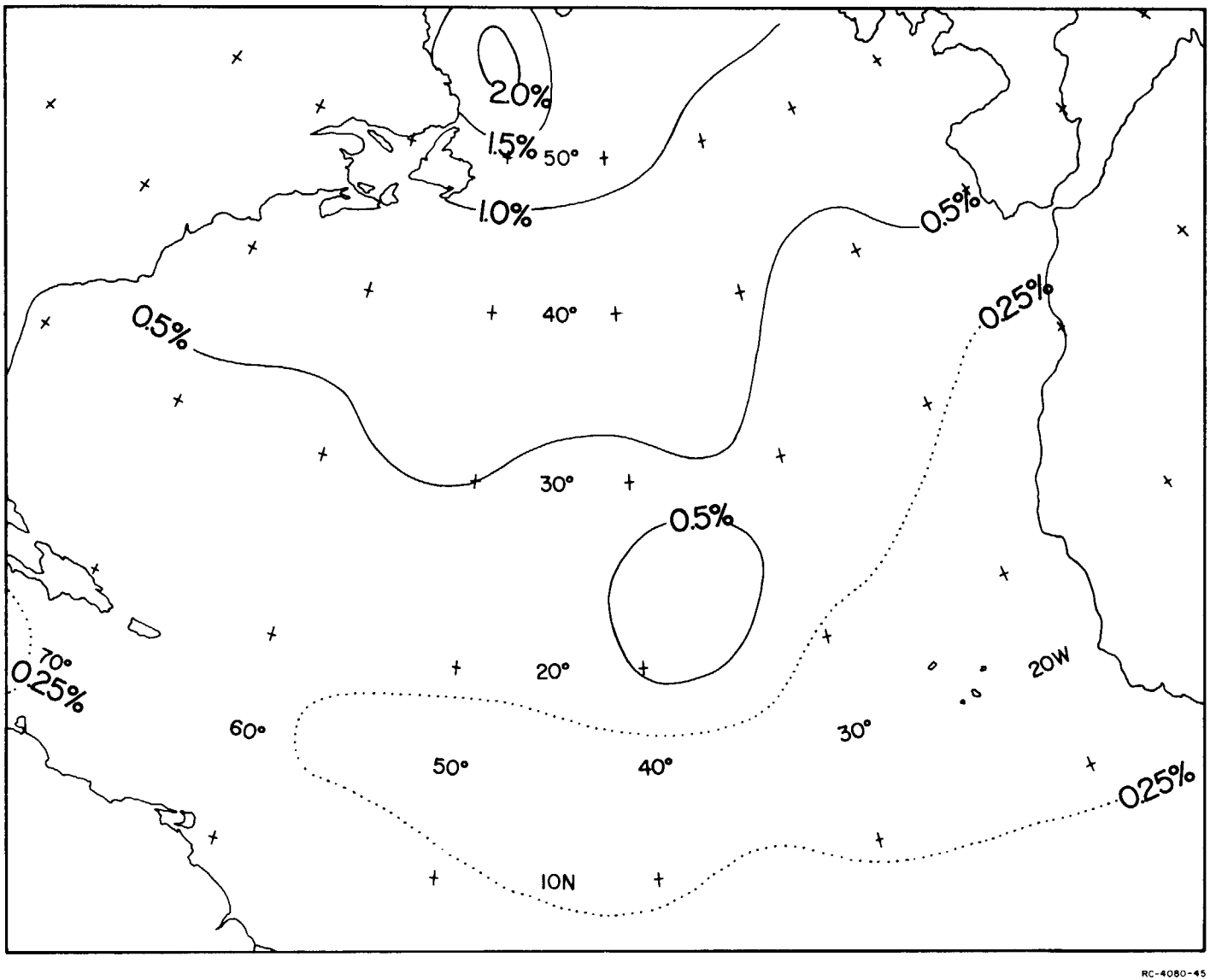

FIG. 28 ESTIMATED PROBABILITY OF OCCURRENCE OF PRECIPITATION DETECTABLE BY SATELLITE RADAR WITH 4-BY-4-MILE RESOLUTION – NORTH ATLANTIC, JANUARY, 3-mm hr THRESHOLD
(Beam filled in vertical)

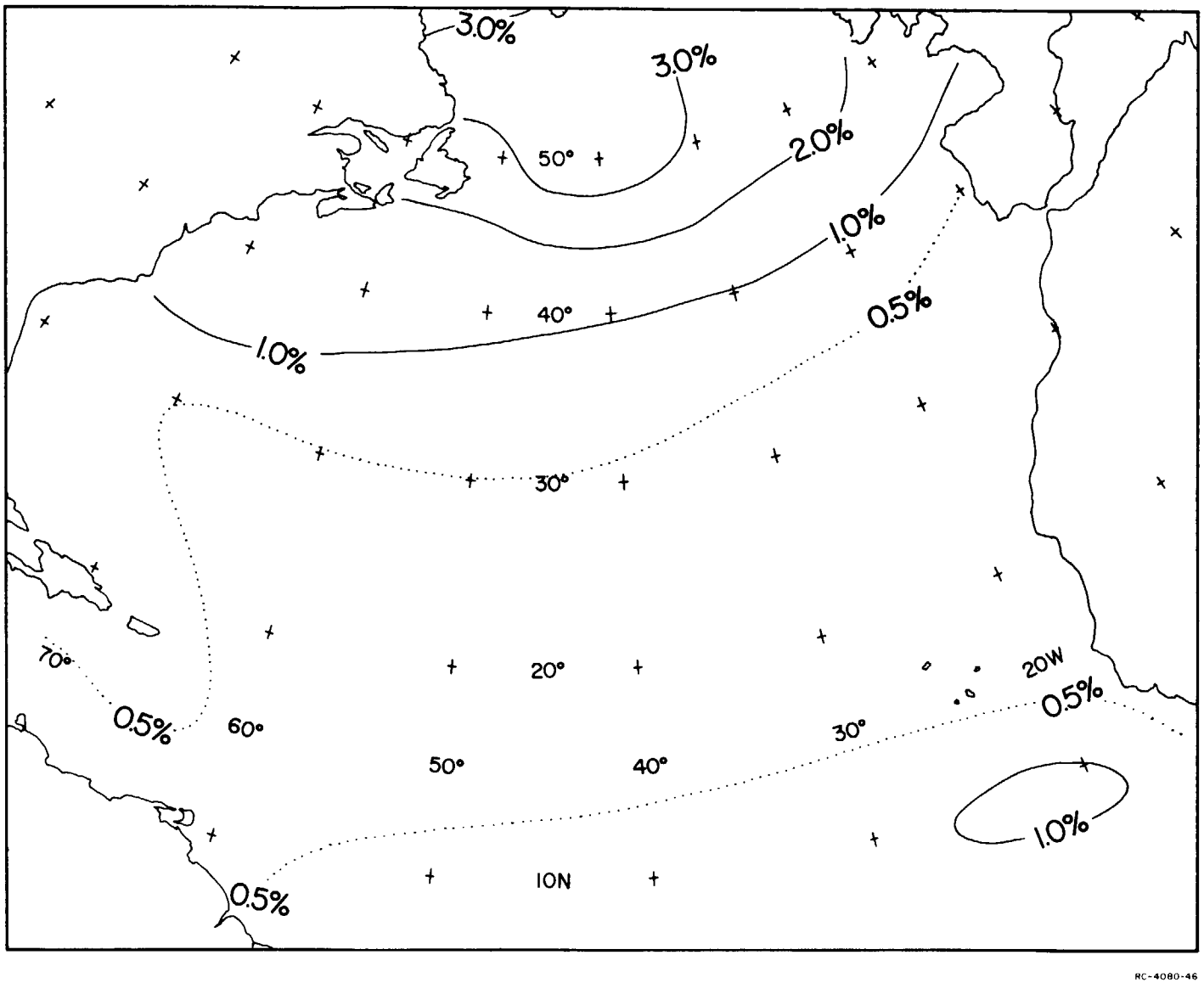

FIG. 29 ESTIMATED PROBABILITY OF OCCURRENCE OF PRECIPITATION DETECTABLE BY SATELLITE RADAR WITH 4-BY-4-MILE RESOLUTION – NORTH ATLANTIC, JULY, 1-mm hr THRESHOLD
(Beam filled in vertical)

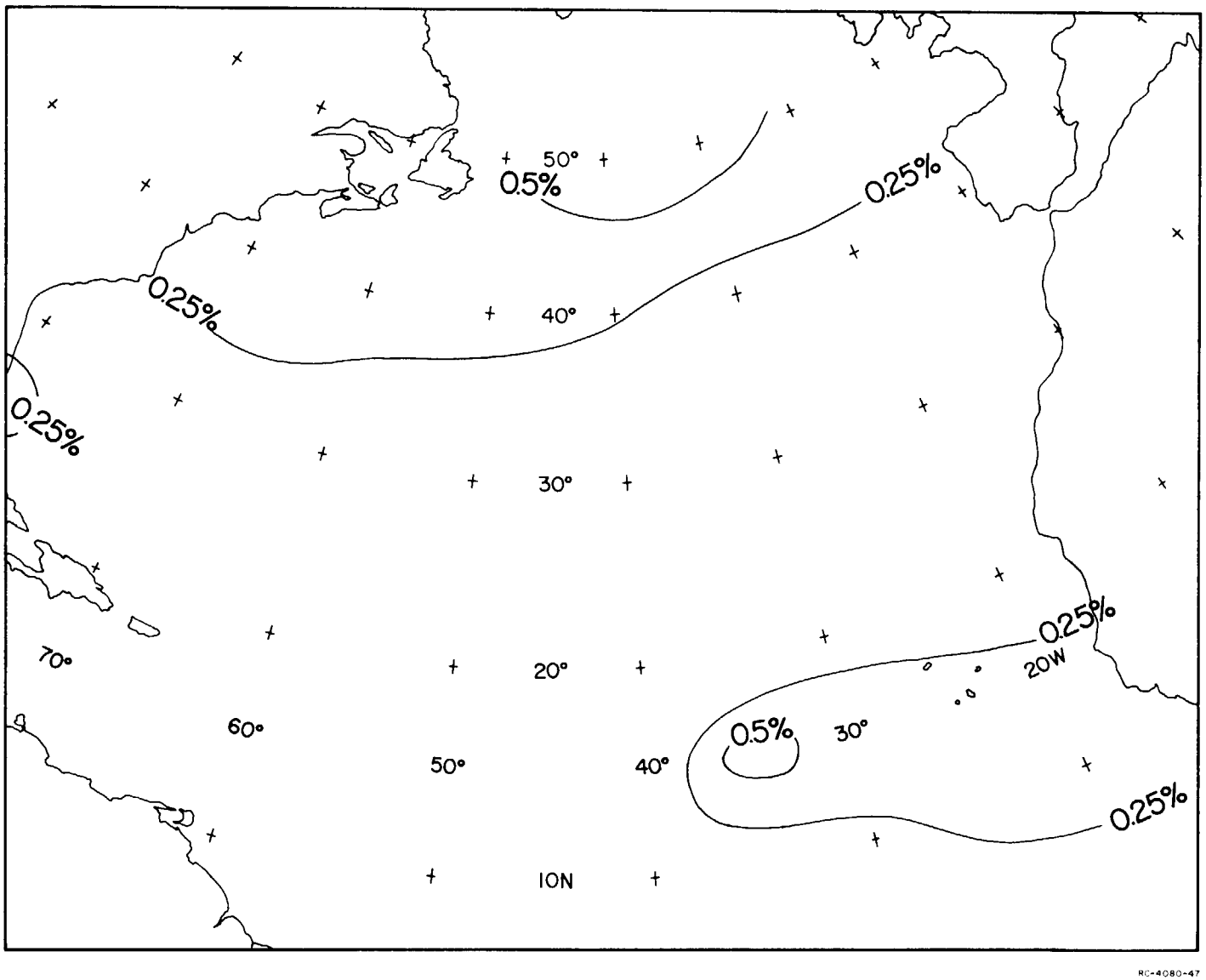

FIG. 30 ESTIMATED PROBABILITY OF OCCURRENCE OF PRECIPITATION DETECTABLE BY SATELLITE RADAR WITH 4-BY-4-MILE RESOLUTION – NORTH ATLANTIC, JULY, 3-mm hr THRESHOLD
(Beam filled in vertical)

No calculations have been performed for land areas. Presumably the results for flat land would reflect mean cyclone tracks and the sub-tropical high-pressure areas just as the oceanic results do. It is doubtful if any system could provide reliable results in mountainous regions (Sec. IV-C, below).

The above results show that a polar orbit would not be most suitable for a weather radar satellite. A satellite in such an orbit would spend one-third of its time at latitudes greater than 60 degrees, where detectable precipitation rarely occurs. Figures 23 through 30 indicate that a more useful orbit would be one crossing the Equator at 45 to 50 degrees orientation, rather than 90 degrees. A satellite radar in such an orbit could concentrate its observations in two bands, around 40-50°N and 40-50°S, effectively monitoring the principal mid-latitude cyclone tracks.

IV ENGINEERING REQUIREMENTS FOR A METEOROLOGICAL SATELLITE RADAR

A. Ultimate Limitations on Performance

Performance standards for a meteorological satellite radar capable of detecting a reasonable fraction of the precipitation in the beam can now be stated. They are (1) the ability to detect continuous rain filling the contributing region at rates as low as 1 mm/hr, (2) horizontal resolution of 4 miles, and (3) vertical resolution of 2 miles. In addition, the radar must be capable of scanning a broad swath if it is to provide data of any meteorological significance whatever. The physical parameters which can be varied in attempts to satisfy these standards include the peak transmitter power, the pulse length, the pulse repetition frequency, the receiver sensitivity, the radio frequency, and the antenna size. The proper choices of these parameters are made more difficult by a multiplicity of relationships among them.

A great deal of work, both published (e.g., Refs. 8-14) and unpublished, has been devoted to attempts to find suitable compromises among the various parameters. No attempt will be made here to review all of this work in detail. Rather, we shall set down what appear to be the most critical performance-limiting factors, comment on some proposals by previous writers concerned with overcoming such limitations, and give a brief description of the form a workable satellite radar would be likely to take.

The basic problem facing a satellite radar designer is that of detecting a signal returned from a thin layer of precipitation against a background of circuit noise, antenna noise, and clutter signals from the earth's surface. Circuit noise can be overcome, in theory at least, by powerful transmitters and sensitive receivers. Antenna noise can be overcome by the use of powerful transmitters. However, surface clutter signals can be overcome only by shaping a beam which prevents their arrival during the periods when precipitation signal is being received

or by finding some means of discriminating against them in the receiver circuits. This is because clutter signals will ordinarily exceed the precipitation signal by some 10 to 30 db (see Sec. IV-C).

The limitations just mentioned apply to the detection problem. Consideration of coverage requirements shows that scanning will be an acute problem if beams sharp enough to eliminate ground clutter are employed. Sufficiently rapid scanning to yield continuous coverage will move the beam approximately its own width during the interval between transmission and receipt of a pulse.

These points will now be taken up in turn, but, because of the multiplicity of relationships involved, no conclusion regarding any parameter can be regarded as final until all parameters have been considered. For the sake of simplicity, discussion will be limited to a satellite radar at an altitude of 600 miles.

B. Power Requirements

The power scattered back toward a satellite radar by precipitation must be detected against a background of random noise, which is contributed by the receiver circuits and by the matter in the antenna beam. These contributions can be described conveniently in terms of an effective receiver noise temperature, T_e, and an antenna temperature, T_a, respectively. The total noise output is equal to that which would result if the receiver were noise-free but the incoming signal contained a noise-like component of mean power

$$P_n = k(T_e + T_a)B \tag{12}$$

where k is Boltzmann's constant, T_e and T_a are in degrees Kelvin, and B is the effective bandwidth. The noise figure, F, of a receiver is related to its effective noise temperature by

$$F = 1 + \frac{T_e}{290^\circ K} \tag{13}$$

where F is ordinarily expressed in decibels.[69]

In the case of microwave antennas pointed skyward, antenna noise is contributed by galactic sources, the gaseous components of the atmosphere, and occasionally by clouds and precipitation. Measured values of T_a at the zenith range from below $5^{\circ}K$ in clear weather to over $100^{\circ}K$ in heavy thunderstorms.[70]

T_a will vary also in the case of an antenna pointed downward from a satellite. It should be emphasized that here we are discussing the earth's gray-body radiation, rather than the familiar surface-clutter interference, which is considered in Sec. IV-C. The antenna temperature observed will be a function of frequency and angle of incidence. It will include radiation from the surface and galactic radiation reflected from the surface, both modified by attenuation in the atmosphere, as well as radiation from the atmosphere itself, including clouds and precipitation. A check of available references indicates that observed values will range from around $150^{\circ}K$ over the sea to near $300^{\circ}K$ over some land surfaces.[69,71]

The use of parametric amplifiers with noise temperatures of a few hundred degrees Kelvin is indicated for satellite application. Masers have been developed which can be operated (under refrigeration) with X-band receivers to yield over-all receiver noise temperatures as low as $27^{\circ}K$.[72] However, antenna noise becomes the performance-limiting factor once T_e is lowered below T_a, so that the full potential of maser systems cannot be realized with downward-looking radars.

A fundamental limitation is imposed by the fluctuating nature of the precipitation echo, whose instantaneous value is due to the existing arrangement of the individual particles in the beam.[44] It is the <u>mean</u> value of the signal intensity which is related to precipitation rate.

There is considerable confusion in the literature concerning the proper criteria to use in establishing the minimum acceptable S/N (mean signal-to-noise) ratio for precipitation echoes. The Meteorological Satellite Laboratory Report No. 4 (Ref. 13) uses standards set by Hall,[73] which were derived in examining the detectability of steady targets in

noise. A more suitable basis for discussion would appear to be Kaplan's treatment of rapidly fading signals--that is, signals statistically the same as the noise.[74]

Kaplan's results were used in the computations of required transmitter power contained in Ref. 14. There, it is proposed to average the returns from 10 pulses with a S/N ratio of 3 db at the threshold rainfall rate, after allowing 10 db for system losses. Kaplan's Fig. 3 shows that this leads to a detection probability of just over 50% for a false-alarm ratio of 10^{-4} at the threshold rate. This false-alarm ratio appears to be low enough to satisfy the meteorological requirements. In Ref. 14, it is implied that the ten returns to be averaged would have to come from ten different pulses, and that the pulses would have to be separated in time by 7 msec or so, this being the time required for particle shuffling to lead to statistical independence at X-band. However, statistical independence is achieved each time the contributing region moves its own length along the beam, while successive pulses are practically independent if the antenna moves through half its own width during one pulse-repetition period.[44]

It will be shown in Sec. IV-D, below, that the pulse length makes a minor contribution to both the horizontal and vertical resolution elements for points off the satellite path. Thus, there is no great loss in resolution if the needed averaging is performed along the beam, rather than over a succession of pulses, provided the pulses are limited to about 1 μsec duration. This approach leads to a reduction in the mean power requirement, but not in the peak power requirement. The former is more likely to be a limiting factor in satellite operation.

We now have established enough conditions to permit an estimate of peak power and mean power requirements for a useful system. For a maser system operating over the oceans, T_a and T_e would be near $150^{\circ}K$ and $30^{\circ}K$, respectively. Frequency-stability considerations show that a satellite radar will need a receiver bandwidth near 2 Mc, and the use of 1-μsec pulses would rule out any great improvement over this. Using Eq. (12) shows that the minimum noise power that can ever

be reasonably expected is -112 dbm. Allowing 10 db for system losses[13,14] and a S/N ratio of 3 db, shows that the minimum detectable input signal from precipitation would have an average peak power of -99 dbm.

The peak transmitter power required for detection of 1-mm/hr rain with such a system can be estimated from the weather radar equation, which yields upon rearrangement,[45]

$$P_t = \frac{8\pi r^2 P_r}{A_e c\tau\eta} \tag{14}$$

where P_t is the transmitter power, r is the target range, A_e is the effective antenna aperture, c is the speed of light, τ is the pulse duration, and η is the radar reflectivity per unit volume, given by

$$\eta = \frac{\pi^5 |K|^2}{\lambda^4} \cdot Z$$

where K, Z, and λ are as defined in Sec. III. As noted above, observations from a swath of several hundred miles would be needed to provide data of meteorological value. At the outer edges of a 500-mile swath, say, the target range to a satellite 600 miles up is 1225 km. Considering the situation at X-band, where η for 1-mm/hr rain is near $10^{-7.2}$ m^{-1}, and setting A_e at 10 m^2 and τ at 1 μsec, we find P_t to be just over 15 kw.

In order to scan a 500-mile swath with 4-by-4-mile resolution while traveling at 4 miles per second, the satellite radar would have to examine 125 resolution elements per second. Directing a 1-μsec pulse of 15 kw peak power at each of these would consume power at a mean rate of 2 watts. When allowance is made for telemetry and heat losses, it appears that 3 to 5 watts would be required. This is somewhat more than the power consumption of present-day communication satellites. If averaging along the beam were not used, 10 pulses would have to be directed at each contributing region, and the mean power requirement would thus be increased by a factor of 10.

Typical radar receivers now in use have noise temperatures of a few thousand degrees Kelvin.[72] A satellite radar with such a receiver would be incapable of detecting 1-mm/hr rain unless the transmitter power were increased accordingly. To give a concrete example, a receiver with a noise temperature of 3000°K would need about 15 times as much power as the maser system considered above. Its mean power output would be near 35 watts. This is a formidable requirement, but presumably could be met if satellite radar data were considered absolutely necessary.

The theoretical power requirements can be reduced if the satellite radar is designed to operate in the K-band, rather than the X-band. This possibility is discussed in Sec. IV-3 below under the heading "Frequency and Attenuation."

C. Possibilities of Precipitation-Clutter Discrimination

The clutter signal returned to a meteorological satellite radar at any instant would be determined by the echo cross-section per unit area of the surface illuminated, which is denoted by σ_o (a dimensionless number). In determining the ratio of surface clutter to precipitation echo intensity, σ_o is to be compared to $(\eta c \tau/2)$, the radar reflectivity per unit volume multiplied by the length of the contributing region along the beam. For 1-mm/hr rain and a 1-μsec pulse at vertical incidence, $(\eta c \tau/2)$ is equal to -50 db.

The clutter signal returned to a satellite radar would be a function of frequency, polarization, angle of incidence, and the nature of the surface illuminated. Clutter signals are often treated as consisting of specular and scattered components, with the relative strength of the two depending upon the statistical properties of the illuminated surface. Care must be exercised in extrapolating such results; a hillside which yields a specular reflection to a stationary radar a mile away would be merely another randomly oriented facet of a rough surface for a satellite radar speeding past at an altitude of 600 miles.

Measurements of σ_o for water surfaces have been published by a number of authors, including Kerr,[43] Wiltse et al.,[75] and Grant and

Yaplee.[76] The specular components are large for angles of incidence approaching 90°, especially during calm conditions, while the scatter components predominate at small angles of incidence. During rough conditions, the scatter component is increased while the specular component is diminished. Roughness thus leads to increased values of σ_o for angles of incidence less than about 70°, but near vertical incidence this trend is reversed. The reported values indicate that, in the X-band and K-band regions, σ_o for water surfaces with moderate winds would range from -5 db at the edge of a 500-mile swath (angle of incidence 70°) to around +5 db at the satellite subpoint.[43,75] Under calm conditions, σ_o at the subpoint might rise as high as +25 db due to specular reflections.[43]

Measurements from aircraft over land show that ground clutter also contains specular and scattered components, but the former tend to be small even at vertical incidence.[77] The function σ_o again shows an angular dependence, usually dropping about 20 db as the angle of incidence decreases from 90° to 65°. However, wooded terrain shows only a weak angular dependence. Reported values of σ_o over land at vertical incidence range from -25 db up to +12 db.[76,78] It is necessary to keep in mind that the statistical properties of a surface vary with the area illuminated, but the mean cross sections observed from a satellite would likely be in the same range. At the edge of a 500-mile swath, one could expect a reduction of some 15 db.

The functions σ_o and $(\eta c \tau/2)$ are not directly comparable at points removed from the satellite subpoint. The fraction of the beam's cross-sectional area impinging upon the surface at the instant the trailing edge of the contributing region reaches it is given by

$$\frac{\frac{c\tau}{2} \cdot \cot \alpha}{r \Phi}$$

where α is the nadir angle and Φ the half-power beamwidth. The ratio of clutter cross section to precipitation cross section is then given by

$$\frac{\frac{c\tau}{2} \cdot \cot \alpha \cdot \sigma_o}{r\Phi \frac{\eta\, c\tau}{2}} = \frac{\cot \alpha \cdot \sigma_o}{r\, \Phi\, \eta}$$

where all symbols are as previously defined in this chapter. At the edge of a 500-mile swath and with a 0.2-degree beam (Sec. IV-D, below), the clutter-precipitation ratio for 1-mm/hr rain is given by $10^4\ \sigma_o$, rather than by $10^5\ \sigma_o$, as it is at the subpoint for a 1-μsec pulse.

In spite of the tremendous range of σ_o existing under various conditions, certain conclusions can be drawn. The first is that the surface clutter will usually exceed the signal from 1-mm/hr rain in the X-band region by at least 20 db. The return from heavy rain could exceed that from the surface occasionally, but, on the other hand, sea clutter at vertical incidence apparently could exceed that from 1-mm/hr rain, which a useful system must detect, by 75 db. The second conclusion is that at least part of the clutter signal will be incoherent--that is, it will be statistically indistinguishable from the precipitation return. In view of the relative intensities of surface and precipitation return, this component alone will typically exceed that from 1-mm/hr rain by several decibels.

The possibility of distinguishing ground clutter from precipitation return by utilizing some difference in the characteristics of the two signals other than relative amplitude has been considered by several authors.

The fluctuating nature of the precipitation echo has been mentioned in some proposals, but the motion of the satellite which yields a statistically independent precipitation return for each pulse will do the same for the scattered component of the sea or ground clutter. Therefore, pulse-to-pulse comparisons of the return from a given contributing region would be meaningless.

A multi-frequency system, proposed by Keigler and Krawitz, would utilize the well known fact that the return from cloud and precipitation increases, for a given antenna size, as the fourth power of the frequency.[8]

Therefore, a comparison of the return at two frequencies from a contributing region containing both precipitation and surface targets (ground or sea clutter) might reveal the presence of the precipitation. The idea has been examined closely by personnel of the Meteorological Satellite Laboratory of the U.S. Weather Bureau and rejected as impractical.[11] To get the same contributing region at the two frequencies, a larger antenna would have to be used at the lower. Therefore, the increase in return at the higher frequency would be reduced to roughly a square-law relationship. To obtain a significant difference in the total returns would require a frequency ratio of perhaps ten, as the precipitation's contribution to the total signal would be small. It is possible, however, that with such a large ratio the clutter return would vary also, thus spoiling the whole principle. Other obvious disadvantages of the system are its complexity and the increase in power requirements.

Circularly polarized radiation scattered by small spheres undergoes a reversal in the direction of rotation. This fact is used in eliminating rain echoes from air search radars.[79] Keigler and Krawitz state, "By the same token, a difference in returned signal for linearly (ground plus precipitation) and circularly (ground only) polarized signals could be used as an indication of the presence of precipitation."[8] The same suggestion has been offered, apparently independently, by two other sources in private communications, but closer scrutiny shows it to be of no value. The difficulty is that, while suppression of the precipitation return itself may run to 25 db, suppression of the precipitation plus ground return can never exceed the ratio of the ground clutter return to the precipitation plus ground return. With ground return 20 db above the precipitation return, to use a typical value, the two signals to be compared would be less than 1 db apart in amplitude, and hence indistinguishable. Furthermore, the clutter signal itself is affected by changes in polarization, so it would not provide any fixed basis of comparison.[75]

Katzenstein and Sullivan have proposed a pulsed Doppler system with a fan beam oriented at 45° to the satellite path, the Doppler shifts associated with the satellite's forward motion being used to locate targets in elevation and position along the beam.[9]

Among various possible objections to Katzenstein and Sullivan's proposal, the following is perhaps most serious. The ground return would not have, as they state, "a discrete Doppler frequency depending only on range." Assuming a reasonable value for the width of their fan beam shows that the Doppler shift at 100 miles from the subpoint would average near 80 kc, but actually extend from 70 kc to 90 kc. As the differential Doppler shift due to altitude in Katzenstein's and Sullivan's scheme is only 150 cycles per 1,000 feet, the indicated vertical resolution is over 100,000 feet. Katzenstein and Sullivan also neglected organized motions of the precipitation particles, including their fall and those produced by the wind or by strong vertical currents in convective cells. A radial component of 22 knots could cancel (or double) the differential Doppler shift associated with an altitude difference of 5,000 feet.*

Keigler and Krawitz also mentioned Doppler radar as a means of distinguishing precipitation and ground return, but concentrated on the Doppler shift arising from the fall velocities of the precipitation particles.[8,10] Obviously, Doppler shifts cannot be used two or three ways at once. Geometric considerations show that significant Doppler shifts are produced, in both the Keigler-Krawitz and Katzenstein-Sullivan systems, by several factors, including the forward motion of the satellite, the earth's rotation, changes in satellite altitude, movement of the precipitation by the wind, and the fall speeds of the precipitation particles. Furthermore, sea clutter can show Doppler

---

*This is a condensation of a simple, independent analysis performed by the present author in June 1962. An earlier and more detailed study by Hilleary, not in our hands at that time, had reached the same conclusion.[12]

shifts, which apparently are due to the motion of wave trains along the surface. These considerations appear to eliminate any chance of success for either the Keigler and Krawitz or the Katzenstein and Sullivan system.

Several individuals have suggested in private communications that a side-looking radar like the airborne one developed in Project MICHIGAN be used on a satellite.[80] This radar achieves fine angular resolution by integrating the return (including phase information) from successive pulses as it is carried along. Resolution is improved only in the direction of motion, which is the least critical for points off the satellite path. No real improvement in the situation could result from its use. As the MICHIGAN radar is basically a Doppler system, all of the ambiguities among target range, angular bearing, height, and radial velocity which arose in the Keigler-Krawitz and Katzenstein-Sullivan systems appear here also.

It should be noted that the individual motions of precipitation particles lead to a broadening of the Doppler shifts associated with them, which would affect all the proposed systems.[81] At 3 centimeters, this broadening would amount to 100 to 200 cps, depending upon the particle size distribution. It appears too that the amplitude fluctuations caused by the varying aspect of the particle arrays in the individual resolution elements sought would also introduce some Doppler components. However, in view of the several apparently decisive arguments already cited against the use of Doppler radars in meteorological satellites, a mathematical analysis of this particular point does not appear to be justified.

D. Beam Geometry

As no satisfactory method of discriminating against the scatter component of the surface clutter return is available, a satellite radar could succeed only by using a beam sharp enough to prevent its arrival simultaneously with the precipitation return.

As a first approximation, we shall consider a beam of uniform gain with a square cross section. Figure 31 illustrates this case at the

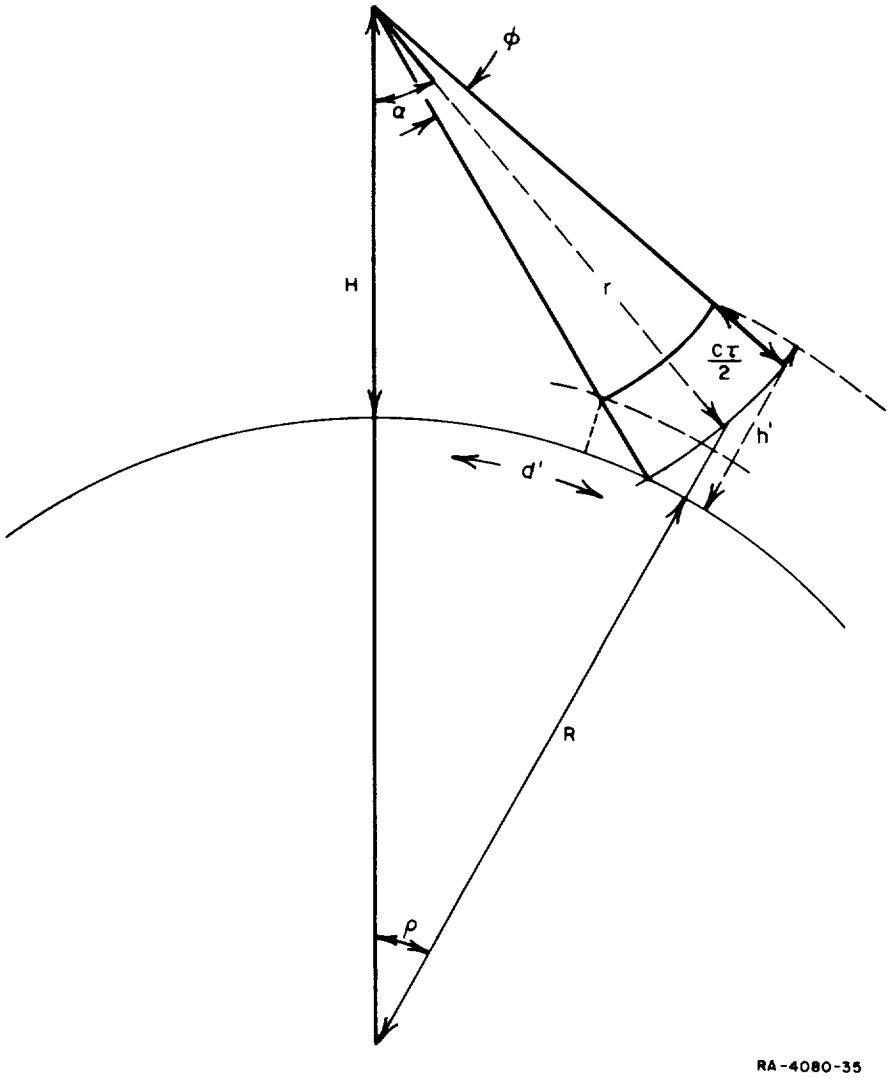

FIG. 31 VERTICAL AND HORIZONTAL RESOLUTION COMPONENTS FOR A PULSED SATELLITE RADAR

instant the contributing region reaches the surface at a point removed from the satellite subpoint.

The resolution in height, h', is given by

$$h' = r\Phi \left[\frac{R + H}{R} \sin \alpha\right] + \frac{c\tau}{2}\left[\frac{R + H}{H} \cos \alpha - \frac{r}{R}\right] \qquad (15)$$

where r is the slant range, Φ is the beam width, R the radius of the earth, H the satellite height, α the nadir angle, c the speed of light, and τ the pulse duration.* The resolution, d', along the Great Circle from subpoint to target is given by

$$d' = r\Phi\left[\frac{R + H}{R} \cos \alpha - \frac{r}{R}\right] + \frac{c\tau}{2}\left[\frac{R + H}{R}\right]\sin \alpha \quad . \qquad (16)$$

Substitution of numerical values shows that the most critical problem is the maintenance of vertical resolution near the edges of the swath, and that the beamwidth term is much larger than the pulse length term in that region. Figure 32 shows the height resolution, as a function of distance from the subpoint and beamwidth, for a radar emitting 1-μsec pulses from an altitude of 600 miles. An increase in τ to 10 μsec, which would result, in effect, if ten contributing regions were averaged along the beam, would increase h' by roughly 1000 feet. Using Fig. 32, the requirement that h' be held down to two miles for points 250 miles from the subpoint can be translated into a maximum permissible beamwidth--namely, 0.2°. This would make d' approximately 3 miles, thus satisfying the horizontal resolution requirements as well.

The beamwidth and gain obtainable from an antenna are functions of its effective aperture and the radio frequency used (e.g., Ref. 32, pp. 27 ff., Ref. 82). For a theoretical beam of uniform gain and small square cross section, we can write

---

*The symbols r, R, and α have been used in earlier chapters with different meanings. In this chapter, they will be used only as defined above.

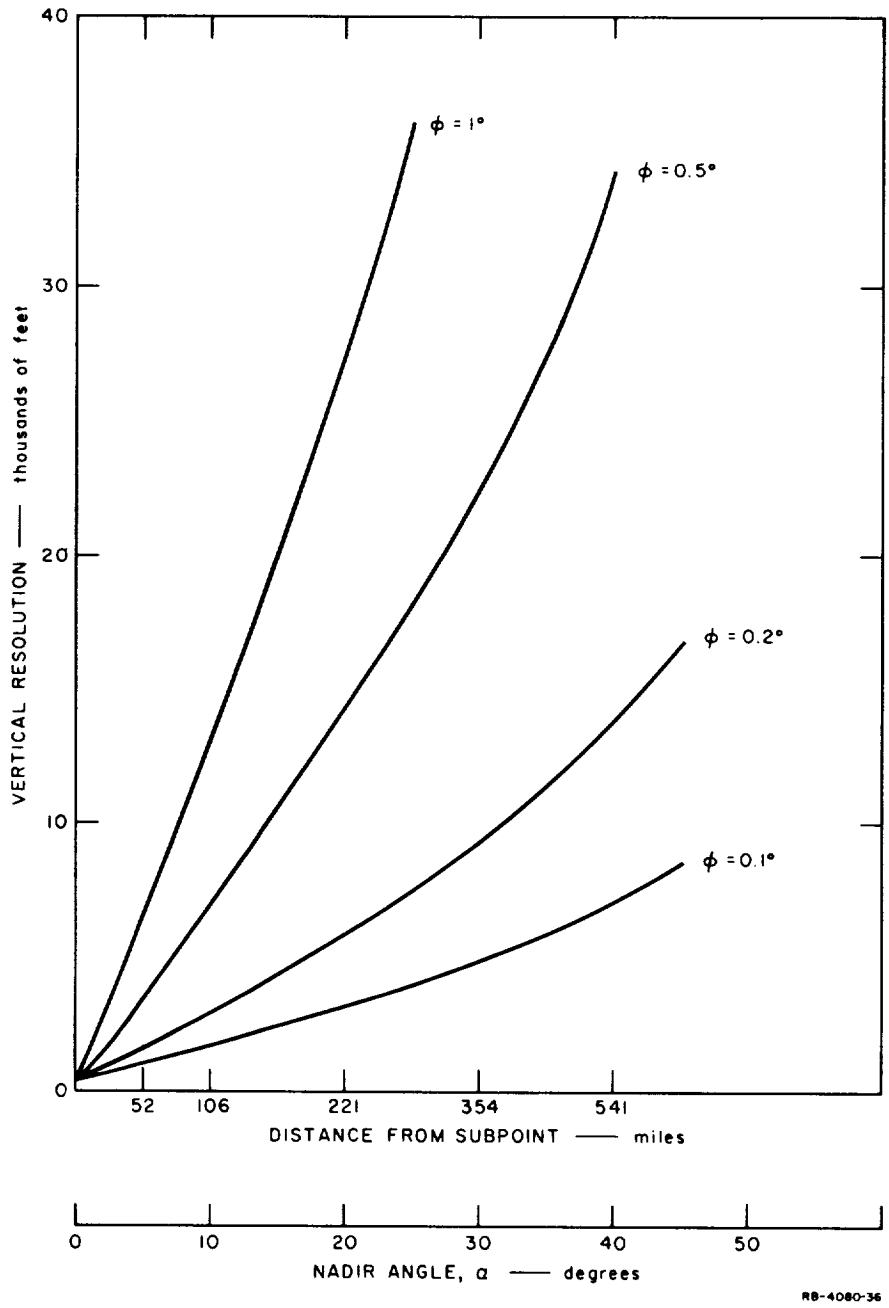

FIG. 32 VERTICAL RESOLUTION AS A FUNCTION OF DISTANCE FROM SUBPOINT (Nadir Angle) AND BEAMWIDTH FOR SATELLITE RADAR AT 600 MILES USING 1-μsec PULSES

$$A_e = (\lambda/\Phi)^2 \qquad (17)$$

where A_e is the effective aperture, λ is the wavelength, and Φ the beamwidth in radians. Equation (17) shows that the shaping of a 0.2° beam at X-band would require that A_e be near 50 m^2. Since, in practice, the effective aperture is roughly 50% of the actual antenna area, a need for a structure nearly 40 feet in diameter is implied. Such an antenna would reduce the power requirements computed in Sec. IV-B by 7 db, but its actual construction would present grave problems.

When actual beams, rather than the above idealization, are considered, further difficulties are revealed. Some sidelobe contributions from the surface will arrive simultaneously with the main-beam precipitation return, except when the radar is directed at the subpoint. Surface clutter signals are sometimes 30 to 70 db above precipitation return at X-band, as noted in Sec. IV-C, above, while typical antenna patterns have sidelobes 12 to 25 db below the main beam.[82] In many cases, therefore, clutter return via sidelobes would seriously interfere with the precipitation return. This could be overcome by more sharply tapering the illumination to improve sidelobe suppression, but this would also necessitate an increase in antenna size.

Scanning a 500-mile swath from 600 miles up involves a sweep through 45 degrees of nadir angle. For continuous coverage this must be completed each time the satellite moves forward one resolution element--that is, about once per second. If the scan is continuous, the antenna will sweep through 0.3 degrees during the 8 msec a pulse takes to get to the ground and back. Thus it would not be able to receive the return from the pulses it transmitted. This indicates a need for stepped scanning, which could not be managed with an unwieldy 20-foot reflector, or a multiple feed-horn system. A shift to phased array antennas is a possibility, but the scanning requirements would lead to a very complex system.

E. Frequency and Attenuation

The results of Secs. IV-C, D, and E all point strongly toward the use of a higher frequency than X-band in a meteorological satellite radar. As the precipitation scattering cross section increases roughly as the fourth power of the frequency, a shift in wavelength from 3.2 cm to 1 cm would ease power requirements by some 20 db. This would bring the mean power, which was estimated at 5 watts for an X-band maser system in Sec. IV-B, down to manageable levels. As sea clutter exhibits very little frequency dependence near vertical incidence,[75] the precipitation-sea-clutter signal ratio would also improve by 20 db. A slightly smaller improvement could be expected over land.[77] This would be enough to eliminate most of the confusion due to ground clutter return via side lobes, provided sidelobe suppression of 25 db could be obtained. (The possible 70-db clutter-precipitation ratio mentioned in Sec. IV-C would only occur when the radar was over a smooth water surface and directed at the subpoint.) Finally, the change would reduce the required antenna diameter for a given beamwidth by a factor of 3.

There are two considerations which offset these advantages to some extent. First, the tolerances for the antenna surface would become extremely close, of the order of 1 mm. This would appear to rule out the use of inflatable structures, which have been suggested as a means of getting a large reflector into orbit--e.g., Ref. 8 and Appendix V of Ref. 13.

Attenuation of satellite radar transmissions by the atmosphere is considered at some length in Ref. 13, making use of earlier computations by Atlas et al.[83] It appears to the present author that attenuation is a relatively minor problem compared to the ones noted above. The distance which the pulses would have to travel through heavy precipitation to reach the ground would never exceed 10 to 12 miles, and would usually be much less. Gunn and East state that the one-way attenuation due to rain in decibels per kilometer is given by $0.22R$ at 0.9 cm, where R is the rainfall rate in mm/hr.[45] Sample calculations show that the ground return, which would be a useful altitude reference,

might be lost occasionally during heavy thunderstorms, but that the percentage of time this would occur should be negligible. In this connection, the results of Secs. III-D and E regarding the low frequency of occurrence of high rainfall rates are of interest. In any event, storm tops would always be accessible to a satellite-borne radar.

It should be noted that a change to the 1-cm region would not render clouds visible to a satellite radar. Vertical-pointing K-band radars are sometimes described as cloud-detection radars, but they do not detect all clouds. They detect clouds containing large particles of the order of 25 microns in diameter, virga, and, of course, precipitation. An increase in range from, say, 2 to 600 miles would render echoes in the first two categories undetectable, leaving only some of the heavier precipitation return.

It will be recalled that the arguments against using satellites as rainfall monitors which are advanced in Secs. I and II are based on the nature of precipitation and the mechanics of satellite orbits, and are independent of the sensor used. A shift to K-band, while easing certain technical requirements, offers no solution to the fundamental limitations outlined in Secs. I and II.

REFERENCES

1. Bjerknes, J., and H. Solberg, "Meteorological Conditions for the Formation of Rain," Geofysiske Publikationer, 2, 3, pp. 1-60 (1921), UNCLASSIFIED.

2. Neiburger, M., and H. Wexler, "Weather Satellites," Scientific American, 205, 1, pp. 80-94 (July 1961), UNCLASSIFIED.

3. Crowson, D. L., "Cloud Observations from Rockets," Bull. Am. Meteorol. Soc., 30, 1, pp. 17-22 (January 1949), UNCLASSIFIED.

4. Bjerknes, J., "Detailed Analysis of Synoptic Weather as Observed from Photographs Taken on Two Rocket Flights over White Sands, N. Mex., July 26, 1948," Report, the RAND Corp., Santa Monica, Calif. (April 1951), UNCLASSIFIED.

5. Wexler, H., "Observing the Weather from a Satellite Vehicle," J. British Interplanetary Society, 13, 5, pp. 269-276 (September 1954), UNCLASSIFIED.

6. Widger, W. K., Jr., and C. N. Touart, "Utilization of Satellite Observations in Weather Analysis and Forecasting," Bull. Am. Meteorol. Soc., 38, 9, pp. 521-533 (November 1957), UNCLASSIFIED.

7. Mook, C. P., and D. S. Johnson, "A Proposed Weather Radar and Beacon System for Use with Meteorological Radar Satellites," Proc. 3rd National Convention on Military Electronics, IRE, pp. 206-209 (1959), UNCLASSIFIED.

8. Keigler, J. E., and L. Krawitz, "Weather Radar Observations from Earth Satellites," Proc. 8th Weather Radar Conference, pp. 237-244 (April 1960), UNCLASSIFIED.

9. Katzenstein, H., and H. Sullivan, "A New Principle for Satellite-Borne Meteorological Radar," Proc. 8th Weather Radar Conference, pp. 505-515 (April 1960), UNCLASSIFIED.

10. Keigler, J. E., and L. Krawitz, "Weather Radar Observations from an Earth Satellite," J. Geophys. Research, 65, 9, pp. 2793-2808 (September 1960), UNCLASSIFIED.

11. Johnson, D., and D. T. Hilleary, "Dual Frequency for Meteorological Satellites," private communication to NASA (1961), UNCLASSIFIED.

12. Hilleary, D. T., "Some Geometric Considerations Pertaining to Meteorological Satellite Doppler Radar," Private communication to NASA from Meteorological Satellite Laboratory, U.S. Weather Bureau (1961), UNCLASSIFIED.

13. Anon., "Requirements and Design Concepts for an Initial Satellite Weather Radar," MSL Report 4, U.S. Weather Bureau, with appendix by Diamond Ordnance Fuze Laboratories (January 1961), UNCLASSIFIED.

14. Anon., "Requirements for a Study Program to Specify the Design of a Satellite-Borne Precipitation Radar," Diamond Ordnance Fuze Laboratories, Washington 25, D.C. (October 1961), UNCLASSIFIED.

15. Smith, G. D., and M. G.H. Ligda, "The Use of Composite Radar Photographs in Synoptic Weather Analysis," Scientific Report 3, Contract AF 19(604)-1564, the A. & M. College of Texas, College Station, Texas (August 1957), UNCLASSIFIED.

16. Senn, H. V., and H. W. Hiser, "The Origin and Behavior of Hurricane Spiral Bands as Observed on Radar," Proc. 7th Weather Radar Conference, pp. K-46 to K-55 (1958), UNCLASSIFIED.

17. Tepper, M., "Mesometeorology--The Link Between Macroscale Synoptic Weather and Local Weather," Bull. Amer. Meteorol. Soc. 40, pp. 56-72 (February 1959), UNCLASSIFIED.

18. Newton, C. W., "Structure and Mechanism of the Prefrontal Squall Line," J. Meteorol. 7, 3, pp. 210-222 (June 1950), UNCLASSIFIED.

19. Wilson, J. W., and E. Kessler, III, "Use of Radar Summary Maps for Weather Analysis and Forecasting," J. Appl. Meteorol., 2, 1, pp. 1-11 (February 1963), UNCLASSIFIED.

20. Byers, H. R., and R. R. Braham, Jr., "The Thunderstorm," Government Printing Office, Washington, D.C. (1949), UNCLASSIFIED.

21. Langleben, M. P., "The Plan Pattern of Snow Echoes at the Generating Level," J. Meteorol., 13, 6, pp. 554-560 (December 1956), UNCLASSIFIED.

22. Fujita, T., "Study of Mesosystems Associated with Stationary Radar Echoes," J. Meteorol., 16, pp. 38-52 (February 1959), UNCLASSIFIED.

23. Ligda, M. G.H., R. T.H. Collis, and R. H. Blackmer, Jr., "A Radar Study of Maritime Precipitation Echoes," Final Report, SRI Project 2829, Contract NOas 59-6170-c, Stanford Research Institute, Menlo Park, California (June 1960), UNCLASSIFIED.

24. Soane, C. M., and V. G. Miles, "On the Space and Time Distribution of Showers in a Tropical Region," Quart. J. Roy. Meteorol. Soc. 81, pp. 440-448 (July 1955), UNCLASSIFIED.

25. Austin, J. M., and R. H. Blackmer, Jr., "The Variability of Cold Front Precipitation," Proc. 5th Weather Radar Conference, pp. 95-101 (1955), UNCLASSIFIED.

26. Goldie, A. H. R., "Rainfall at Fronts of Depressions," Geophysical Memoirs, No. 69, H. M. Stationery Office, London (1936), UNCLASSIFIED.

27. Bristor, C. L., and M. A. Ruzecki, "TIROS I Photographs of the Midwest Storm of April 1, 1960," Monthly Weather Review 88, pp. 315-326 (September-December 1960), UNCLASSIFIED.

28. Boucher, R. J., and R. J. Newcomb, "Synoptic Interpretation of Some TIROS Vortex Patterns: A Preliminary Cyclone Model," J. Appl. Meteorol. 1, 2, pp. 127-136 (June 1962), UNCLASSIFIED.

29. Serebreny, S. M., E. J. Wiegman, and R. G. Hadfield, "Investigation of the Operational Use of Cloud Photographs from Weather Satellites in the North Pacific," Final Report, SRI Project 3858, Contract Cwb 10238, Stanford Research Institute, Menlo Park, California (November 1962), UNCLASSIFIED.

30. Fujita, T., and T. Ushijima, "Investigation of Squall Lines with the Use of Radar and Satellite Photographs," Proc. 9th Weather Radar Conference, pp. 186-192 (1961), UNCLASSIFIED.

31. Nagle, R. E., and S. M. Serebreny, "Radar Precipitation Echo and Satellite Cloud Observations of a Maritime Cyclone," J. Appl. Meteorol. 1, 3, pp. 279-295 (September 1962), UNCLASSIFIED.

32. Nagle, R. E., and R. H. Blackmer, Jr., "The Use of Synoptic-Scale Weather Radar Observations in the Interpretation of Satellite Cloud Observations," Final Report, SRI Project 3947, Contract AF 19(628)-284, Stanford Research Institute, Menlo Park, California (December 1962), UNCLASSIFIED.

33. Nagle, R. E., "Comparisons of Time-Integrated Radar-Detected Precipitation with Satellite Observed Cloud Patterns," Proc. 10th Weather Radar Conference (1963), UNCLASSIFIED.

34. Boucher, R. J., "Synoptic-Physical Implications of 1.25-Cm Vertical Beam Radar Echoes," J. Meteorol. 16, 3, pp. 312-326 (June 1959), UNCLASSIFIED.

35. Kreitzberg, C. W., "Preliminary Results of a Study of Pacific Storms Using 1.87-Cm Radar," Tech. Note 1, Contract AF 19(604)-5192, University of Washington, Seattle, Washington (1961), UNCLASSIFIED.

36. Huff, F. A., and J. C. Neill, "Rainfall Relations on Small Areas in Illinois," Bull. 44, Illinois State Water Survey Division, Urbana, Illinois (1957), UNCLASSIFIED.

37. Noel, T. M., and A. Fleisher, "The Linear Predictability of the Radar Signal," Proc. 8th Weather Radar Conference, pp. 323-334 (1960), UNCLASSIFIED.

38. Wexler, R., "Theory and Observation of Radar Storm Detection," in Compendium of Meteorology, pp. 1283-1289 (Amer. Meteorol. Soc., 1951), UNCLASSIFIED.

39. Grunow, J., "Investigations on the Structure of Precipitation," Final Report, Contract No. DA-91-591-EUC-1386, OI-4346-60, Deutscher Weterdienst (April 1961), UNCLASSIFIED.

40. Dryden, W. A., "Useful Satellite Orbits for Some High-Altitude Weather Observations," Scientific Report 1, Contract AF 19(604)-1754, Dept. of Meteorology, Florida State University, Tallahassee, Florida (August 1958), UNCLASSIFIED.

41. Jones, D. L., D. S. Cooley, and J. A. Carey, "A Survey of Observational Requirements from Meteorological Satellites, 1963-1966," Report 7086-32, Contract GE 214-A 92505, The Travelers Research Center, Inc., Hartford, Connecticut (July 1962), UNCLASSIFIED.

42. Ryde, J. W., "Echo Intensities and Attenuation Due to Clouds, Rain, Hail, Sand, and Dust Storms," Report 7831, General Electric Co., England (1941), UNCLASSIFIED.

43. Kerr, D. E., "Propagation of Short Radio Waves," pp. 481-640, Vol. 13, Radiation Laboratory Series (McGraw-Hill Book Company, Inc., New York, N.Y., 1951), UNCLASSIFIED.

44. Marshall, J. S., and W. Hitschfeld, "Interpretation of the Fluctuating Echo from Randomly Distributed Scatterers: Part I," Canadian J. Physics, 31, pp. 962-995 (1953), UNCLASSIFIED.

45. Gunn, K. L. S., and T. W. R. East, "Microwave Properties of Precipitation Particles," Quart. J. Roy. Meteorol. Soc. 80, pp. 522-545 (October 1954), UNCLASSIFIED.

46. Fujiwara, M., "An Analytical Investigation of the Variability of Size Distribution of Raindrops in Convective Storms," Proc. 8th Weather Radar Conference, pp. 159-166 (April 1960), UNCLASSIFIED.

47. Gunn, K. L. S., and J. S. Marshall, "The Distribution with Size of Aggregate Snowflakes," J. Meteorol. 15, pp. 452-461 (October 1958), UNCLASSIFIED.

48. Douglas, R. H., "Size Distributions, Water Contents and Radar Reflectivities of Hail in Alberta," Proc. 8th Weather Radar Conference, pp. 127-134 (April 1960), UNCLASSIFIED.

49. Bigler, S. G., and P. L. Hexter, Jr., "Radar Analysis of Hurricane Debra," Proc. 8th Weather Radar Conference, pp. 25-32 (1960), UNCLASSIFIED.

50. Peltzer, R. G., R. B. Crane, and O. L. Tiffany, "An Airborne Radar for Weather Reconnaissance," Proc. 8th Weather Radar Conference, pp. 339-346 (1960), UNCLASSIFIED.

51. Wilk, K. E., "Research Concerning Analysis of Severe Thunderstorms," Final Report, Contract AF 19(604)-4940, Illinois State Water Survey, Urbana, Illinois (December 1961), UNCLASSIFIED.

52. Battan, L. J., Radar Meteorology, pp. 85-90, University of Chicago Press (1959), UNCLASSIFIED.

53. Wexler, R., and P. M. Austin, "Radar Signal Intensity from Different Levels in Steady Snow," Research Report 23, Contract DA 36-039 SC-42625, Massachusetts Institute of Technology, Cambridge, Mass. (March 1954), UNCLASSIFIED.

54. Kotsch, W. J., " An Example of Colloidal Instability of Clouds in Tropical Latitudes," Bull. Am. Meteorol. Soc., 28, 2, pp. 87-89 (February 1947), UNCLASSIFIED.

55. Marshall, J. S., "Grey Scale and CAPPI in Operation," Proc. 8th Weather Radar Conference, pp. 279-286 (1960), UNCLASSIFIED.

56. Donaldson, R. J., Jr., "Analysis of Severe Convective Storms Observed by Radar," J. Meteorol. 15, 1, pp. 44-50 (February 1958), UNCLASSIFIED.

57. Hartel, H. W., R. A. Clark, and V. E. Moyer, "Investigation of Space and Time Variations of Convective Precipitation as Revealed by Radar Reflectivity Measurements," Proc. 9th Weather Radar Conference, pp. 83-89 (October 1961), UNCLASSIFIED.

58. Newell, R. E., "Some Radar Observations of Tropospheric Cellular Convection," Proc. 8th Weather Radar Conference, pp. 315-322 (1960), UNCLASSIFIED.

59. Blackmer, R. H., Jr., and S. M. Serebreny, "Dimensions and Distributions of Cumulus Clouds as Shown by U-2 Photographs," Scientific Report 4, SRI Project 3245, Contract AF 19(604)-7312, Stanford Research Institute, Menlo Park, California (July 1962), UNCLASSIFIED.

60. Bussey, H. E., "Microwave Attenuation Statistics Estimated from Rainfall and Water Vapor Statistics," Proc. IRE 38, 7, pp. 781-785 (July 1950), UNCLASSIFIED.

61. Hudson, H. E., Jr., G. E. Stout, and F. A. Huff, "Studies of Thunderstorm Rainfall with Dense Raingauge Networks and Radar," Report of Investigation No. 13, Illinois State Water Survey, Urbana, Illinois (1952), UNCLASSIFIED.

62. Hamilton, P. M., and J. S. Marshall, "Weather-Radar Attenuation Estimates from Raingauge Statistics," Scientific Report MW-32, Contract AF 19(604)-2065, McGill University, Montreal, Canada (January 1961), UNCLASSIFIED.

63. Langleben, M. P., "The Terminal Velocity of Snowflakes," Quart. J. Roy. Meteorol. Soc. 80, 334, pp. 174-181 (April 1954), UNCLASSIFIED.

64. Gunn, K. L. S., "Snowfall Rates at Montreal," Proc. 8th Weather Radar Conference, pp. 175-178 (1960), UNCLASSIFIED.

65. Cole, A. E., and N. Sissenwine, "Rate of Rainfall Frequencies Over Selected Air Routes and Destinations" (U), Air Force Surveys in Geophysics No. 66, Geophysics Research Directorate, U.S. Air Force (1955), SECRET.

66. Russak, S. L., and J. W. Easley, "A Practical Method for Estimating Rainfall Rate Frequencies Directly from Climatic Data," Bull. Am. Meteorol. Soc. 39, 9, pp. 469-472 (September 1958), UNCLASSIFIED.

67. U.S. Navy Marine Climatic Atlas of the World, Volume I: North Atlantic Ocean, NAVAER 50-1C-528 (December 1956), UNCLASSIFIED.

68. U.S. Navy Marine Climatic Atlas of the World, Volume II: North Pacific Ocean, NAVAER 50-1C-529 (July 1956), UNCLASSIFIED.

69. Hansen, R. C., "Low-Noise Antennas," Microwave J. 2, 6, pp. 19-24 (June 1959), UNCLASSIFIED.

70. Hogg, D. C., and R. A. Semplak, "Effect of Rain and Water Vapor on Sky Noise at Centimeter Wavelengths," Bell System Tech. J. 40, pp. 1331-1348 (September 1961), UNCLASSIFIED.

71. Chen, S. N., and W. H. Peake, "Apparent Temperatures of Smooth and Rough Terrain," Trans. IRE, PGAP-9, 6, pp. 567-572 (November 1961), UNCLASSIFIED.

72. Robbiani, R. L., "Application of Maser to Nuclear Weather Surveillance Radar," USASRDL Tech. Report 2151, U.S. Army Signal Research and Development Laboratory (September 1960), UNCLASSIFIED.

73. Hall, W. M., "Prediction of Pulse Radar Performance," Proc. IRE 44, 2, pp. 224-231 (February 1956), UNCLASSIFIED.

74. Kaplan, E. L., "Signal-Detection Studies, with Applications," Bell System Tech. J. 34, 2, pp. 403-437 (March 1958), UNCLASSIFIED.

75. Wiltse, J. C., S. P. Schlesinger, and C. M. Johnson, "Back-Scattering Characteristics of the Sea in the Region from 10 to 50 kMc," Proc. IRE 45, 2, pp. 220-228 (February 1957), UNCLASSIFIED.

76. Grant, C. R., and B. S. Yaplee, "Back Scattering from Water and Land at Centimeter and Millimeter Wavelengths," Proc. IRE 45, 7, pp. 976-982 (July 1957), UNCLASSIFIED.

77. Moore, R. K., and C. S. Williams, Jr., "Radar Terrain Return at Near-Vertical Incidence," Proc. IRE 45, 2, pp. 228-238 (February 1957), UNCLASSIFIED.

78. Edison, A. R., R. K. Moore, and B. D. Warner, "Radar Terrain Measured at Near-Vertical Incidence," Trans. IRE, PGAP-8, 3, pp. 246-254 (May 1960), UNCLASSIFIED.

79. Ridenour, L. N., Radar System Engineering, pp. 81-85, Vol. 1, Radiation Laboratories Series (McGraw-Hill Book Company, Inc., New York, N.Y., 1947), UNCLASSIFIED.

80. Cutrona, L. J., W. E. Vivian, E. N. Leith, and G. O. Hall, "A High-Resolution Radar Combat-Surveillance System," Trans. IRE, PGMIL-5, 2, pp. 127-131 (April 1961), UNCLASSIFIED.

81. Barlow, E. J., "Doppler Radar," Proc. IRE 37, 4, pp. 340-355 (April 1949), UNCLASSIFIED.

82. Silver, S., Microwave Antenna Theory and Design, pp. 168 ff., Vol. 12, Radiation Laboratory Series (McGraw-Hill Book Company, Inc., New York, N.Y., 1949), UNCLASSIFIED.

83. Atlas, D., V. G. Plank, W. H. Paulson, and A. C. Chmela, "Atmospheric Attenuation of the Short Microwaves," Part II of Weather Effects on Radar, Air Force Surveys in Geophysics No. 23, Geophysics Research Directorate, U.S. Air Force (December 1952), UNCLASSIFIED.

109

STANFORD RESEARCH INSTITUTE

MENLO PARK
CALIFORNIA

Regional Offices and Laboratories

Southern California Laboratories
820 Mission Street
South Pasadena, California

Washington Office
808 17th Street, N.W.
Washington 5, D.C.

New York Office
270 Park Avenue, Room 1770
New York 17, New York

Detroit Office
The Stevens Building
1025 East Maple Road
Birmingham, Michigan

European Office
Pelikanstrasse 37
Zurich 1, Switzerland

Japan Office
911 Iino Building
22, 2-chome, Uchisaiwai-cho, Chiyoda-ku
Tokyo, Japan

Representatives

Honolulu, Hawaii
Finance Factors Building
195 South King Street
Honolulu, Hawaii

London, England
19 Upper Brook Street
London, W. 1, England

Milan, Italy
Via Macedonio Melloni 40
Milano, Italy

London, Ontario, Canada
P.O. Box 782
London, Ontario, Canada